Forschungsbericht 2006-02

Particle Emissions from Aviation: Microphysics, Chemistry, and Climate Impact

Andreas Petzold

Deutsches Zentrum für Luft- und Raumfahrt
Institut für Physik der Atmosphäre
Oberpfaffenhofen

96 Seiten
43 Bilder
8 Tabellen
104 Literaturstellen

Deutsches Zentrum
für Luft- und Raumfahrt e.V.
in der Helmholtz-Gemeinschaft

Particle Emissions from Aviation: Microphysics, Chemistry, and Climate Impact

Partikelemissionen des Luftverkehrs:

Mikrophysik, Chemie und Klimawirkung

Department of Physics of the Ludwig-Maximilians-University Munich

Thesis for postdoctoral lecture qualification in Meteorology

der Fakultät für Physik der Ludwig-Maximilians-Universität München
zur Habilitation in Meteorologie vorgelegte wissenschaftliche Arbeit

Dr. rer. nat. Andreas Petzold

June 2005

To

Sabine

Abstract

Particulate emissions from aviation during cruise, their physical and chemical properties and the potential effects on Earth's atmosphere and climate constitute a rich and complex research area. Their relevance for the global climate system was identified in the early 1990s, and gains today increasing attention because of their likely role in the life cycle of upper tropospheric ice clouds or cirrus, respectively. An understanding of the impact mechanisms of aviation-related particle emissions on atmosphere and climate requires research on particle formation in gas turbines, on particle processing in chemically active exhaust plumes, on atmospheric processing and transformation of particles released into the upper troposphere and lowermost stratosphere, and also on the background aerosol of this particular atmospheric layer which forms the sink for the aircraft engine exhaust particles. Simultaneously, techniques have to be developed for improving the available measurement capabilities for relevant particle properties and constituents. The presented experimental work approaches the scientific subject from all necessary directions: The physical and chemical properties of emitted particles were identified under cruise altitude conditions and with more detailed methods during ground-test studies. The quantification of emissions for various aircraft resulted in a validated average emission index for particulate black carbon which is today widely used for the calculation of the aviation-related particle emissions in climate models and impact studies. The results achieved from this extensive experimental field work contributed considerably to the international assessment of the climate effects of aviation at the turn to the 21st century. A European research programme on the properties and the processing of particles forming in an aircraft engine under controlled test-stand conditions was defined which built on the knowledge gained during the studies on aviation particle emissions at cruise. The project PartEmis was of high relevance also for the European aircraft engine industry and provided extensive new knowledge on particle emissions from aircraft engines. Particularly the connection of particle chemical and physical properties with the potential activation of combustion particles for the formation of cloud droplets will promote the understanding of the aerosol-cloud interaction concerning combustion particles. Furthermore, a robust method for the measurement of aerosol light absorption and thus for black carbon was developed and evaluated. Multi-Angle Absorption Photometry turned out to be widely applicable for measurements in engine exhaust as well as in the remote background atmosphere on mountain sites. Results from a first 2–years data record on black carbon in the free troposphere over central Europe were used in combination with the determined particle emission factors for aircraft engines for estimating the black carbon load of the free troposphere and for assessing the climate impact of particle emissions from aviation. The estimated magnitude of the expected aerosol radiative forcing is in close agreement with recent results from the European project TRADEOFF which represents today's state of knowledge on the subject of aviation radiative forcing.

Zusammenfassung

Partikelemissionen von Flugzeugen in Reiseflughöhe, deren physikalische und chemische Eigenschaften and potentielle Auswirkungen auf die Atmosphäre und das Klima der Erde bilden ein reichhaltiges und komplexes Forschungsgebiet. Die Bedeutung der Partikelemissionen für das globale Klimasystem wurde in den frühen 1990er Jahren erkannt und erfährt heute wegen einer möglichen Beeinflussung des Lebenszyklus hoher Eiswolken eine steigende Aufmerksamkeit. Das Verständnis der Wirkungsmechanismen der von Flugzeugen ausgestoßenen Partikeln auf die Atmosphäre und auf das Klima erfordert wissenschaftliche Arbeiten auf den Gebieten der Partikelbildung in Gasturbinen, der Partikelprozessierung in einer chemisch reaktiven Abgasfahne und in der Atmosphäre, sowie auf dem Gebiet der grundlegenden Charakterisierung des Aerosols der oberen Troposphäre, das letztlich die Senke für die emittierten Partikel darstellt. Gleichzeitig müssen Messverfahren weiterentwickelt werden, um als wichtig identifizierte Aerosolparameter besser erfassen zu können. Die hier vorgestellten experimentellen Arbeiten nähern sich dem Thema von allen erforderlichen Richtungen an: Die physikalischen und chemischen Eigenschaften der emittierten Partikel wurden unter Reiseflugbedingungen und bei Bodentests untersucht. Die Quantifizierung der Emissionen unterschiedlicher Flugzeugtypen führte zur Validierung eines mittleren Emissionsindex für schwarzen Kohlenstoff, der heute in vielen Arbeiten zur Berechnung der Partikelemissionen des Luftverkehrs in Klimamodellen und Wirkungsstudien Verwendung findet. Die Ergebnisse aus den vielfältigen experimentellen Arbeiten trugen wesentlich zur Beurteilung der Klimawirksamkeit des Luftverkehrs an der Wende zum 21. Jahrhundert bei. Ein europäisches Forschungsprogramm zur Untersuchung der Partikelbildung und Prozessierung in Gasturbinen unter kontrollierten Prüfstandsbedingungen fußte im Wesentlichen auf den zuvor erzielten Ergebnissen aus den Studien zur Partikelemission aus Flugzeugen in Reiseflughöhe. Das Projekt PartEmis hatte auch für die europäische Luftfahrtindustrie eine große Bedeutung und lieferte umfangreiches neues Wissen über dieses Gebiet. Insbesondere die Verknüpfung der chemischen und physikalischen Eigenschaften der Partikel mit ihrer Fähigkeit, Wolkentropfen zu bilden wird das Verständnis der Aerosol-Wolken Wechselwirkung für Verbrennungspartikel befördern. Darüber hinaus wurde eine einfache Methode zur Messung der Lichtabsorption durch Partikel und damit indirekt zur Messung des schwarzen Kohlenstoffs entwickelt und validiert. Es stellte sich heraus, dass die Mehrwinkel –Absorptionsphotometrie eine breit anwendbare Methode ist, die sowohl bei Messungen im Abgas von Gasturbinen als auch in der Hintergrundatmosphäre auf einer Bergstation eingesetzt werden kann. Erste Resultate einer sich über zwei Jahre erstreckenden Datenreihe des schwarzen Kohlenstoffs in der freien Troposphäre über Mitteleuropa wurden zusammen mit den Ergebnissen der Emissionsstudien genutzt, um die Massenkonzentration des schwarzen Kohlenstoffs in der oberen Atmosphäre und den möglichen Klimaeffekt zusätzlich emittierter Kohlenstoffpartikel aus dem Luftverkehr abzuschätzen. Die ermittelte Größenordnung des erwarteten aerosolbedingten Strahlungsantriebs stimmt sehr gut mit jüngsten Ergebnissen der europäischen Studie TRADEOFF überein, die den aktuellen Stand des Wissens zu diesem Themenkomplex repräsentiert.

Content

1 Introduction

The investigation of the atmospheric and climate impact of particulate emissions from aviation requires studies on the formation conditions for particulate pollutants in the aircraft engine as well as in the engine plume after its release into the atmosphere. The physical and chemical properties of the emitted particles have to be known, because they determine their potential role in atmospheric chemistry, cloud formation and aerosol-climate-interaction. These particle properties have to be studied under ground-test conditions as well as under real cruise conditions. The latter type of experiment requires challenging and extensive aircraft-borne measurements. Appropriate measure-ment methods have to be developed which make the important aerosol properties accessible. As a final pre-requisite, all assessments of the impact of the particle emissions from aviation require high-level knowledge on the properties of the aerosol of the upper free troposphere and lowermost stratosphere and of the respective natural variability. This knowledge must be available in particular for 9 to 13 km altitude where the largest fraction of intercontinental air transport is concentrated. Without the knowledge on the aerosol of the background atmosphere, no conclusion can be drawn on the potential climate effects of particles which are released by aviation into the pre-existing background aerosol.

The publications and the related new material discussed in this work cover all the addressed research topics. After a brief overview on emissions from aviation in general and on particle effects on climate in the Introduction, the publications and the presentation of new material are organised in seven sections. The content of each section and the related publications are summarised briefly for guiding the reader through the manuscript.

Section 2: *Particle emissions at cruise altitude*

The properties of particles in the exhaust plume of civil aircraft are studied in terms of particle type, particle number density and particle size. Particular emphasis is put on the influence of the fuel sulphur content on the properties of the particles in the aircraft engine exhaust plume.

Included publications:

[1] Petzold, A., R. Busen, F.P. Schröder, R. Baumann, M. Kuhn, J. Ström, D.E. Hagen, P.D. Whitefield, D. Baumgardner, F. Arnold, S. Borrmann, and U. Schumann (1997) Near field

measurements on contrail properties from fuels with different sulfur content, *Journal of Geophysical Research, 102*, 29,867-29,880.

[2] Petzold, A., J. Ström, S. Ohlsson and F.P. Schröder (1998) Elemental composition and morphology of ice crystal residual particles in cirrus clouds and contrails, *Atmospheric Research, 49,* 21-34.

Section 3: *Microphysical properties and chemical composition of aircraft engine exhaust particles*

The chemical compositions of the sulphur containing species and in particular of the carbonaceous fraction of the exhaust aerosol are determined from filter samples. The results from the chemical analytical studies are related to the particle microphysical properties determined from ground and in-flight experiments.

Included publications:

[3] Petzold, A. and F.P. Schröder (1998) Jet engine exhaust aerosol characterisation, *Aerosol Science and Technology, 28*, 62-76.

[4] Petzold, A. and A. Döpelheuer (1998) Re-examination of black carbon mass emission indices of a jet engine, *Aerosol Science and Technology, 29,* 355-356.

[5] Petzold, A., J. Ström, F.P. Schröder, and B. Kärcher (1999) Carbonaceous aerosol in jet exhaust: Emission characteristics and implications for heterogeneous reactions, *Atmospheric Environment*, *33,* 2689-2698.

Section 4: *Quantification and prediction of engine emission factors for particulate black carbon*

The emission of carbonaceous particles is quantified for various aircraft during in-flight studies. The obtained results are used for the validation of an empirical prediction method for the emission of carbonaceous matter, and for the calculation of a aircraft fleet averaged particle emission factor.

Included publications:

[6] Petzold, A., A. Döpelheuer, C.A. Brock, and F.P. Schröder (1999) In situ observations and model calculations of black carbon emission by aircraft at cruise altitude, *Journal of Geophysical Research*, *104*, 22171-22181.

Section 5: *A new measurement method for aerosol light absorption and black carbon*

The new simple and robust method Multi-Angle Absorption Photometry MAAP for the measurement of aerosol light absorption and the closely related black carbon is presented. Results from an extensive instrument evaluation study, the Reno Aerosol Optics Study 2002 are discussed.

Included publications:

[7] Petzold, A., and M. Schönlinner (2004) Multi-angle absorption photometry - a new method for the measurement of aerosol light absorption and atmospheric black carbon, *Journal of Aerosol Science*, *35,* 421-441.

[8] Petzold, A., H. Schloesser, P.J. Sheridan, W.P. Arnott, J.A. Ogren, and A. Virkkula (2004) Evaluation of multi-angle absorption photometry for measuring aerosol light absorption, *Aerosol Science and Technology*, *39*, 40-51, 2005.

Section 6: *Formation conditions, physical and chemical properties, and potential interaction of aircraft engine exhaust particles with atmospheric water vapour; the European project PartEmis*

The effects of engine combustor operation conditions, fuels sulphur content and engine turbine section on the emission properties for particulate matter and gaseous precursors for particle formation are extensively studied in a unique European experiment. An overview over the results with particular emphasis on particle microphysical properties and combustion particles is given.

Included publications:

[9] Petzold , A., et al. (2003) Properties of jet engine combustor particles during the PartEmis experiment. Microphysical and chemical properties. *Geophysical Research Letters, 30***,** 1719, doi:10.1029/2003GL017283.

[10] Petzold, A., et al. (2005) Particle emissions from aircraft engines – A survey of the European project PartEmis,
Meteorologische Zeitschrift, *14*, 465-476.

Section 7: *The effects of hydrocarbon and sulphur-containing compounds on the CCN activation of combustion particles*

New material from the PartEmis experiment is presented which builds the bridge from particle emission to atmospheric effects by investigating the link from particle physical and chemical properties to the potential for cloud condensation nuclei activation. Part of the material was presented by the author as an invited lecture on the International Workshop on „Ice, Soot and Aviation: What Impact on the Environment?“, organised by CNES in La Londe (France), 10. – 14. Mai 2004 and on the 8th International Conference on Carbonaceous Particles in the Atmosphere, held in Vienna, 14 – 16 October 2004. The entire Section 7 was recently published in *Atmospheric Chemistry and Physics*.

Petzold, A., M. Gysel, X. Vancassel, R. Hitzenberger, H. Puxbaum, S. Vrochticky, E. Weingartner, U. Baltensperger , and P. Mirabel (2005) On the effects of organic matter and sulphur-containing compounds on the CCN activation of combustion particles, *Atmos. Chem. Phys., 5*, 3187–3203, 2005.

Section 8: *Assessment of the atmospheric impact of particle emissions from aviation*

The results from the presented studies on particle emission properties are combined with atmospheric observations of the aerosol of the upper free troposphere and lowermost stratosphere. The atmospheric observations are used to estimate the loading of the upper free troposphere with combustion particles which are so far not accessible to a direct measurement. The gained estimated magnitudes for the climate effects of aviation-related particle emissions are discussed and compared to the recent European TRADEOFF study which is the latest international modelling study on the expected radiative forcing of climate caused by aviation. The atmospheric observations used for this assessment originate from the first long-term measurement of atmospheric black carbon on the European high-alpine research station Jungfraujoch in Switzerland using a MAAP, and from studies of the vertical variability of the atmospheric aerosol, conducted under the lead of the author.

1.1 Emissions from Aviation

Blue sky covered by a large number of condensation trails (see Figure 1.1) impressively illustrates a likely impact of growing air transportation on the global climate, caused by its emissions released by aviation into the atmosphere. Of what nature are the compounds emitted by aircraft at high altitudes and what might be their effects?

Figure 1.1. *Aircraft exhaust plume, young contrail and aged contrails spreading over the sky (EC, 2001b).*

The gaseous and particulate emissions from aircraft engines are products of an incomplete combustion process. Burning hydrocarbon fuel with natural sulphur impurities, using air as an oxidant, results in the emission of water vapour H_2O and carbon dioxide CO_2 as the major products, and nitrogen oxides NO_x, sulphur oxides SO_2 and H_2SO_4, carbon monoxide CO, and particulate matter as minor exhaust constituents. The atmospheric effects of these exhaust products are manifold and partially connected. This work focuses on the properties of the emitted particles, their formation conditions and the expected effects on the atmosphere.

Among the exhaust products, the particulate matter forms a complex sub-set. During the combustion process of hydrocarbon fuel in the flame, carbonaceous particles are forming in zones of a high ratio of fuel to oxygen. The formation of combustion particles is a well-known phenomenon of combustion processes at fuel-rich conditions (Glassman, 1996), i.e., when there is not enough oxygen available for a complete combustion of the fuel. The combustion particles are in general composed of carbonaceous material, which is divided into

elemental and organic carbon, EC and OC, respectively. The separation follows mainly from the applied chemical analytical methods and is still a matter of scientific debate (see e.g., Schmid et al., 2001). The light absorbing component of the carbonaceous matter is referred to as black carbon BC. Without going into details, BC ≅ EC.

In general terms, the elemental or black carbon is thermally stable up to approximately 600 K, not extractable by organic solvents and chemically inert (Goldberg, 1985). The specific abundance of OC and EC in a combustion particle depends on the details of the combustion process. The entire group of gas–phase hydrocarbon compounds being present in the exhaust gas are designated separately as HC without further specification.

Additional to the combustion particles, another class of particles may form from gaseous precursors emitted from the engine, which reach supersaturation in the expanding and cooling plume. In the case of emissions from an aircraft engine, the condensable gaseous compound of highest abundance is gaseous sulphuric acid H_2SO_4 which forms by oxidation from the sulphur impurities in the fuel. In combination with the water being present in the exhaust plume, H_2SO4 and H_2O can form new particles by nucleation and condensation growth. Contrary to the combustion particles, these nucleated particles are thermally unstable at higher temperatures above approximately 400 K. Because of this feature, they are classified as being volatile, while the thermally stable combustion particles are classified as being nonvolatile. Figure 1.2 illustrates schematically the particles emitted from an aircraft engine.

1.2 Particle Effects on Climate

Before entering the discussion of potential effects of particulate emissions from aviation on the global climate, a brief excursion summarises the role of aerosol particles in the global climate system on a very general level.

Inspired by Twomey's (1977) publication on the effect of aerosols on cloud radiative properties and thus on climate, Charlson and co-workers published their pioneering work on the role of airborne aerosol particles in the global climate system (Charlson et al., 1989, 1990, 1991). Of key interest was the potential of airborne particles for scattering incoming solar radiation back into space. The follow-on paper by Penner et al. (1992) extended this discussion by including the aspect of light absorption by aerosol particles on the atmospheric

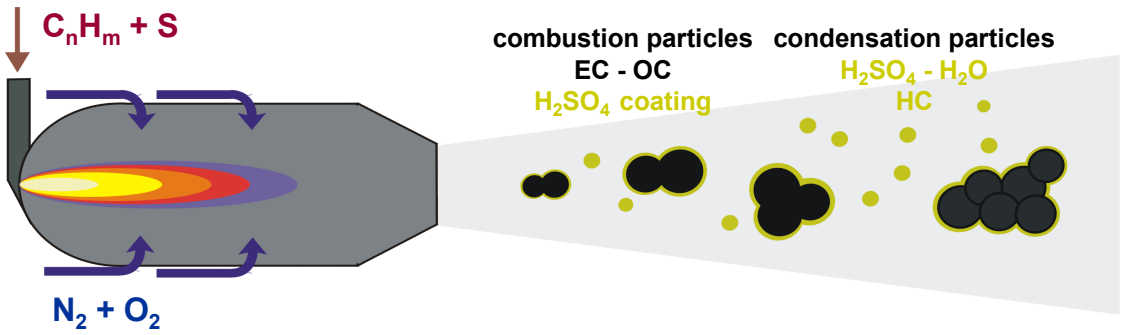

Figure 1.2. *Schematic representation of particles emitted from an aircraft engine.*

radiation balance. An international conference on "Aerosol Forcing of Climate", held 1994 in Berlin (Charlson and Heintzenberg, 1995) reviewed the current knowledge on this subject. A contemporary theoretical treatment of the processes of light scattering and light absorption by small particles is given in the textbook of Bohren and Huffman (1983).

As is schematically shown in Figure 1.3, the atmospheric aerosol can interact with the solar and infrared radiation in the Earth-atmosphere system in different ways. Focusing first on the solar radiation spectrum (0.25 μm ≤ λ ≤ 4 μm), two categories of effects are known: The *direct effect* of the atmospheric aerosol on climate is based on the interaction of aerosol particles with the incoming solar radiation. Electro-magnetic radiation can either be scattered or absorbed by particles. Elastic light scattering results in the modification of the direction of propagation of radiation without affecting its wavelength (see yellow arrows in the left part of Figure 1.3). Inelastic light scattering processes like Raman scattering which also modify the wavelength of radiation will be neglected in this discussion.

One result of scattering of solar radiation by aerosol particles is an increase of the planetary albedo α_P, which characterises the fraction of incoming solar radiation S_0 scattered back into space from the Earth-atmosphere system. The planetary albedo α_P of a considered Earth-atmosphere system is determined to a large extent by the properties of the underlying surface. Figure 1.3 contains exemplary the two most important cases of a water surface and a land surface. The α_P values refer to the maximum of the solar spectrum at a wavelength of $\lambda = 550$ nm.

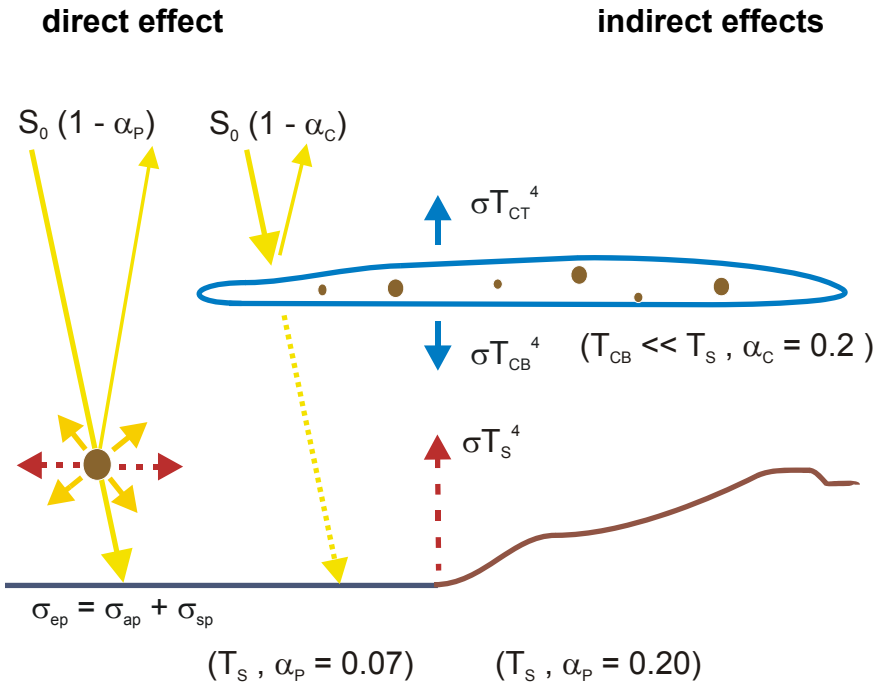

Figure 1.3. *Basic impact processes of atmospheric aerosol particles on the global climate; for explanation of the parameters see the discussion in the text.*

An increase in the fraction of back scattered solar radiation $S_0 \times \alpha_P$ reduces the radiation energy deposited in the Earth-atmosphere system $S_0 \times (1 - \alpha_P)$ which is available for heating the system. Hence, an increased loading of the atmosphere by light scattering particles results in a net cooling of the entire system compared to the reference case without particle loading. This effect is also referred to as negative radiative forcing, because the additional loading of the atmosphere by light scattering particles increases the flux of radiative energy from Earth into space, i.e., it extracts energy from the system compared to the reference case without particle loading.

Light absorption by particles, however, transforms the radiation energy into heat which can then be transferred from the particles to the embedding atmosphere (see red arrows in the left part of Figure 1.3). Depending on the specific properties of the light-absorbing particles, a higher atmospheric loading tends to increase the net radiation energy deposited in the Earth-atmosphere system compared to the reference case without higher loading of light absorbing aerosol. Opposite to a higher loading of the atmosphere with light scattering particles, an increased loading with light absorbing particles may cause a positive radiative forcing.

Table 1.1: Effects of main aircraft engine exhaust constituents on the global climate

Exhaust constituent	Impact on Atmosphere and climate
CO_2	*Troposphere and stratosphere* greenhouse gas ⇒ positive radiative forcing
H_2O	*Troposphere* greenhouse gas ⇒ positive radiative forcing contrail formation ⇒ positive radiative forcing *Stratosphere* Greenhouse gas ⇒ positive radiative forcing formation of polar stratospheric clouds (PSC) ⇒ ozone destruction ⇒ increasing UV-B radiation modification of O_3 chemistry ⇒ ozone destruction ⇒ increasing UV-B radiation
NO_x	*Troposphere* Ozone formation in the upper free troposphere Greenhouse gas ⇒ positive radiative forcing, reduced UV-B radiaton CH_4 destruction ⇒ negative radiative forcing *Stratosphere* O_3 formation below 18 – 20 km ⇒ reduced UV-B radiation O_3 destruction above 18 – 20 km ⇒ increased UV-B radiation increasing PSC formation ⇒ O_3 destruction, increasing UV-B radiation
SO_x , H_2SO_4 , sulphate particles	*Troposphere* increasing atmospheric concentration of sulphate particles ⇒ negative radiative forcing contrail formation ⇒ positive radiative forcing modification of O_3 chemistry by heterogeneous processes on particle surfaces *Stratosphere* Modification of O_3 chemistry by heterogeneous processes on particle surfaces
Combustion particles	*Troposphere* increasing atmospheric concentration of light-absorbing carbonaceous particles ⇒ positive radiative forcing contrail formation ⇒ positive radiative forcing modification of cirrus occurrence and life cycle ⇒ positive radiative forcing *Stratosphere* increasing atmospheric concentration of light-absorbing carbonaceous particles ⇒ positive radiative forcing
Contrails	*Troposphere* reducing the emission of infrared radiation from the Earth surface into space, increasing the solar radiation scattered back into space ⇒ positive radiative forcing

The *indirect effects* result from the interaction of aerosol particles with the water vapour contained in the atmosphere. Depending on their chemistry and size, particles may act very efficiently as nuclei for the formation of water droplets and thus of clouds. Clouds, however, can scatter solar radiation even more efficiently than aerosol particles. The light scattering properties of clouds in turn depend directly on the number of cloud droplets and on their size. Increasing the number of aerosol particles in an air mass increases also the number of potential cloud condensation nuclei CCN. Clouds forming in a polluted air mass thus tend to contain more but smaller cloud droplets. As a consequence, they may scatter solar radiation more efficiently because of the larger number of light scattering centres (Twomey, 1977). Another consequence of the smaller droplet size is the reduced formation of precipitation in polluted clouds.

In a cloudy atmosphere, the planetary albedo α_P is replaced by the reflectivity or cloud albedo, respectively, α_C, which depends on the cloud microphysical properties like droplet size and number concentration, cloud thickness, and droplet shape in case of ice-containing mixed-phase clouds and ice clouds or cirrus, respectively. Over a "dark" surface, there is $\alpha_C > \alpha_P$, while over "bright" surfaces $\alpha_C \leq \alpha_P$. Thus, clouds can have a net cooling effect or a net warming effect, depending on the surface, over which they are occurring. Clouds do not only interact with the solar radiation but also with infrared radiation in the terrestrial radiation band ($\lambda > 4$ μm). The emission of infrared radiation from the surface of the Earth follows the Stefan-Boltzmann law and is proportional to the surface temperature T_S, according to $\propto \sigma (T_S)^4$ with σ being the Stefan-Boltzmann constant. Correspondingly, the emission of infrared radiation from clouds into space depends on the temperature at the cloud top T_{CT}, i.e., $\propto \sigma (T_{CT})^4$, and the re-emission of infrared radiation to the Earth surface depends on the temperature at the cloud base T_{CB}. Since water and ice clouds absorb radiation in the terrestrial spectral range almost perfectly, they have a strong impact on the atmospheric radiation balance.

Exemplary effects can be summarised in a simplified manner:

- bright clouds at low altitude over water with $T_{CT} \cong T_S$ have almost no impact on the atmospheric budget of infrared radiation, but increase the albedo because $\alpha_C > \alpha_P$: net cooling effect;

- bright clouds at low altitude over land with $T_{CT} \cong T_S$ have almost no impact on the atmospheric budget of infrared radiation, the impact on the albedo depends strongly on the surface: net cooling or heating effect;
- thin ice clouds at high altitude with $T_{CT} << T_S$ reduce the infrared emission from the Earth's surface into space, the albedo effect depends strongly on could thickness: net heating effect.

The above schematic discussion of the effects of clouds and particles on the planetary albedo and on the infrared atmospheric radiation budget follows the excellent presentation of this subject in the textbook by Hartmann (1994). The treatment of the subject is far from being adequate, but is expected to give a sufficient overview over this highly complex area. The entire subject of aerosol – climate interaction is widely discussed in the latest report of the International Panel on Climate Change (IPCC, 2001), including the current state of knowledge.

Table 1.1 gives an overview over the most important gaseous and particulate exhaust products emitted from aircraft engines and their impact on the troposphere and the stratosphere. Since one key component of aircraft exhaust particles is the solar radiation absorbing black carbon which also participates in the formation of contrails, it is obvious that a possible impact of the black carbon emissions from aviation on the radiative properties of the atmosphere and thus on the global climate needs to be investigated.

1.3 The Atmospheric Effects of Aviation – a Historical Perspective

Research on the global environmental impact of growing aviation was initiated in the early 1970's by the expected effects of a globally operating supersonic fleet which was assumed to cruise mainly in the stratosphere (Crutzen, 1971; Johnston, 1971). First priority was given to the investigation of the impact of nitrogen oxide emissions and emissions of carbon monoxide and hydrocarbons on stratospheric ozone.

An early indication for aviation being a strong source for particulate matter in the lower stratosphere originated from balloon-borne observations of a particle layer in the lower stratosphere (Hoffmann and Rosen, 1978). Measurements in the aged exhaust plume of aircraft operating in the stratosphere like the high-altitude research aircraft ER-2 of NASA

Table 1.2: Historical development of the research on the impact of aviation emissions on regional and global climate

Period	Subject of research
since 1960	Impact of noise emissions and emissions of combustion particles (smoke) on the close environment of airports
since 1970	Impact of NO_X emissions of a supersonic fleet operating in the stratosphere on the stratospheric ozone layer
since 1990	Impact of the emissions of the sub-sonic aviation operating in the upper free troposphere and lowermost stratosphere on the global atmosphere: - formation conditions, lifetime and radiative impact of contrails - impact of NO_X emissions on the ozone chemistry of the upper troposphere and lowermost stratosphere - modification of the background aerosol of the upper free troposphere and lowermost stratosphere and expected climate impact - occurrence, properties and life cycle of aviation-induced cirrus clouds, so called contrail-cirrus, and expected climate impact
since 2000	Impact of particulate emissions of aviation on - occurrence, properties and life cycle of natural cirrus clouds and resulting impact on the atmospheric radiation budget - an indirect effect of aviation on natural cirrus - airport air quality with special emphasis on the emissions of volatile and nonvolatile ultrafine particles

(Fahey et al., 1995a) and the Concorde supersonic aircraft (Fahey et al., 1995b) confirmed the high concentration of particles in the plume of those aircraft in the stratosphere. At this time, however, virtually nothing was known about the characteristics of particles emitted from an aircraft engine in the upper troposphere, as well as about the emission properties of aircraft engines at cruise conditions.

Another even stronger key driver for international research programmes on the environmental impact of aviation was the predicted growth rate of up to 5% per year for the air transportation sector. Thus, in the late 1980s, the effects of gaseous emissions from aviation became again a topic of large interest (Brühl and Crutzen, 1988). In 1990, an international colloquium on "Air-Traffic and the Environment" organised by DLR provided an overview on the current state of knowledge on the impact of global air traffic on the atmosphere (Schumann, 1990).

As the globally operating aircraft fleet was identified as a major source for gaseous pollutants in the most frequently used and very sensitive altitude band of 9 – 13 km, extensive research programmes on the expected impact of subsonic aviation on the chemical, physical and

radiative properties of the upper free troposphere and lowermost stratosphere were launched both in Europe and in the USA. An overview over the historical development of this research area is compiled in Table 1.2.

Besides the effect of gaseous emissions from aviation on the ozone chemistry in the upper free troposphere and lowermost stratosphere, another well known phenomenon of aviation became of growing importance – the condensation trails or contrails which form from emitted water vapour in the cooling exhaust plume behind a cruising aircraft. Although jet condensation trails and their formation conditions were known since the 1940s (see Schumann (1996) for an overview), the expected effects on the global climate made them an important subject of research not until the 1990s. In the context of contrail formation, the particle emissions of aviation during cruise appeared for the first time on the scientific agenda of the atmospheric research community (Pitchford et al., 1991).

The report of the Intergovernmental Panel on Climate Change IPCC of the World Meteorological Organisation WMO on the impact of aviation on the atmosphere (IPCC, 1999), the EU Report on European Research in the Stratosphere (EC, 2001a), and the European Workshop on Aviation, Aerosol, Contrails and Cirrus Clouds in 2000 (2001b) summarised the state of knowledge on the expected climate effects and possible mitigation strategies. The European Conference on Aviation, Atmosphere and Climate in 2004 put a particular emphasis on the interaction of aviation with cirrus clouds and defined the scientific key objectives for the upcoming research on the climate effects of aviation. The selected publications [1] – [6] and [9] – [10], which are discussed in detail in the corresponding sections, made essential contributions to these reports and workshops.

1.4 The Atmospheric Effects of Particle Emissions from Aviation

At the beginning of the international research activities on the particle emissions from aviation and expected atmospheric effects, the level of knowledge on this subject was very poor. A number of pressing questions was raised by the scientific community and tackled by dedicated research activities. In the following, the key questions and the contributions of the author are highlighted.

Figure 1.4. *View from the cockpit of the research aircraft Falcon to the source aircraft B737-300 of Lufthansa during the experiment SULFUR VI (Schröder et al., 2000).*

(i) What are the characteristic physical and chemical properties of particles emitted from aviation at cruise conditions?

The first systematic investigation of particles emitted from subsonic aircraft at cruise was conducted under the lead of DLR Institute of Atmospheric Physics within the framework of the SULFUR experiments (Schumann et al., 1996; [1]; [5]; for an overview of the entire set of experiments, see Schumann et al., 2002) and the POLINAT study in the North Atlantic flight corridor (Hagen et al., 1996). Particularly as part of the SULFUR experiments, unique measurements were conducted with the instrumented research aircraft Falcon of DLR in the plume of source passenger aircraft. The author was responsible for the entire analysis of these experimental flights. Figure 1.4 illustrates the closest approach of less than 50 m flight distance ever achieved for the research aircraft towards the source aircraft.

The chemical composition of aircraft exhaust particles was studied first by Petzold and Schröder ([3]; [4]). First results on the chemical composition of particles enclosed in contrail ice crystals were reported simultaneously by Petzold et al. [2] and Twohey and Gandrud. (1998).

(ii) What are reliable particle emission factors for aviation, to be used for emission inventories and climate modelling?

Particle emission factors for various aircraft-engine combinations were reported from several field experiments by Schumann et al. (1996), by Petzold et al. ([1]; [4]; [5]), and by Anderson et al. (1998a). The experimental quantification of emission factors of several aircraft engines for combustion particles by Petzold et al. [6], including the validation of an empirical prediction model for emission properties of aircraft engines at cruise provided finally the required values for emission inventories and model studies.

(iii) What is the nature of ultrafine particles observed in aircraft plumes at cruise altitude?

Parallel to the investigation of the emission of carbonaceous combustion particles, extensive efforts were undertaken on the observation and modelling of particles which nucleate in the cooling exhaust plume from gaseous precursors, i.e., mainly from gaseous sulphuric acid H_2SO_4. Key results were published by Schumann et al. (1996), Anderson et al. (1998b), Schröder et al. (1998), Brock et al. (2000) and Schröder et al. (2000), containing essential contributions by the author.

(iv) How do particles emitted from aircraft engines influence the contrail formation process?

Since the initial investigation of the particle emissions from aviation where driven by the expected impact on the forming contrail, modelling studies were conducted for improving the understanding of the role of the different particle types. Already at an early state of research, it turned out from modelling results, that contrail formation can be explained only from an interaction of the emitted carbonaceous combustion particles and the nucleating sulphuric acid – water particles.

Schumann and Busen (1995) using pioneering observations, and Miake-Lye and co-workers (1994) as well as Kärcher (1996) and Kärcher and co-workers (1995, 1996) using modelling studies, concluded that the basic process required for the explanation of the observations is a coating of the combustion particles by sulphuric acid which activates them for the formation of water droplets and ice crystals during the contrail formation. The observations of particle and contrail microphysical properties during the SULFUR studies ([1]; [2]; Kuhn et al. (1998)) provided the observational basis for the verification of the models by Kärcher et al. (1998).

(v) Which aerosol properties determine the atmospheric effects of particle emissions from aviation – and how are they measured?

The results from the model studies on aerosol-contrail interaction and first indications that particle emitted from aviation might influence the formation conditions and properties of cirrus clouds (Boucher, 1999) raised the question of how particle emissions from aviation should be characterised with respect to expected climate effects. So far, only the "smoke number", which refers to the visibility of the exhaust plume, was used for the regulation of particle emissions from aircraft engines. The discussion on this subject was started by the International Civil Aviation Organisation ICAO, a body of the United Nations. Technical support was requested by ICAO from the E-31 Particulate Subcommittee of the International Society of Automotive Engineers SAE.

In the recent Aerospace Information Report (AIR 5982) which was prepared under the responsibility of the E-31 Particulate Subcommittee, all methods are reviewed, which are available for particle measurements in the exhaust of aircraft engines during the engine certification procedure as determined by ICAO. The author contributed the section on the measurement of particle mass.

Combustion particles composed of black and organic carbon are the major fraction of particles emitted by aviation. Aviation is considered the major intra-atmospheric source of light-absorbing nonvolatile combustion particles (IPCC, 1999; EC 2001a). The problem of measuring particulate black carbon is, however, still not sufficiently solved. Considerable and substantial progress on the subject of measuring black carbon particles by an optical method was achieved by the author. Starting from the investigation of deficiencies of available routine methods (Petzold and Niessner, 1995a; Petzold et al., 1997), the new method of multi-angle absorption photometry MAAP (Petzold et al., 2002a; [7]) was developed and successfully evaluated [8].

(vi) Do particles emitted from aviation influence clouds?

Observations of long-living contrails which transform into a cirrus cloud (see e.g., Schröder et al., 2000) and the analysis of satellite data (Boucher, 1999) which reported a possible correlation between air traffic and cirrus cloud occurrence, indicated a possible interaction path from aviation particle emissions to cirrus clouds.

In year 2000, one key activity in this area of the atmospheric research community was the European experiment on Interhemispheric Differences in Clouds from Anthropogenic Emissions INCA, which was focussing on the differences in cloud properties at midlatitudes in the polluted atmosphere of the northern hemisphere and the clean atmosphere of the southern hemisphere. Although the aerosol loading of the southern hemispheric upper troposphere at midlatitudes was three times less than in the corresponding part of the northern hemisphere (Minikin et al., 2003), the differences in cloud properties where only of minor significance (Gayet et al., 2002, 2004). The author contributed significantly to these investigations.

Parallel to the INCA study, the European project PartEmis ("Measurement and prediction of emissions of aerosols and gaseous precursors from gas turbine engines") focused on the investigation of the effect of engine operation parameters and fuel composition on the properties of the emitted particles. Within PartEmis internationally leading research under the experimental co-ordination of the author was performed in this field. An overview over the technological aspects of this challenging experiment is given by Wilson et al. (2004). Petzold et al. [10] summarises the scientific knowledge gained from PartEmis. Besides experimental coordination, the author contributed the investigation of the aerosol microphysical properties to the project. The key findings on particle exhaust properties are presented by Petzold et al. [9]. Possible interactions with clouds by particle activation are discussed by Gysel et al. (2003), Hitzenberger et al. (2003), Vancassel et al. (2003), and Nyeki et al. (2004).

(vii) The future: Is there an indirect effect of aviation on cirrus clouds?

Since the aerosol impact on the cirrus clouds turned out to be far from being fully understood and quantified, it is expected that the research on the environmental impact of aviation will even more focus on the question, whether there is an indirect effect of aviation on cirrus clouds, i.e., do particles emitted from aviation have an influence on the cirrus occurrence, lifetime and properties? This topic is a core subject of the European project QUANTIFY ("Quantifying the Climate Impact of Global and European Transport Systems") co-ordinated by DLR Institute of Atmospheric Physics where the authors participates in several sub-projects.

The assessment of the impact of particle emissions from aviation on the aerosol of the upper troposphere and lowermost stratosphere and thus on cirrus clouds forming in this part of the atmosphere still suffers from a lack of data. To overcome this situation, a European consortium has formed which is working on the “Integration of routine aircraft measurements into a global observing system”. Within the project IAGOS, the author is responsible for the development of particle measurement instrumentation which can be routinely operated on board of civil aircraft.

Only the synopsis of characterisation studies on particle emissions from aviation at cruise altitude, of studies of particle properties under controlled conditions in engine test stands, and of the investigation of the variability of the atmospheric background aerosol permits a first-order assessment of the possible effects of particle emissions from aviation on the global climate from an observational perspective. Any modelling study has to rely on those observations. Furthermore, the development of appropriate measurement technologies has to close gaps in the observation capabilities. Any in-depth assessment of the climate effects of aviation will build on those high-quality observations, and requires them as an essential pre-requisite.

In the following sections, ten publications in peer-reviewed journals are discussed in their respective scientific context. The publications provide contributions to all of the named elements – source characterisations under cruise conditions, controlled test-rig studies, measurement technology development, and atmospheric observations.

Section 2 deals with particulate emissions from aviation under cruise conditions. First, a characterisation of the particles observed in aircraft exhaust plumes at cruise altitude is presented in terms of number, volatility, and size [1]. The effect of the fuel sulphur content on the properties of the emitted particles in the exhaust plume is discussed [1]. Particles being enclosed in contrail ice particles are classified in terms of physical and chemical properties, including the identification of carbonaceous particles in the residuals from evaporated contrail ice crystals [2].

In Section 3, the chemical composition of exhaust particles is investigated from filter samples collected during engine ground tests [3]. The emission indices for carbonaceous matter and

sulphate-containing compounds are determined for various engine operation conditions and fuel sulphur contents [4]. Particular emphasis is put on the properties of black carbon particles emitted from an aircraft at ground and during cruise [5].

Section 4 focuses on the quantification of the emission index of several civil aircraft concerning carbonaceous particulate matter [6]. An empirical correlation method for the prediction of black carbon mass emission indices from engine operation conditions is validated. The model is applied to the calculation of a fleet-averaged black carbon mass emission index which is used in emission data bases and in global climate models.

Section 5 discusses the development of a new simple and robust optical method for the determination of the aerosol absorption coefficient and thus for the black carbon mass concentration. The section starts with a review of deficits of conventional methods (Petzold et al., 1997) and describes then the new method of multi-angle absorption photometry [7]. Results from an intensive method evaluation experiment are presented [8].

Section 6 deals with the investigations of the effects of fuels sulphur content and engine operation conditions on the physical and chemical properties of the emitted particles, as obtained during the experiment PartEmis [9; 10]. Particle properties under investigation cover the formation of new particles from gaseous precursors as well as the activation of particles for forming cloud condensation nuclei. First successful applications of the new measurement method for black carbon to measurements in the exhaust gas of an aircraft engine are presented.

Section 7 presents new material on the key question of how chemical and physical properties of combustion particles influence the activation for cloud condensation nuclei. This section treats one of the key issues of the entire PartEmis experiment.

Section 8 concludes the discussion of integrated publications with an assessment of expected atmospheric effects of aviation-related particle emissions in the upper free troposphere and lowermost stratosphere. The assessment applies particle emission properties determined under cruise conditions [6]. Observations of atmospheric background aerosol during the first long-term operation of the new aerosol absorption measurement method on the European high-

alpine research station Jungfraujoch in Switzerland as well as the vertical distribution of background aerosol properties measured during several field experiments in continental Europe under the author's participation are used for this assessment.

2 Particulate Emissions from Aviation at Cruise Conditions

This section discusses the properties of particles emitted from aircraft at cruise altitude. Particle microphysical properties like number concentration and size are studied from observations during aircraft chasing experiments (see Fig. 1.4). The impact of the fuel sulphur content (FSC) on the formation of volatile particles via nucleation from the gas phase is investigated. The chemical composition of particles collected from evaporated contrail and cirrus ice crystals is analysed and discussed with respect to the role of exhaust particles in contrail formation.

In accordance with the nomenclature used in aerosol science, particles in the size range $D_p \leq 15$ nm are termed ultrafine condensation nuclei UCN or nucleation mode particles, respectively, particles with sizes 15 nm $\leq D_p \leq 100$ nm are referred to as Aitken mode particles, and particles with sizes 100 nm $\leq D_p \leq 1000$ nm constitute the accumulation mode of the aerosol.

2.1 Near-field Studies on Aerosol and Contrail Properties from Fuels with Different Sulphur Content [1]

The first paper within this section reports on the investigation of microphysical properties of aircraft engine exhaust aerosol and contrails in the near field of the emitting aircraft for fuels with different sulphur contents. The measurements were performed in the frame-work of the SULFUR experiments series. The instrumented research aircraft Falcon 20 was operated in the plume of the research aircraft ATTAS, both of DLR, and of an Airbus A310-300 of Lufthansa, using fuels with sulphur contents of 6 (low), 850 (standard) and 2700 mg kg^{-1} (high).

At flight distance 1800 m (plume age ≈ 10 s) to the ATTAS aircraft, maximum total number concentrations in the plume were 1.0 and 3.5 x 10^4 cm^{-3} for low and high sulphur fuel, respectively. Figure 2.1 shows two examples of plume encounters for high and low fuel sulphur content. The effect of the fuel sulphur on the number of detected particles is obvious. In Figure 2.2, the data are sorted according to the flight distance. Particle number concentrations increase because of the higher fuel sulphur content by a factor of 3 to 4. Although, the impact of the fuel sulphur on the emission of particles is significant, its influence is weak, because an increase in the fuel sulphur content by a factor of 450 translates into an increase in particle number concentration in the plume of only 3 – 4.

The ultrafine condensation nuclei mode UCN which is dominated by new particles nucleating from gaseous sulphuric acid contributed on the average 30% to the total aerosol when low sulphur fuel was burned, and 43%, when high sulphur fuel was burned. In the background aerosol outside the plume, this fraction was less than 10%.

The accumulation mode aerosol in the size range $D_p > 100$ nm which is expected to be constituted by large combustion particles, did not vary significantly from low sulphur fuel to

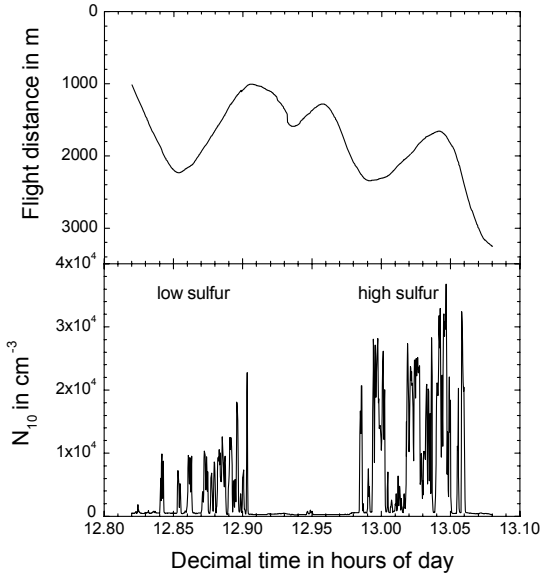

Figure 2.1. *Flight distance and number concentration of particles larger than 10 nm in diameter (N_{10}) for a plume measurement in the exhaust of the DLR ATTAS research aircraft.*

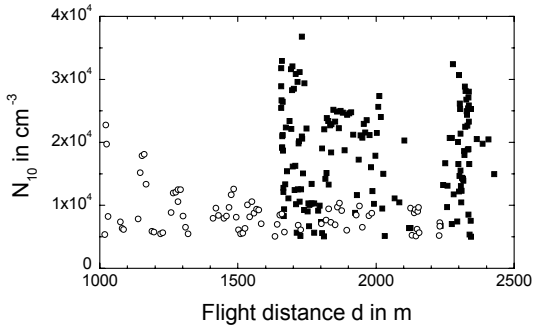

Figure 2.2. *Particle number concentration as a function of flight distance and fuel sulphur content in the plume of the DLR ATTAS research aircraft.*

high sulphur fuel. It ranged at about 3400 cm^{-3} for a plume age of approximately 2 s. It has to be mentioned, however, that combustion particles contribute significantly also to the sub-100 nm fraction of the aerosol. A distinction of sulphuric acid particles from combustion particles in the sub-100 nm range was not possible at this state of the experiments.

Using high sulphur fuel, the typical number concentrations of contrail particles were increased by about one third with respect to low sulphur fuel, while the effective diameter of the contrail particle size distribution was shifted from 1.8 μm to 1.5 μm at a fuel sulphur independent ice water content of 2 mg m^{-3}. Measurements at a distance < 400 m (plume age ≤ 2.5 s) behind a Lufthansa Airbus A310-300 yielded an accumulation mode number concentration of 5450 cm^{-3}. This high number concentration coincided with a high number concentration of small contrail particles ($N = 1380$ cm^{-3}, $D_e = 1.3$ μm). The differences in microphysical contrail properties between normal sulphur (850 mg kg^{-1}) and high sulphur (2700 mg kg^{-1}) fuel were below significance.

Major fuel sulphur induced differences occurred in the contrail particle phase at the plume age of approx. 10 s. Ice water content and mean surface concentration of the contrail remained almost unaffected by the fuel sulphur. The contrail particles were smaller in size and larger in number when high sulphur fuel was burned. The picture of contrail formation obtained from the measurements followed theoretical predictions: The contrail at a plume age of less than 2 s is dominated by heterogeneous freezing of activated engine exhaust particles which are expected to be mainly combustion particles. After 10 s of ageing, the number of contrail particles is increasing by a factor of 1.7 (low sulphur fuel) to 2.7 (high sulphur fuel) compared to the plume age of < 2 s. The enhanced formation of contrail particles in the high sulphur fuel case is assumed to be caused by additional homogeneous freezing of nucleated H_2SO_4-H_2O droplets. The homogeneous freezing process requires a much longer time scale than heterogeneous freezing and thus cannot be observed to full extent in the short distance measurements. Hence, the influence of the fresh exhaust aerosol on contrail properties seems to be restricted to the very young state of contrail development.

The most pronounced effect of the fuel sulphur was observed with respect to nucleated H_2SO_4-H_2O particles in the sub-20 nm size range. The fuel sulphur content showed almost no effect on the emitted large carbonaceous combustion particles. Part of the difference in

contrail particles between high and low sulphur fuel and between different aircraft were probably caused by different ambient conditions. However, the presented observations indicated a strong influence of engine properties on the emissions of particles and of wake properties on the forming contrails.

Comparisons of the measurements behind an Airbus A310-300 with the ATTAS measurements gave evidence for an effect of the emitted primary exhaust aerosol on the properties of the young contrail (age ≤ 2 s). The Airbus plume exhibited both an increased number of exhaust aerosol particles and an increased number of contrail particles with respect to the ATTAS contrail. Effects of fuel sulphur content on plume and contrail properties were not observable for the Airbus A310-300 case because the fuel sulphur content was varied by a much smaller factor.

2.2 Composition and Morphology of Ice Crystal Residual Particles in Cirrus Clouds and Contrails [2]

In the second publication discussed in this section, results of the chemical and morphological signatures of aerosol particles associated with contrail formation are reported. The results originated from the analysis of aircraft-sampled residual particles from evaporated ice crystals, using a Counter-flow Virtual Impactor CVI. Samples of crystals taken in both contrails and cirrus clouds were compared with interstitial aerosols found in natural cirrus. The samples were analysed with a Scanning Electron Microscope equipped with a windowless energy-dispersive X-ray microanalysis system (SEM/EDX), which allows the identification of carbon-rich combustion aerosol via both X-ray emission and morphology. The CVI was mounted on board the DLR Falcon research aircraft to sample contrail and cirrus crystals with aerodynamic diameters larger than 4.5 μm. The CVI separates cloud elements larger than about 4.5 μm aerodynamic size by inertia from the surrounding atmosphere into a warm, dry, and particle-free air. Residual particles left behind by the evaporated cloud elements were collected on Nuclepore™ membrane filter substrates for subsequent SEM/EDX analysis.

The samples were taken during flights conducted on October 14, 15, and 17, 1996, during the AEROCONTRAIL campaign over southern Germany near the Austrian border. This area was heavily affected by air traffic during the experiment; following EUROCONTROL data, approximately 10 flights per hour were passing this region.

Table 2.1: Relative abundance of major elements in the interstitial aerosol sampled inside a cirrus; the characteristic diameter of sampled interstitial aerosol particles was < 0.8 μm [2]

	Interstitial aerosol (cirrus)		
Particle type	Black Carbon	Silicate	Metallic
Relative abundance in %			
C	68	0	4
O	22	49	37
Si	4	41	2
S	0	3	3
Cr + Fe + Ni	6	7	54
Fraction of interstitial aerosol in %			
FL 290 (approx. 9500 m altitude)	95	< 5	≈ 1
FL 260 (approx. 8500 m altitude)	80	20	0
FL 230 (approx. 7600 m altitude)	< 70	> 30	0

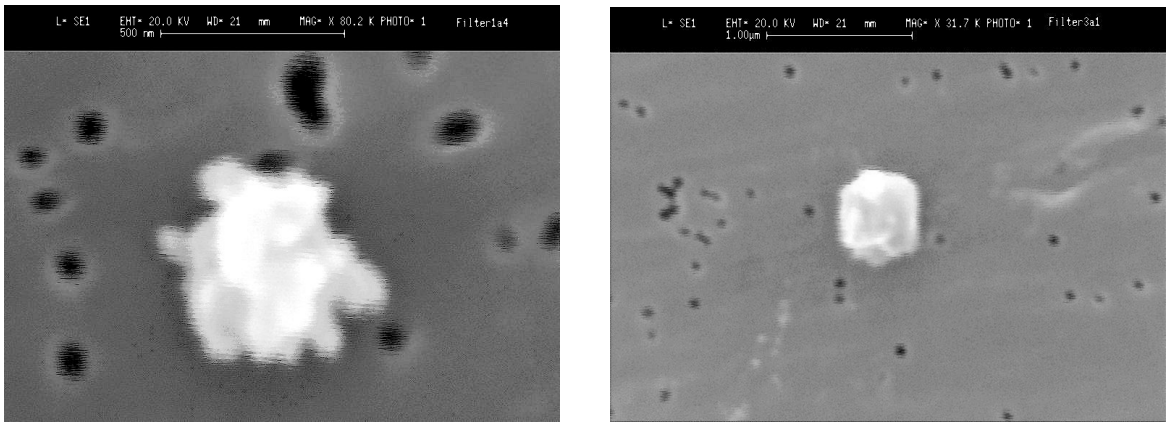

Figure 2.3. *Black carbon agglomerate from a B747 contrail (left panel) and one silicate particle from the interstitial aerosol inside a cirrus cloud (right panel).*

Three different aerosol types (black carbon BC, metallic particles, silicate) were distinguishable by their morphology, while the elemental composition of representative particles of each aerosol type was determined via EDX analysis. Figure 2.3 shows a carbonaceous particle sampled from a contrail of a B747 and a silicate particle sampled from the interstitial aerosol inside a natural cirrus cloud. The morphological signatures of the carbonaceous agglomerate formed from sub-100 nm primary particles and the crystal structure of the SiO_2 rich particle are clearly visible. The abundance ratios of major elements were derived from background corrected EDX spectra.

In the contrail and cirrus cases, black carbon (BC) particles dominated the residual size spectra for particles smaller than 1 µm. The coarse residual particle mode ($D_p \geq 1.5$ µm) in contrails consisted almost completely of mechanically generated metallic particles which contributed only about 1 % to residual particle number. Observed particle number concentrations and BC mass concentration of the residual particles were 0.2 cm^{-3} and 16 ng m^{-3} inside the contrail and 0.02 cm^{-3} and < 2 ng m^{-3} inside the cirrus.

The fraction of fine BC particles (0.1 µm $< D_p <$ 0.8 µm) in the interstitial aerosol samples increased with altitude from < 70 % at 7.6 km to 95 % at 9.5 km near the air traffic corridors with number concentrations of ≈ 0.1 cm^{-3}. Table 2.1 taken from [2] highlights this indication of the impact of aircraft exhaust particles on the aerosol in the upper troposphere.

The high abundance of carbonaceous particles in the residuals from evaporated contrail ice particles confirmed on an observational basis the hypothesis from modelling studies that carbonaceous combustion particles play a key role in contrail formation. However, the results discussed in this publication did not permit a separation of carbonaceous particles attached to the surface of already existing contrail ice crystals from those carbonaceous particles which were incorporated in the contrail particle during formation.

This separation was possible from observations reported by Kuhn et al. (1998) under the guidance of the author. In this paper the refractive index of contrail particles was measured which contained light-absorbing inclusions. The size of the inclusions was estimated using the Maxwell-Garnett approach and agreed very good with the average size of the residual particles determined from the filter samples. Combining the refractive index analysis with the chemical analysis presented in [2], experimental evidence for particulate carbonaceous inclusions in contrail ice particles was achieved.

The large fraction of carbonaceous particles observed in the cirrus samples suggested that particulate aircraft emissions can influence also clouds other than the contrails formed directly behind the aircraft. Since wide regions of the airspace over continental Europe is covered by air traffic corridors, in turn this yields a very large area where cirrus clouds are potentially affected

3 Physical and Chemical Properties of Aircraft Engine Exhaust Particles

Section 3 is focusing on a quantitative physical and chemical characterisation of the particle emitted from an aircraft engine. The chemical composition of the carbonaceous and the sulphate-containing fraction of the aerosol is determined from filter samples collected during ground-test operations of an aircraft engine [3]. Emission indices for carbonaceous matter are determined from these analyses [4]. The connection between aircraft engine emissions during ground operation and at cruise is discussed in [5], based on observations in the exhaust plume of the same aircraft on ground [3] and at cruise.

3.1 Aircraft Engine Exhaust Aerosol Characterisation [3]

The exhaust aerosol of an aircraft engine was characterised using a set of techniques to measure mass concentrations of carbonaceous matter and of particulate sulphate, and the particle size distribution. Measurements were performed in the exhaust plume of a Rolls Royce/SNECMA M45H Mk501 turbofan engine of the ATTAS aircraft of DLR. During sampling the engine was operated at various engine thrust levels from idle run to 70% of take-off, burning fuels with low (6 mg kg^{-1}) and high (2700 mg kg^{-1}) sulphur content. The analysis of the filter samples collected during the different engine thrust levels yielded that the ratio of black carbon BC to total carbon TC varied from 11 % with the engine in idle run to > 80 % at 70% of take-off thrust, see Figure 3.1. These chemical analyses were the first ones reported for a combustion aerosol emitted from an aircraft engine.

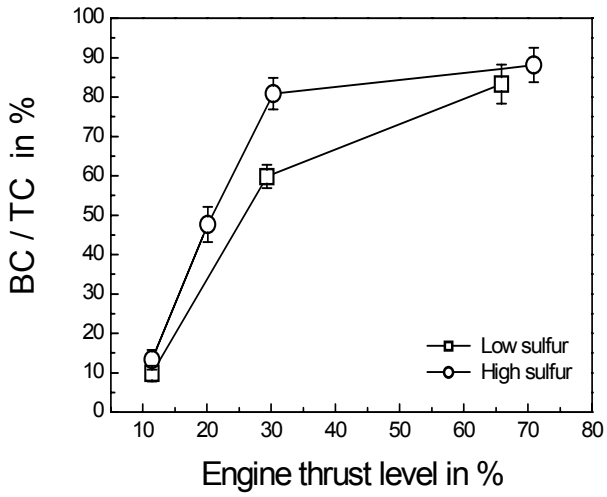

Figure 3.1. *Black carbon (BC) fraction of total carbon (TC) as a function of engine thrust level; low sulfur and high sulfur correspond to a fuel sulfur content 6 mg kg^{-1} and 2700 mg kg^{-1}, respectively.*

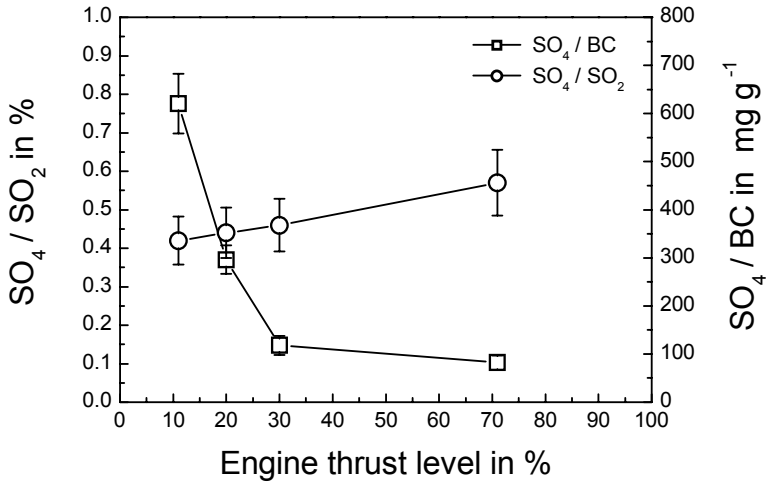

Figure 3.2. *Abundance ratios of SO_4^{2-}/SO_2 and SO_4^{2-}/BC plotted as functions of engine thrust level for a sulfur fuel content of 2700 mg kg^{-1}.*

The main conclusions which were drawn from the chemical analyses for the carbonaceous matter are: The BC fraction of TC is strongly affected by combustion conditions or engine operation conditions, respectively. The obtained OC-BC split suggests that the carbonaceous aerosol which is emitted by an aircraft engine at cruise power of 50% contains between 20% and 30% organic matter of total carbon mass. The BC as well as the TC mass concentrations are of comparable magnitude at distinct thrust levels for fuels with high sulphur and low sulphur content. BC formation is thus almost independent from the fuel sulphur content.

The ratio of particulate sulphate to gaseous SO_2 , which corresponds to the overall conversion rate of SO_2 to particulate H_2SO_4 seemed to be almost independent from the engine thrust level, as is shown in Figure 3.2. The observed upper limit was 0.8 % on a mass scale and 0.5 % on a number scale for plume ages < 1 s. The conversion rate from SO_2 molecules into particulate SO_4^{2-} inside the young exhaust of < 0.5 % with only a slight dependence on engine thrust level was in agreement with theoretical values based on the conversion of SO_2 via OH oxidation and a reaction of the formed SO_3 with H_2O to sulphuric acid. A formation of particulate sulphuric acid via the catalytic oxidation of SO_2 on the surface of the BC particles was excluded, because no correlation between sulphate and BC was observed (Figure 3.2).

The reported results provided a first chemical characterisation of the carbonaceous fraction of an aircraft engine exhaust aerosol and were used in the follow-on short-communication paper [4] for a quantitative determination of mass and number emission indices concerning carbonaceous matter.

3.2 Mass Emission Indices for an Aircraft Engine [4]

The black carbon (BC) emission index EI_{BC} in terms of mass and number is an important parameter to characterise the environmental impact of jet engine exhaust aerosol. The mass emission index describes the mass of carbonaceous matter emitted from an engine, when 1 kg of fuel is consumed. The respective index for particle number is defined equivalently.

Whenever the emission of carbonaceous matter from aviation and the expected effects are modelled, reliable emission indices are needed, because on a global scale, only the fuel consumption of the globally operating aircraft fleet is known. The mass and number emission indices were calculated from the measured mass and number concentrations of combustion particles [3] via the relation

$$EI_{BC} = \frac{c_{BC}\,(T_{air}\,, p_{air}\,)}{\rho_{air}\,(T_{air}\,, p_{air}\,)}\,N$$

with c_{BC}, BC mass concentration, ρ_{air}, density of air at measurement conditions (T_{air}, p_{air}), and N, air to fuel ratio of the engine. For the Rolls Royce/SNECMA M45H Mk501 turbofan engine at ground test conditions N varies from 70 at idle run conditions to 52 at take-off thrust. In Figure 3.3, the results are shown for the mass emission index at different engine operation conditions. The emission index varies from 0.015 g kg^{-1} at idle to 0.27 – 0.33 g kg^{-1} at 70% of take-off thrust. The emission of carbonaceous particulate matter depends thus strongly on the operation conditions of the engine. The values observed for the two investigated extreme cases extend over a factor of 20.

The respective number emission indices were estimated from measured mass concentrations and size distributions. For idle run and take-off conditions, emission values of 1×10^{14} kg^{-1} and 8.7×10^{14} kg^{-1}, were obtained. The emission indices reported in this note, were the first values

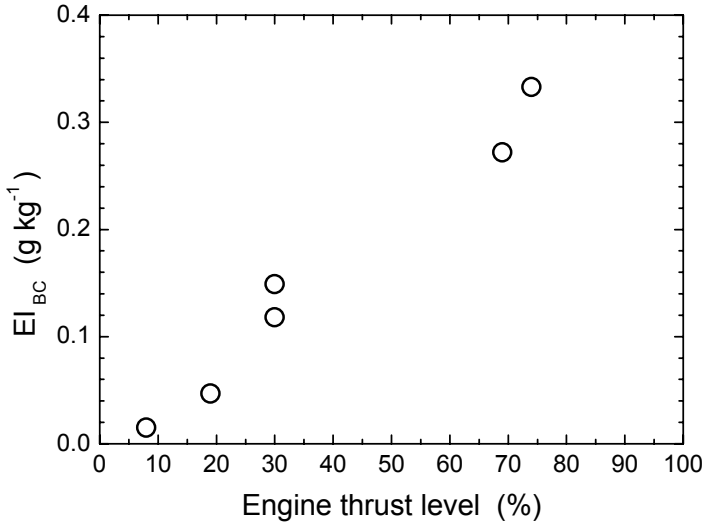

Figure 3.3. *Black carbon mass emission index EI_{BC} (in g BC per kg fuel) as a function of engine thrust level.*

derived from chemical analyses of the emitted aerosol. At the time of publication, they were widely used in the literature for the calculation of black carbon mass emissions from aviation.

3.3 Carbonaceous Aerosol in Aircraft Engine Exhaust [5]

This publication puts particulate emphasis on the carbonaceous particles in the exhaust of aircraft engines both during ground operation and at cruise. The question behind was, to what extent results from ground test studies – which are easy to perform – can be transferred to conditions at cruise altitude.

Characteristic parameters of black carbon aerosol (BC) emitted from aircraft engine were measured during ground tests and in-flight behind the same aircraft. The studies attempted to combine airborne measurements of the exhaust aerosol size distribution and chemical analyses of aircraft-sampled contrail and cirrus crystal residuals [2] with ground-based measurements of aerosol size distribution and chemical composition [3] to obtain a more detailed picture of the aircraft engine exhaust aerosol than having been available at the time of the studies. The results were based on a series of experimental flights which were conducted in 1996 and 1997 behind the ATTAS research aircraft of DLR above southern Germany.

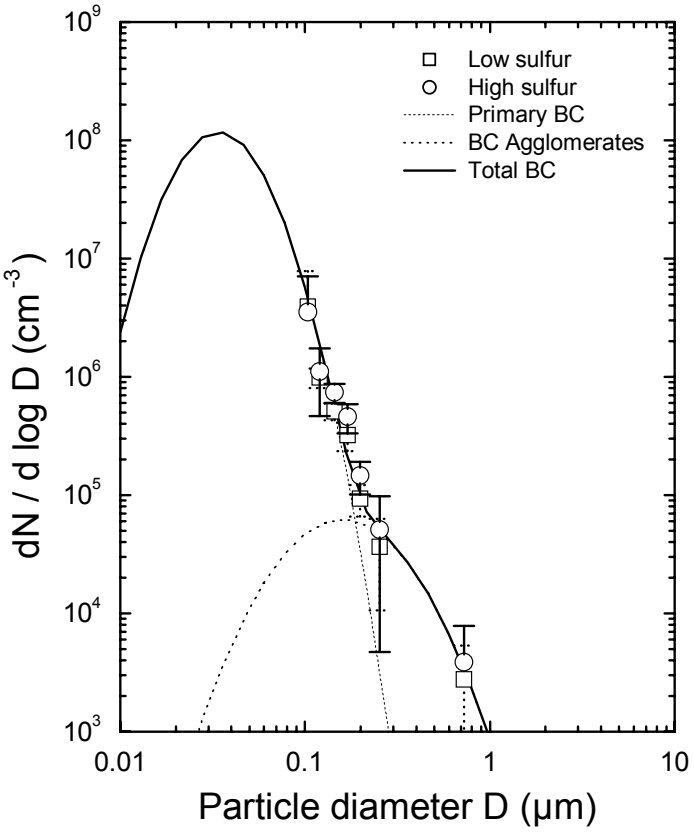

Figure 3.4. *Particle size distribution in the plume of the DLR ATTAS research aircraft at cruise altitude.*

In-flight aerosol characterisation inside the exhaust plume of the ATTAS was performed during the SULFUR 5 experiment in 1997. The instrumentation used for the measurement of the exhaust aerosol on board the Falcon was extended compared to the experiment SULFUR 4 [1] towards a separation of volatile and nonvolatile particles by heating one branch of the sampling line for removing volatile material. This technique permits the differentiation between volatile H_2SO_4 –H_2O particles and nonvolatile carbonaceous combustion particles during the airborne measurements. The size distribution of the combustion particles was obtained from log-normal model size distributions which were adjusted to measured exhaust aerosol size distributions in the accumulation mode size range. The total number concentration of the combustion aerosol was fixed by the measured total number of nonvolatile particles.

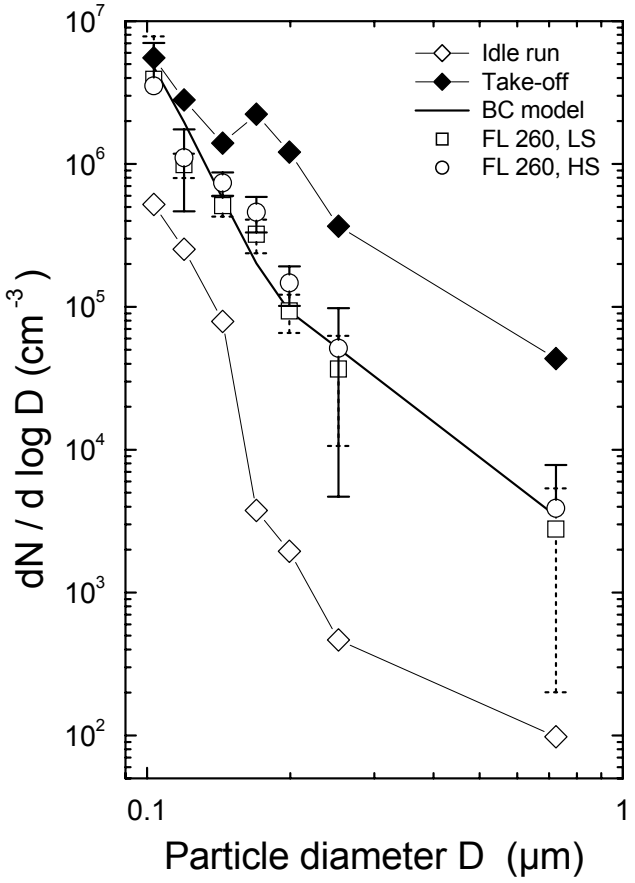

Figure 3.5. *Particle size distribution in the exhaust gas of the DLR ATTAS research aircraft during ground operation at idle and take-off conditions, and at cruise altitude.*

Size distribution features of the ATTAS exhaust aerosol were a primary BC mode at a modal diameter $D_p \cong 0.045$ µm, and a BC agglomeration mode at $D_p < 0.2$ µm. The total BC number concentration at the engine exit was 2.9×10^7 cm^{-3}. Figure 3.4 shows an example for the ATTAS exhaust aerosol.

The variability of size distributions of accumulation mode combustion particles is demonstrated in Figure 3.5. All size distributions showed a steep increase towards small particles in the sub-100 nm range. Only in the case of take-off larger combustion particles in the accumulation mode regime were emitted. This mode was completely missed for idle run conditions. However, the comparison of size distributions plotted in Figure 3.5 from ground test and in-flight measurements indicated that characteristic features of the BC size distribution were almost independent of altitude, i.e., from pressure and temperature.

In-flight BC mass emission indices ranged from 0.11 to 0.15 g BC (kg fuel) $^{-1}$. The measured in-flight particle emission value was $1.75 \pm 0.15 \times 10^{15}$ kg $^{-1}$ with corresponding ground test values of $1.0 - 8.7 \times 10^{14}$ kg $^{-1}$. These values were within the range of values reported for the extreme engine operation conditions idle and take-off as published in [4]. They compared to a thrust level of ≅ 30%.

Concluding, both size distribution properties and mass emission indices can be scaled from ground test to in-flight conditions, as long as the operation conditions are well known. The remaining question left open was, how representative the engine of the ATTAS aircraft was compared to the contemporary aviation fleet average. To answer this highly important question, further measurements in the plume of commercial aviation aircraft had to be performed.

4 Quantification and Prediction of Black Carbon Emissions by Aircraft at Cruise Altitude [6]

For answering the question of what are the particle emission properties of aircraft engines currently in service, the exhaust aerosol of two aircraft, the ATTAS and a Boeing 737-300 were extensively characterised at cruise conditions during the SULFUR 6 study. The old-technology aircraft ATTAS, equipped with Rolls Royce/Snecma M45H Mk501 engines (certification year 1971) was investigated again, because an extensive data set existed already concerning the emission properties of this aircraft. The Boeing B737-300 was equipped with CFM International CFM56-3B1engines (certification year 1983) which are among the cleanest aircraft engines on the market.

The measurement capabilities were again extended compared to SULFUR 4 [1] and SULUR 5 [5] such, that an important measurement gap concerning the nucleation mode particles in the sub-20 nm range was closed. Furthermore, an optical absorption photometer was operated aboard the Falcon which permitted for the first time the measurement of the black carbon mass emission index in the plume without any assumptions on particle shape and size.

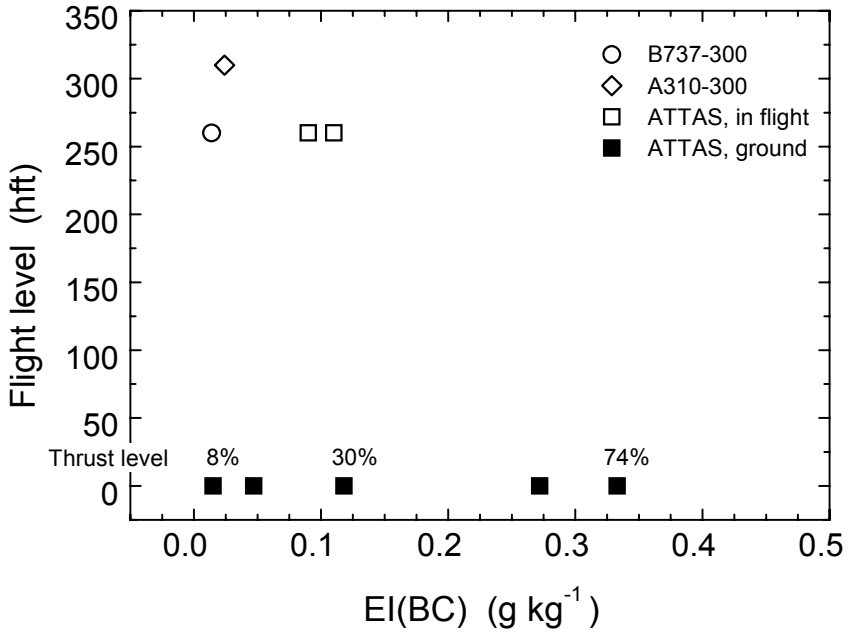

Figure 4.1. *BC mass emission index EI(BC) at different flight levels and for ground conditions.*

The analysis presented in this publication used all measurement flights performed so far during the SULFUR experiments in the exhaust plume of the DLR ATTAS research aircraft [1; 5], one Lufthansa Airbus A310-300 [1], and one Lufthansa Boeing B737-300 [6]. The particle size distributions, measured in the different exhaust plumes, provided the key features for particles emitted from old-technology (ATTAS) and modern-technology (B737-300) engines.

It turned out, that the old-technology engine emitted larger particles with a higher number EI than the more modern engine. The size distribution of the exhaust aerosol from the modern CFM56-3B1 engine was characterised by a primary BC mode at a particle diameter of ≅ 25 nm and an agglomeration mode at ≅ 150 nm. The corresponding modal diameters of the Rolls Royce/Snecma M45H Mk501engine exhaust aerosol were a primary mode at ≅ 35 nm m and an agglomeration mode at 150 – 160 nm. The size distribution properties of the ATTAS exhaust aerosol were highly reproducible for two measurements during the SULFUR 5 [5] and the SULFUR 6 [6] studies.

The BC number and mass emission indices EI(N) and EI(BC) varied from 3.5×10^{14} kg^{-1} and 0.011 g kg^{-1} for a modern CFM56-3B1 engine under cruise conditions to 1.7×10^{15} kg^{-1} and 0.11 g kg^{-1} for the older ATTAS engine. Figure 4.1 compiles the mass emission indices measured so far for various engines during ground tests and cruise altitude measurements. Similar to the mass emission indices, modern engines emit considerably less combustion aerosol particles by number than older engines. Figure 4.2 implies, that the number emission indices of modern engines are < 10^{15} kg^{-1}. It has to be mentioned, that Figure 4.2 contains also an emission index for a 1963 years technology engine flown on a Boeing B707, which is the highest value measured so far.

The observational results obtained during the measurements of the SULFUR 6 study confirmed several hypotheses stated earlier:

(1) The mass and number emission indices for nonvolatile combustion particles are almost independent from the fuel sulphur content. This behaviour was expected from the results obtained during the SULFUR 4 study [1] for the larger accumulation mode fraction of the combustion aerosol.

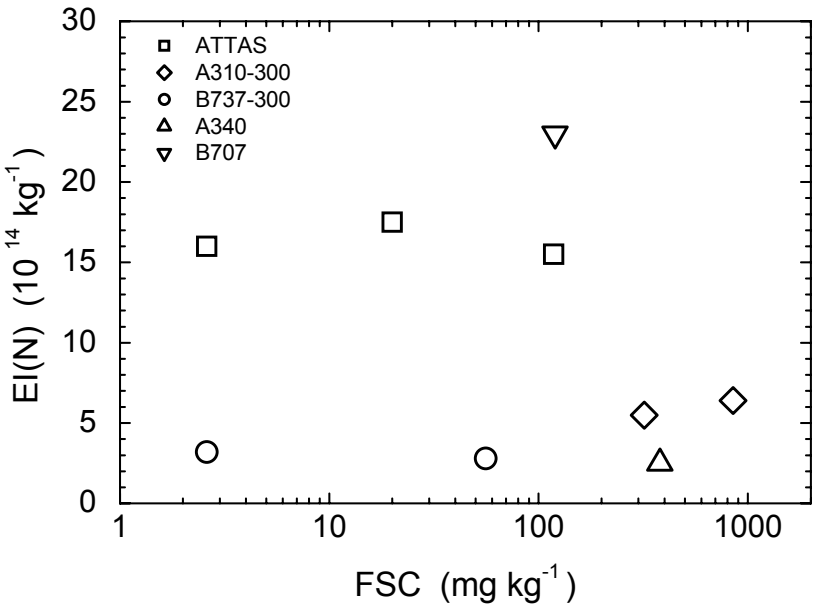

Figure 4.2. *Particle emission index EI(N) for non-volatile BC particles at different fuel sulfur contents FSC.*

(2) The black carbon mass concentrations estimated from the integral volume of the modelled size distributions of nonvolatile particles in the plume was in good agreement with the mass concentration measured with the aerosol absorption photometer. This result confirmed the assumption [1; 5], that the non-volatile aerosol is predominantly composed of carbonaceous matter.

(3) The effect of engine properties on the exhaust aerosol is probably larger than the effect of the fuel sulphur content [1]. Since modern engines emit smaller but more particles than older engines, differences in the activation for contrail particle formation might occur.

Another highly relevant issue reported in [6] is the validation of an empirical model which predicts the black carbon emissions from an engine from its operation conditions. The determination of the BC emissions from a globally operating aircraft fleet requires the application of a fleet-averaged BC mass emission index EI(BC). In global inventories, the average composition of the aircraft fleet is available together with information on the fuel use in different altitudes and geographical regions of the world. The fleet-averaged emission index permits the determination of released black carbon mass per kg of burnt fuel. For

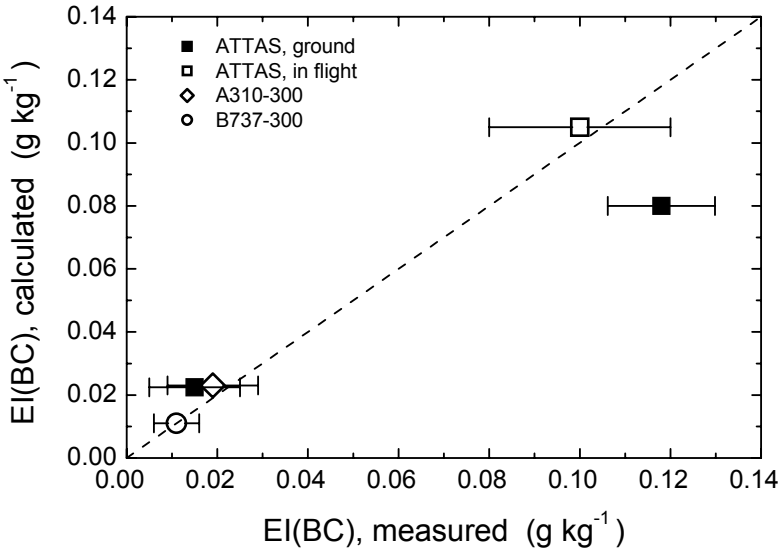

Figure 4.3. *Comparison of calculated and measured BC mass emission indices EI(BC).*

providing such a value, a method for predicting EI(BC) for a set of airframe engine combinations must be developed and validated.

The empirical model was developed by Döpelheuer (1997, 2002), while the crucial task of model validation was tackled in [6] under the lead of the author. The method calculates the mass concentration of black carbon in the exhaust of the engine under consideration for ground test conditions from engine certification data. In the second step, the mass concentration is estimated for cruise altitude conditions from the changed operation conditions. In the final step, the total amount of emitted BC mass is calculated and converted into a mass emission index.

Figure 4.3 shows the comparison of mass emission indices EI(BC) determined from measurements in the aircraft plumes at cruise altitude and predicted by the model, when the detailed information on the engine operation parameters during the measurements is used. Although there are only very few data available, the agreement between measurement and prediction is excellent, and the model is successfully validated.

By using the size information form the measurements, the mass emission indices EI(BC) from the model were converted into number emission indices EI(N). Again, very good agreement between predicted and measured emission indices was obtained. In a final step, the model was applied to an average aircraft fleet operating in the North Atlantic flight corridor. The fleet-averaged mass emission index is

$$EI(BC)_{\text{fleet average}} = 0.038 \text{ g BC (kg fuel)}^{-1}$$

which may be interpreted as a "conversion efficiency" of hydrocarbon fuel mass into carbonaceous particulate matter of < 0.004%. The combustion process is thus very clean concerning the emission of carbonaceous particles. The average EI(BC) value is widely used in global emission inventories and modelling activities for the calculation of the global BC mass emissions from aviation.

The investigation of the characteristics of combustion particle emissions by aviation during cruise is closed by the results presented in [6]. The vertical distribution of black carbon emissions and the resulting atmospheric effects are discussed in detail in Section 8.

5 Measurement Methods for the Aerosol Absorption Coefficient and Black Carbon

As is pointed out in the discussions in Sections to 4, particulate black carbon is a key component of the particle emissions from aviation. Furthermore, it is known since the late 1970s, that graphitic-like black carbon is because of its broadband absorption of radiation (Bohren and Huffman, 1983) the most efficient light-absorbing aerosol species in the visible spectral range.

The measurement of black carbon is strongly related to the measurement of aerosol light absorption in the visible part of the radiation spectrum. The relationship between the aerosol absorption coefficient σ_{ap} (in m^{-1}) and the corresponding black carbon mass concentration c_{BC} (in g m^{-3}) is established by an aerosol mass-specific absorption coefficient $b_{ap}^{(BC)}$ (in $m^2 g^{-1}$) via

$$\sigma_{ap} = c_{BC} \times b_{ap}^{(BC)} \quad .$$

There is a variety of $b_{ap}^{(BC)}$ values reported in the literature (Horvath, 1993). The relationship between aerosol absorption and black carbon mass concentration is therefore not unambiguous for different kinds of black carbon containing aerosol particles. In an extensive inter-comparison study on current black carbon sensitive optical and thermal measurement methods, which was

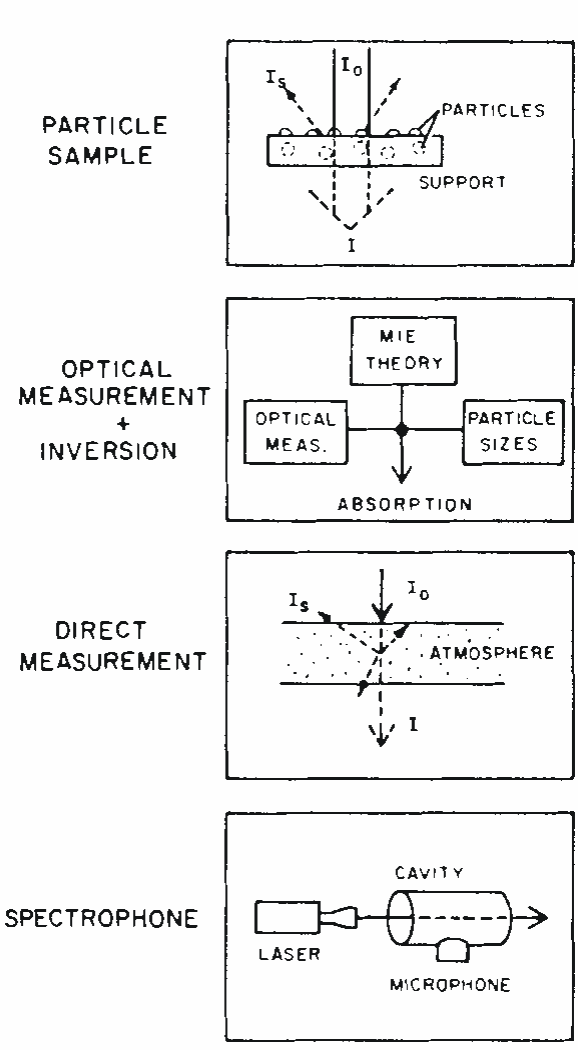

Figure 5.1. *Sketches of the major categories of measuring light absorption by aerosol particles, the graph is taken from the Proceedings of the First International Workshop on Light Absorption by Aerosol Particles (Gerber and Hindman, 1982).*

conducted on behalf of the German Umweltbundesamt, Petzold and Niessner (1995a) demonstrated the large variability of correlation factors connecting aerosol absorption and black carbon mass for different measurement methods.

Despite its importance, the problem of measuring aerosol absorption is still not sufficiently solved (Andreae, 2001; Heintzenberg et al., 1997). The situation did not change substantially since 1980, when the First International Workshop on Light Absorption by Aerosol Particles was held at the Colorado State University in Fort Collins, USA (Gerber and Hindmann, 1982). Even during the latest 8th International Conference on Carbonaceous Particles in the Atmosphere 2004 in Vienna, an entire session was focussing on the relationship between black carbon mass and aerosol absorption, and on possible improvements in measurement methods.

Optical techniques like Raman scattering (Rosen et al., 1978) and laser induced incandescence LII (Melton, 1984; Baumgardner et al., 2004) turned out to be useful methods for the identification of graphitic-like compounds in atmospheric aerosol samples (Raman scattering) and for detecting light absorbing particles in flames (LII), but so far they did not reach the state of maturity which is required for an application to atmospheric monitoring purposes and routine measurements.

The methods used for the determination of the aerosol absorption coefficient are based on optical techniques. Figure 5.1 summarises schematically the major categories of measurement methods from top to bottom: (1) intrusive techniques using particles collected on filters, (2) in situ measurements of optical and microphysical aerosol properties combined with data inversion using Mie theory for scattering and absorption of light by spheres, (3) direct measurement of atmospheric light transmission and scattering, e.g., by sun photometry, (4) photoacoustic spectroscopy which measures the sound wave generated by an absorbing aerosol in a cavity. All methods aim at the measurement of the aerosol absorption coefficient σ_{ap}, reported in m^{-1} or $Mm^{-1} \equiv 10^{-6}\,m^{-1}$. For measurements in exhaust gases, only methods from categories (1) and (4) can be used.

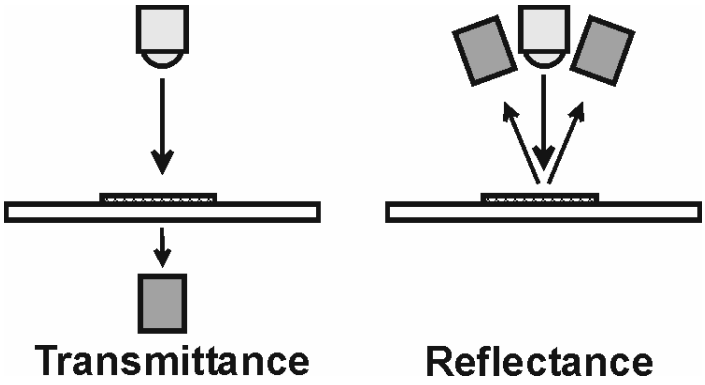

Figure 5.2. *Schematic of transmittance and reflectance methods for the measurement of particle absorption from filter samples.*

Chemically-based methods applied to the determination of the total and the elemental carbon in aerosol samples use mainly thermal filter analysis techniques (Puxbaum, 1979; Cachier et al., 1989).

The applicability of the photoacoustic method to absorption coefficient measurement tasks was proven by several groups (e.g., Adams, 1988; Petzold and Niessner, 1995b, 1996; Arnott *et al.*, 1999), but a detection limit of $\geq 10^{-6}$ m^{-1} makes it a useful technique only for measurements in polluted air masses or exhaust gases. Furthermore, it requires a complex instrument set-up which limits the application for long-term monitoring purposes. However, its in-situ capabilities and the almost entire absence of measurement artefacts make photoacoustic spectroscopy a candidate for a reference method for measuring aerosol absorption coefficients.

Current intrusive methods for the measurement of the aerosol light absorption use mainly the analysis of filter-deposited particles. For this type of technique the particles are collected on a filter substrate which is then analysed by optical means. The advantage of these methods is their capability of sampling over a long period of time which lowers the minimum detectable absorption well below the threshold of 10^{-6} m^{-1}. Two different instrumental set-ups are at present in use, which both rely on the modification of optical properties of filter matrices caused by deposited particles, Figure 5.2 shows the two instrumental set-ups schematically. Filter transmittance (TRANS) and reflectance (REF) methods measure the change in filter transmittance (reflectance) caused by the deposited aerosol particles.

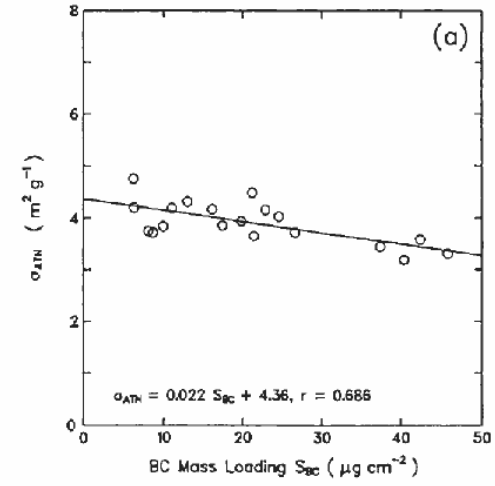

Figure 5.3. *Specific attenuation cross section σ_{ATN} which links light attenuation to mass loading as a function of the black carbon mass loading of the filter (Petzold et al., 1997).*

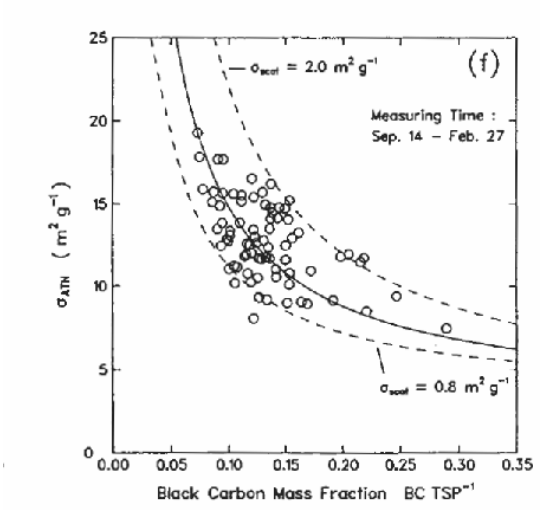

Figure 5.4. *Specific attenuation cross section σ_{ATN} as a function of the black carbon mass fraction of the collected aerosol (Petzold et al., 1997).*

The filter transmittance T/T_0 (reflectance R/R_0) of a filter sample is defined as the ratio of light intensities transmitted through (reflected from) a particle-loaded and a particle free filter, respectively. From these definitions, the method-dependent coefficients $\sigma_{0\,(TRANS)}$ and $\sigma_{0\,(REF)}$ which describe the attenuation of light by the aerosol deposited on the investigated filter are calculated as

$$\sigma_{0\ (TRANS)} = \frac{A}{V} \ln\left(\frac{T_0}{T}\right) \;;\; \sigma_{0\ (REF)} = \frac{1}{2}\frac{A}{V} \ln\left(\frac{R_0}{R}\right)$$

The property A refers to the active filter area while V gives the sampled volume. The ratio A/V thus represents the inverse length of the aerosol column sampled through the filter spot.

In the case of transmission measurement methods, a widely used empirical relationship links the light attenuation to the mass loading of the filter via the attenuation coefficient

$$\ln\left(\frac{T_0}{T}\right) = \sigma_{ATN} \frac{Mass_{BC}}{A} \quad .$$

The attenuation coefficient σ_{ATN} is proportional to the aerosol mass-specific absorption coefficient $b_{ap}^{(BC)}$ (in $m^2 g^{-1}$), but not equal.

Methods measuring the change in light transmission through a filter are the so-called the Laser Transmission method and the Aethalometer (Rosen and Novakov, 1983; Hansen et al., 1984), Integrating Plate methods (Lin et al., 1973; Clarke et al., 1987; Hitzenberger, 1993) and the Particle Soot Absorption Photometer PSAP (Bond et al., 1999). The change in filter reflectance is analysed by a reflectometer (e.g., Delumyea et al., 1980). The Integrating Sphere (Heintzenberg, 1982) can be used as a diffuse detector for both the transmitted or reflected radiation.

The methods differ by the applied filter matrices which are plane polycarbonate membrane filters (Integrating Plate methods) or glass or quartz fibre filters (Laser Transmission method, Aethalometer, PSAP). Among these methods, only the Aethalometer and the PSAP provide real-time data while all other methods require post-sampling filter analysis. In the case of polycarbonate membrane filters, the particles are collected at the surface. Fibre filters, are depth filters where the particles are collected not only at the very surface of the filter but penetrate to some extent also into its interior. Advantages of this filter type are a very high deposition efficiency for even sub-100 nm particles and simple handling and robustness during sampling. This makes it a valuable filter matrix for field work.

However, an absorbing aerosol not only absorbs light, but generally, to an even higher extent, scatters light. Unfortunately, fibre filter based methods show a severe cross-sensitivity to particle-related scattering effects and multiple scattering effects caused by the filter fibres (e.g., Liousse et al., 1993; Petzold et al., 1997). Similar cross-sensitivities are known for filter membrane-based methods (Hitzenberger et al., 1993):

(1) The light scattered by the particles can interact with the absorbing species contained in the particles, which results in turn in an overestimation of aerosol absorption if the aerosol contains a large light-scattering fraction.

(2) In the case of fibre filters, an additional light scattering by the filter fibres has also to be taken into account.

(3) The method sensitivity to deposited particles changes with the loading of the filter, i.e., the blank clean filter is more sensitive to deposited particles than a filter which is to some extend already loaded with particles.

In Figures 5.3 and 5.4, the effects of filter loading (Figure 5.3) and aerosol light scattering components (Figure 5.4) on the attenuation coefficient $\sigma_{ATN} \propto \sigma_{0(TRANS)} / c_{BC}$ for the Aethalometer method are demonstrated for ambient aerosol (Petzold et al., 1997). As outlined above, the attenuation coefficient σ_{ATN} decreases with increasing filter loading, i.e., the method responds to a given mass concentration c_{BC} less efficient for a loaded filter than for a clean filter. The attenuation of light increases with an increasing contribution of light scattering, expressed by a decreasing mass fraction of black carbon to the total suspended particulate matter TSP.

In the case of a transmittance method, the consideration of the effects of aerosol light scattering which is proportional to the aerosol single scattering albedo ω_0, and of filter loading, which is proportional to the filter transmittance T/T_0 in the determination of the aerosol absorption coefficient σ_{ap} from the measured coefficient $\sigma_{(TRANS)}$ requires the introduction of a correction function for filter loading $f(T/T_0)$ and for aerosol light scattering $C(\omega_0)$, according to

$$\sigma_{ap} = \sigma_{0(TRANS)} \; f_{(TRANS)}(T/T_0)\, C_{(TRANS)}(\omega_0)$$

Without a precise knowledge of the correction functions $f(T/T_0)$ and $C(\omega_0)$, absorption coefficient measurements with filter transmittance methods may give incorrect results. For reflectance methods, the situation is identical.

The only real-time method so far which circumvents the extensive correction of absorption coefficient measurements is the recently introduced Multi-Angle Absorption Photometry MAAP. In Section 5.1 a detailed discussion of the method is given. In the course of the Reno Aerosol Optics Study, performed 2002 at the Desert Research Institute in Reno NV, USA (Sheridan et al., 2004), the response characteristics of multi-angle absorption photometry to aerosols of different composition showed close agreement with a reference absorption

measurement. Supported by the results from other laboratory studies and field experiments, MAAP turned out to improve the measurement of the aerosol absorption coefficient by filter-based robust methods significantly. The results of the method evaluation during the Reno Aerosol Optics Study are presented in Section 5.2.

5.1 Multi-Angle Absorption Photometry [7]

Multi-angle absorption photometry is designed as method for an aerosol absorption measurement which is less sensitive to light scattering aerosol components than existing methods. It is to some extent a combination of transmittance and reflectance techniques. The absorption coefficient of the filter-deposited aerosol is calculated from the optical properties of the entire filter system which are determined by a two-stream-approximation radiative transfer scheme. Figure 5.5 illustrates the two-layer system of a particle-loaded filter, the method has to deal with. It shows a cross sectional cut through a particle-loaded glass fibre filter. Particle deposition is observed only within the upper 10-15% of the filter sample thickness.

An investigation of the angular distribution of light back-scattered from and transmitted through a fibre filter has shown that the transmitted radiation is completely diffuse and can be parameterised by a *cos* θ relationship with θ being the scattering angle relative to the incident radiation. The back scattered radiation contains a diffusely scattered fraction proportional to

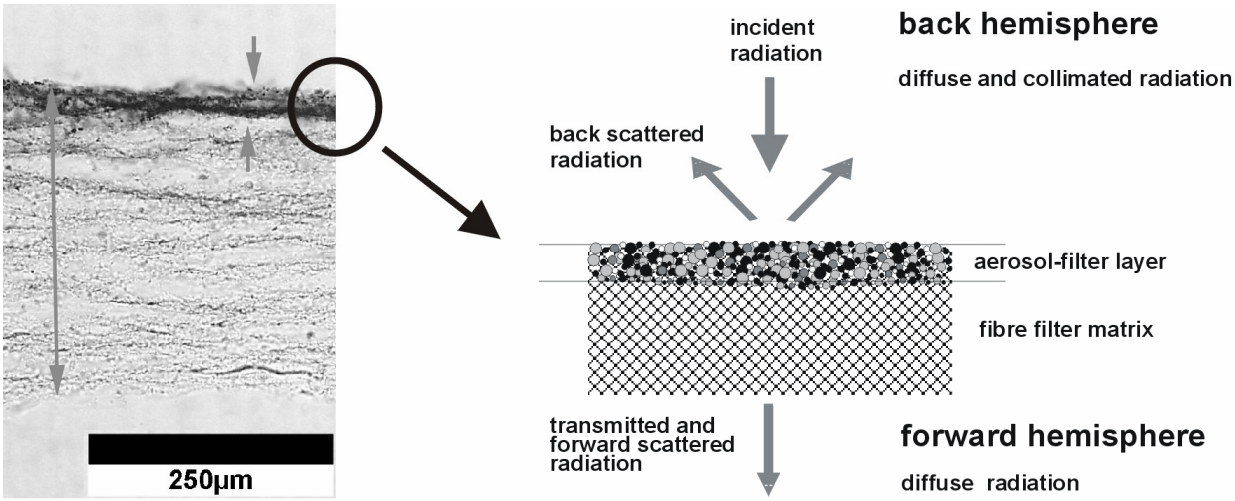

Figure 5.5. *Schematic of the two layer system of particles deposited in a fibrous filter matrix.*

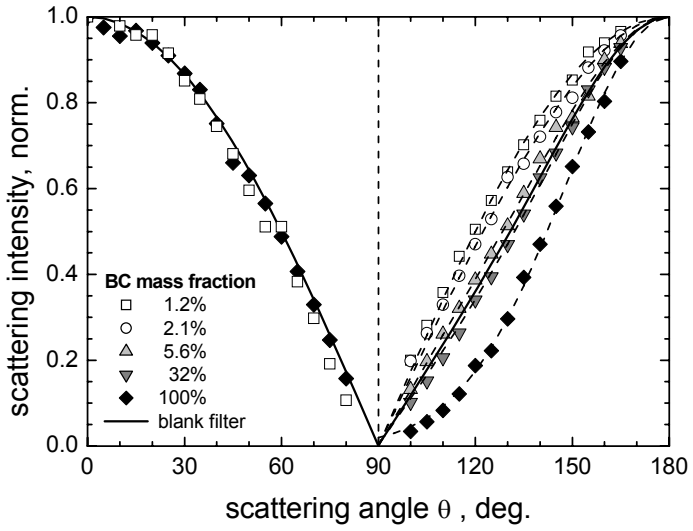

Figure 5.6. *Angular distribution of radiation scattered from glass fibre filters loaded with a mixture of light-absorbing black carbon and light-scattering sodium chloride aerosol.*

cos $(\theta - \pi)$, and a fraction which is parameterised best by a Gauss law proportional to *exp* $[-\frac{1}{2}(\theta - \pi)^2 / \rho^2]$ with ρ being a measure for the surface roughness of the aerosol layer deposited on the filter. The Gaussian-distributed fraction of the back scattered radiation can be taken as radiation "reflected" from a rough surface. The partitioning of back scattered radiation between diffuse and Gaussian type depends on the sampled aerosol. Figure 5.6 shows the data which were used for this analysis.

In order to cover the effect of the aerosol composition on the angular distribution of the back scattered radiation, irradiance measurements are needed at several detection angles in the back hemisphere. In the forward hemisphere, a single measurement is sufficient because the radiation in the forward hemisphere is diffuse. A detailed analysis of the angular distribution provided a distribution of detectors as shown in Figure 5.7. This sensor permits the full determination of the irradiances in the forward and back hemispheres relative to the illuminating light source. The exact position of the detection angles was chosen such that the partitioning between diffuse and Gaussian types can be determined with highest resolution.

The determination of the aerosol absorption coefficient of the deposited aerosol uses radiative transfer techniques. The particle-loaded filter is treated as a two-layer system: the aerosol-

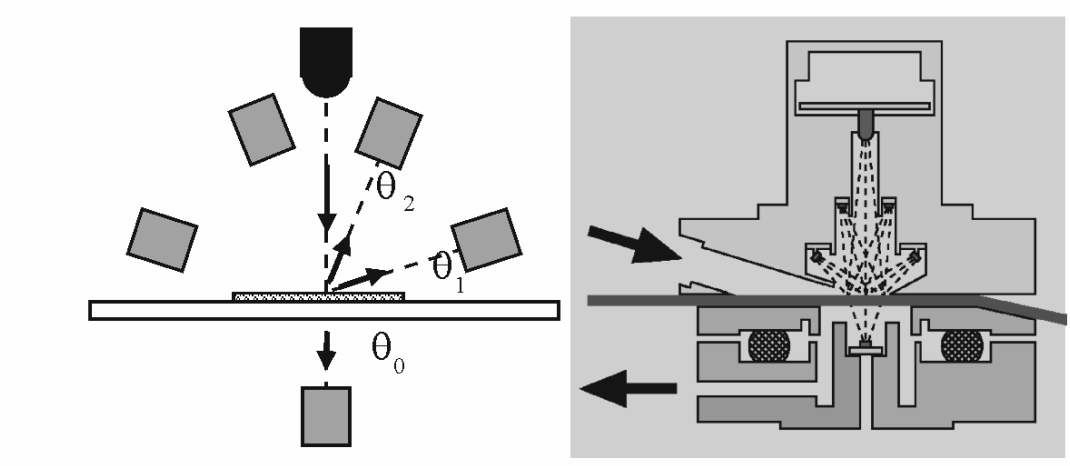

Figure 5.7. *Optical sensor of the multi-angle absorption photometer MAAP; left: position of the photo detectors at detection angles $\theta_0 = 0°$, $\theta_1 = 130°$, and $\theta_2 = 165°$ with respect to the incident light beam ($\lambda_{MAAP} = 670$ nm); right: layout of the MAAP sensor unit, arrows indicate the airflow through the sensor unit across the filter tape [8].*

loaded layer of the filter and the particle-free filter matrix. Radiative processes inside the layer of deposited aerosol and between this layer and the particle-free filter matrix are taken separately into account. The treatment of radiative processes which are relevant in such a two-layer system has to consider the fraction of transmitted radiation T, the fraction of forward scattered radiation F, the fraction of back scattered radiation B, and the fraction of radiation penetrated through the particle-loaded filter P with $P = T + F$.

The optical properties of the particle-free filter matrix (subscript M), the aerosol-loaded filter layer (subscript L), and the entire filter composed of the aerosol-loaded filter layer and the particle-free filter matrix (subscript F) have to be included. Diffuse (superscript *) and collimated (no superscript) incident radiation have to be distinguished. The consideration of multiple scattering effects between the particle-loaded filter layer and the particle-free filter matrix, and scattering processes inside the aerosol layer yield the following budget equations for the ratio of radiation passed through a particle-loaded and a blank filter, $P_F / P_F^{(0)}$, and for the ratio of radiation scattered from a particle-loaded and a blank filter, $B_F / B_F^{(0)}$:

$$\frac{P_{\mathrm{F}}}{P_{\mathrm{F}}^{(0)}} = \frac{T_L + F_L}{1 - B_L^{*}\, B_M}$$

$$\frac{B_{\mathrm{F}}}{B_{\mathrm{F}}^{(0)}} = P_L^{*}\, \frac{T_L + F_L}{1 - B_L^{*}\, B_M} + \frac{B_L}{B_M}\,.$$

The quantities $P_{\mathrm{F}} / P_{\mathrm{F}}{}^{(0)}$ and $B_{\mathrm{F}} / B_{\mathrm{F}}{}^{(0)}$ are directly measurable, while the properties F_{L}, B_{L}, $P_{\mathrm{L}}{}^{*}$, and $B_{\mathrm{L}}{}^{*}$ of the aerosol-loaded filter layer have to be calculated via radiative transfer methods (Hänel, 1987).

For treating the propagation of radiation through a system of light scattering and light absorbing components, the two-stream approximation for the equation of radiative transfer as proposed by Coakley and Chylek (1975) was used. The solution of the equation of radiative transfer yields equations for the quantities F_{L}, B_{L}, $P_{\mathrm{L}}{}^{*}$, and $B_{\mathrm{L}}{}^{*}$ as functions of the ratio of light scattering to light extinction by the aerosol-loaded filter, which is the single-scattering albedo of the aerosol-loaded filter layer $\mathrm{SSA_L}$. The budget equations are solved numerically via the variation of the variable layer optical depth $\mathrm{LOD} = \ln T_{\mathrm{L}}$, which corresponds to the optical depth of the aerosol-loaded filter layer, and the variable $\mathrm{SSA_L}$, until both budget equations are simultaneously satisfied.

It has to be noted, that the properties LOD and $\mathrm{SSA_L}$ are mainly determined by the light-scattering characteristics of the fibrous filter matrix. The contribution of light scattering to light extinction by the filter sample is obtained from the product $\mathrm{LOD} \times \mathrm{SSA_L}$. However, a further separation into contributions of particles and filter fibres to light scattering by the particle-loaded filter cannot be given from the applied radiative transfer approximation method. In the case of light absorption, the situation is different, because the quartz or glass fibres do not contribute to light absorption in the spectral range selected for this instrument (λ_{MAAP} = 670 nm). The method-dependent coefficient $\sigma_{0\,(\mathrm{MAAP})}$ related to aerosol light absorption can thus be determined from the final values LOD and $\mathrm{SSA_L}$ as

$$\sigma_{0\ (MAAP)} = -\frac{A}{V}\left(1 - \mathrm{SSA_L}\right) \mathrm{LOD}\ .$$

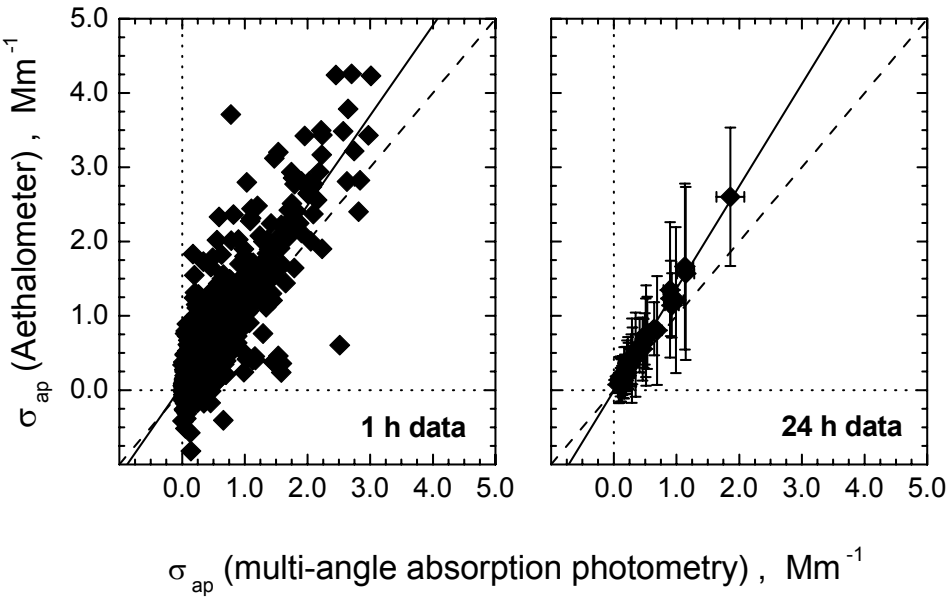

Figure 5.8. *Aerosol absorption coefficients (λ = 0.67 µm) measured at the high-alpine site Jungfraujoch; multi-wavelength Aethalometer data were converted to an aerosol absorption coefficient by applying the method of Weingartner et al. (2003). Solid lines indicate the linear regression lines, dashed lines represent 1:1 lines.*

Similar to the transmittance and reflectance methods, no a priori knowledge is available whether for MAAP also correction functions for aerosol light scattering and filter loading have to be applied, i.e.

$$\sigma_{ap} = \sigma_{0\,(MAAP)}\, f_{(MAAP)}\,(LOD)\, C_{(MAAP)}\,(\omega_0)$$

The expectation, however, is that

$$f_{(MAAP)}\,(LOD)\, C_{(MAAP)}\,(\omega_0) \cong 1.0\,.$$

Proving this expectation required extensive evaluation studies which are discussed in the following section 5.2. An assessment of all sources for measurement uncertainties provided an overall uncertainty for $\sigma_{0\,(\mathrm{MAAP})}$ is 12%. Operating the multi-angle absorption photometer at an averaging time of 1 hour with the sample flow set to 1 $\mathrm{m^3\,h^{-1}}$, yielded a detection limit of $0.05 - 0.07\ \mathrm{Mm^{-1}}$. This limit may be further reduced when the averaging period is extended.

First applications of the method to urban aerosol and background aerosol showed a strong correlation between black carbon mass concentration and aerosol light absorption. The applicability of the method to clean background air was also successfully demonstrated at the remote high-alpine measurement site Jungfraujoch in Switzerland (Figure 5.8). This first application under rough environmental conditions indicated that the absorption coefficients reported so far from conventional Aethalometers are to high by about 40%.

5.2 Evaluation of Multi-Angle Absorption Photometry [8]

A detailed evaluation of the method was performed during the Reno Aerosol Optics Study RAOS in 2002 (Sheridan et al., 2004). During RAOS, test aerosols of different composition and optical properties were generated and exposed to an extensive set of aerosol extinction, aerosol scattering and aerosol absorption measurement methods. Briefly summarised, "white" ammonium sulphate particles and polystyrene latex spheres were mixed with "black" combustion particles which were generated with a kerosene burner and graphite particles emitted from a graphite vane pump. The mixing chamber was a 76 L stainless steel vessel. The single-scattering albedo $\omega_0 \equiv \sigma_{sp} / \sigma_{ep}$ of generated particle mixtures varied from about 0.30 for pure "black" aerosol to 0.70 – 0.98 for externally mixed aerosols, and 1.0 for pure "white" aerosol. Additional to these test runs, measurements were performed with filtered particle-free air for testing the instruments' baseline behaviour, and with ambient aerosol. As reference method for the aerosol absorption measurement, aerosol extinction (σ_{ep}) measured with a folded-path optical extinction cell minus aerosol scattering (σ_{sp}) measured with an integrating nephelometer (model TSI 3563) was chosen, i.e., $\sigma_{ap} = \sigma_{ep} - \sigma_{sp}$.

The absorption coefficient was also measured in situ by a photoacoustic spectrometer. Deployed filter-based absorption measurement methods were a single-wavelength particle soot absorption photometer PSAP (Bond et al., 1999), one 3-wavelength PSAP, two multiple-wavelength Aethalometers, and one single-wavelength MAAP. The adjustment between different wavelengths was obtained from multiple-wavelength measurements by interpolation.

MAAP showed close agreement with the reference absorption measurement by extinction minus scattering. The slopes of regression lines varied between 0.99 ± 0.01 and 1.07 ± 0.02 for pure black carbon particles and external mixtures with ammonium sulphate to 1.03 ± 0.05

for ambient aerosol. No effect of the filter aerosol loading or the single-scattering albedo ω_0 of the sampled aerosol on the MAAP response characteristics was observed. Thus, indeed,

$$f_{(MAAP)}(LOD)\, C_{(MAAP)}(\omega_0) = 1.0$$
$$\sigma_{0(MAAP)} = \sigma_{ap} \quad .$$

Figure 5.9 demonstrates this result for the effect of filter loading on the instrument response, which is expressed as the method-dependent coefficient σ_0 normalised to the reference value $\sigma_{ap} = \sigma_{ep} - \sigma_{sp}$.

In contrast, transmittance and reflectance methods showed a clear impact of ω_0 and the filter loading on the response characteristics, see again Figure 5.9. These dependencies require the application of a correction function for the reliable determination of the aerosol absorption coefficient.

There were three major conclusions from the RAOS study:

(1) Multi-angle absorption photometry is a new and promising approach for the measurement of the aerosol absorption coefficient by filter-based methods, which requires no off-line data correction or parallel-measured aerosol light scattering coefficients for correction purposes.

(2) Filter-based absorption measurement methods which do not include an adequate treatment of the effects of the filter matrix and the aerosol light scattering component in the data analysis, give incorrect results caused by aerosol light scattering effects and by the aerosol loading of the filter.

(3) If filter-based methods treat the perturbing effects properly, e.g., as by off-line corrections using simultaneously measured light scattering coefficients for PSAP data, or by considering these effects in the data analysis algorithm like MAAP does, filter-based approaches for aerosol absorption coefficient measurements are comparable to in situ methods with respect to a reliable σ_{ap} – measurement.

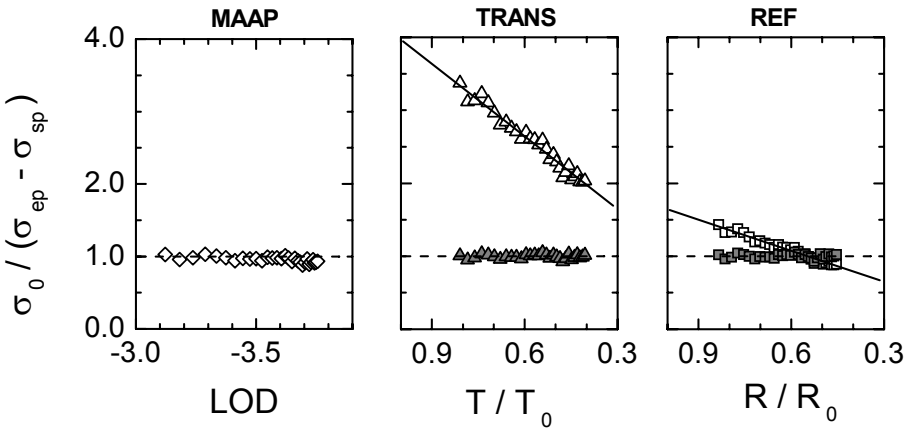

Figure 5.9. *Response functions for methods MAAP, TRANS and REF with respect to pure black carbon aerosol ($\omega_0 \cong 0.30$), solid lines represent the dependency of $\sigma_0 / (\sigma_{ep} - \sigma_{sp})$ on the filter loading in units of layer optical depth LOD (MAAP), filter transmittance T / T_0 and filter reflectance R / R_0, respectively; dashed lines represent the line of equality, filled symbols correspond to data corrected for the filter loading effect.*

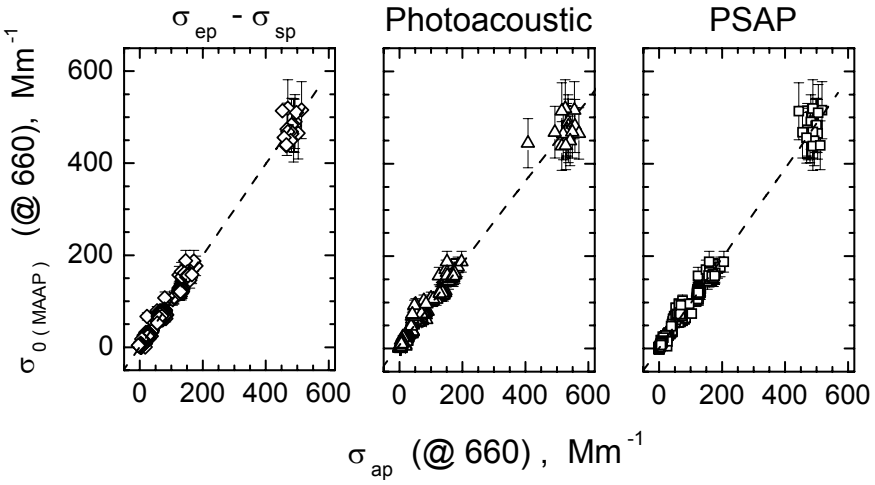

Figure 5.10. *Method comparison of MAAP and reference method extinction – scattering, photoacoustic spectroscopy, and PSAP: externally mixed kerosene/graphite soot – ammonium sulphate aerosols, PSAP data are corrected for light-scattering and filter loading; dashed lines give the linear regression lines. Extinction – scattering, photoacoustic spectroscopy and PSAP were operated at different wavelengths, adjustment to the MAAP wavelength of 660 nm was obtained by interpolation.*

The latter conclusion is illustrated in Figure 5.10 which shows the correlation between MAAP and the reference method extinction minus scattering, photoacoustic spectroscopy, and a filter-loading and scattering-corrected transmittance method PSAP.

Combining the method development described in [7] and the method evaluation described in [8], a promising new method for a simple and robust measurement of the aerosol absorption coefficient, and – keeping the ambiguities of converting aerosol absorption into black carbon mass in mind – for the particulate black carbon is presented.

This method was used for the on-line measurement of black carbon emissions from aircraft engines in [9; 10] and for the estimation of the black carbon mass concentration in the free troposphere for assessment purposes as discussed in Section 8.

6 Particle Emissions by Aircraft Engines Under Simulated Cruise Conditions [9; 10]

The experimental investigations of the microphysical and chemical properties of particles emitted from aircraft engines during cruise and also from ground tests [1] – [5], combined with the quantification of the black carbon emissions from a globally operating aircraft fleet [6], initiated the European research project PartEmis on the "Measure-ment and prediction of emissions of aerosols and gaseous precursors from gas turbine engines". In the course of PartEmis, the impact of engine operation conditions, fuel sulphur content and particle processing in the turbine section of an aircraft engine simulator was investigated.

Particular emphasis was put on the investigation of the connection between particle chemistry and the formation of cloud droplets on these combustion particles, because this is the key process with respect to any indirect effects of aviation-related particles on the global climate, see Section 1. This category of experiments was needed for providing the knowledge on particle formation and particle processing in the engine which cannot be gained from airborne studies like conducted in the SULFUR experiments. PartEmis was thus expected to close the important gap of knowledge concerning particle emissions from aviation and their interaction with the atmosphere.

The author was responsible for the definition and coordination of the entire measurement methodologies applied during PartEmis. The key scientific subject of the author was the effect of engine operation conditions on the aerosol microphysical properties like particle number

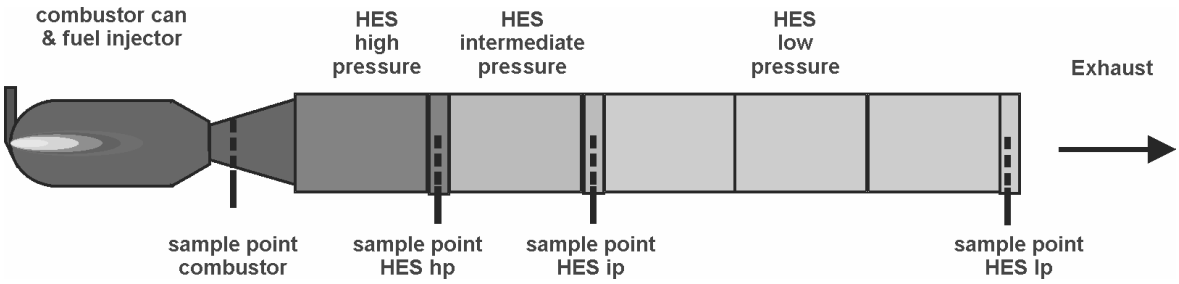

Figure 6.1. *Schematic of the PartEmis combustor and Hot End Simulator HES; the HES is composed of three separate heat exchanger stages, referred to as high (hp), intermediate (ip) and low pressure (lp) stage; taken from [10].*

density, particle size, aerosol mixing state, formation conditions for nucleating volatile particles, and particulate black carbon.

In the series of integrated journal publications two papers on PartEmis are discussed: (1) The effects of fuels sulphur content variation and combustor operation conditions on the microphysics and chemistry of particles in the exhaust plume [9], and (2) the summary of results gained during PartEmis [10]. Contrary to the preceding sections, these publications will be discussed in a single section, because a separation of the presented results is arbitrary.

As will be reported in Section 7 with more detail, the author also investigated one of the key subjects of PartEmis, the important effects of aerosol chemistry and potential cloud condensation nuclei activation of the emitted combustion aerosol. The material presented in Section 7 is not yet published, but is considered the synthesis of the PartEmis experiment.

Multi-Angle Absorption Photometry was applied in PartEmis for the first time to the exhaust from an aircraft engine. Keeping the ambiguities of the relation between aerosol light absorption and black carbon in mind, MAAP permitted the first time-resolved measurements of black carbon emissions form an engine. Since MAAP was also used for the measurement of the aerosol absorption coefficient and thus indirectly for black carbon in the free troposphere on the high alpine research station Jungfraujoch in Switzerland [7], data on the black carbon mass concentration were available for both exhaust plume and free troposphere, but measured with the same technique. These data are thus directly comparable without the

need for assessing different measurement methods. The conclusions from this comparison of concentration levels are discussed extensively in Section 8.

PartEmis was focussed on the characterisation and quantification of exhaust emissions from a gas turbine engine. The engine was composed of a combustor and a unit to simulate a 3-shaft turbine section (referred to as Hot End Simulator HES). The simulator is schematically shown in Figure 6.1. A comprehensive suite of aerosol, gas and chemi-ion measurements were conducted under different combustor and HES operating conditions and for different fuel sulphur concentrations. Measured aerosol properties were mass and number concentration, size distribution, mixing state, thermal stability of internally mixed particles, hygroscopicity, CCN activation potential, and chemical composition. PartEmis was a three-year program with experiments on the combustor in 2001 and on the combustor-HES combination in 2002.

The combustor operation conditions corresponded to modern and older engine gas path temperatures at cruise altitude, with fuel sulphur contents FSC of 50, 410, and 1270 mg kg^{-1}. The combustor behaved like a typical aircraft engine combustor with respect to thermodynamic data and main emissions, which suggested that the PartEmis database may be applicable to contemporary aircraft engines. Table 6.1 summarises the operation conditions of the combustor. PartEmis emission indices for the medium fuel sulphur content case are shown in Figure 6.2 together with mass and number emission indices from various in-flight studies. The order of aircraft types on the y-axis corresponds to an increasing engine certification year from bottom to top. The PartEmis emission indices fit well into this picture and represent a range of engines which are currently in use.

Table 6.1: Combustor operating conditions during the 2001 Combustor and 2002 HES campaigns.

Combustor Parameters	Combustor Campaign		HES Campaign	
	old	modern	old	modern
T combustor inlet, K	566	766	566	760
T combustor outlet, K	1125	1448	1125	1360
P combustor inlet, 10^5 Pa	7.05	8.2	7.05	8.2
Air mass flow, kg s^{-1}	2.12	2.12	1.90	2.05
Fuel flow, kg s^{-1}	0.032	0.042	0.030	0.035
Air fuel ratio	66	50.3	66	58

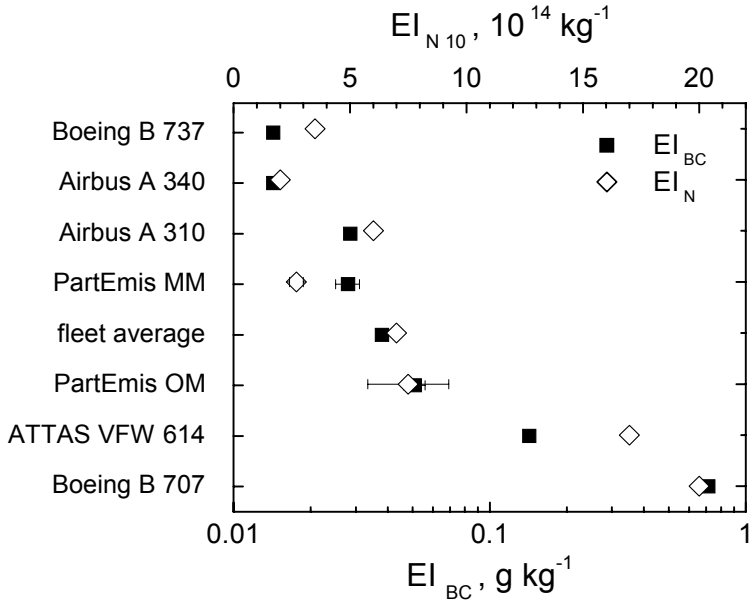

Figure 6.2. *Particle emission characteristics of the PartEmis combustor operated with medium FSC, plotted in the context of emission characteristics measured for aircraft at cruise conditions([6]; Schumann et al., 2002); taken from [9].*

The carbonaceous combustion aerosol was characterised in terms of number density, average size, black carbon mass concentration and total carbon mass concentration. Figure 6.3 summarises the behaviour of these properties for the entire PartEmis experimental matrix, i.e., for engine operation conditions “old” and “modern”, for three different fuel sulphur content levels, and for the combustor exit and the exit of the low pressure stage, corresponding to engine exit.

The combustor operating conditions had only a weak influence on the size, number and mass of emitted particles. The emissions for modern engines were lower than for older engines for all considered properties. This observation is in agreement with the results from earlier in-flight studies, see also Figure 6.2. Mean count median diameter values were 37 – 41 nm for old engine and 40 – 44 nm for modern engine conditions. The geometric standard deviation of the size distribution was 1.67 (1.6 – 1.8) for both operation conditions. Size distributions with comparable median diameters were observed during in-flight studies, e.g., [5].

Also the processing of the combustion particles during their transport through the engine turbine section did not show a significant influence on aerosol microphysical properties.

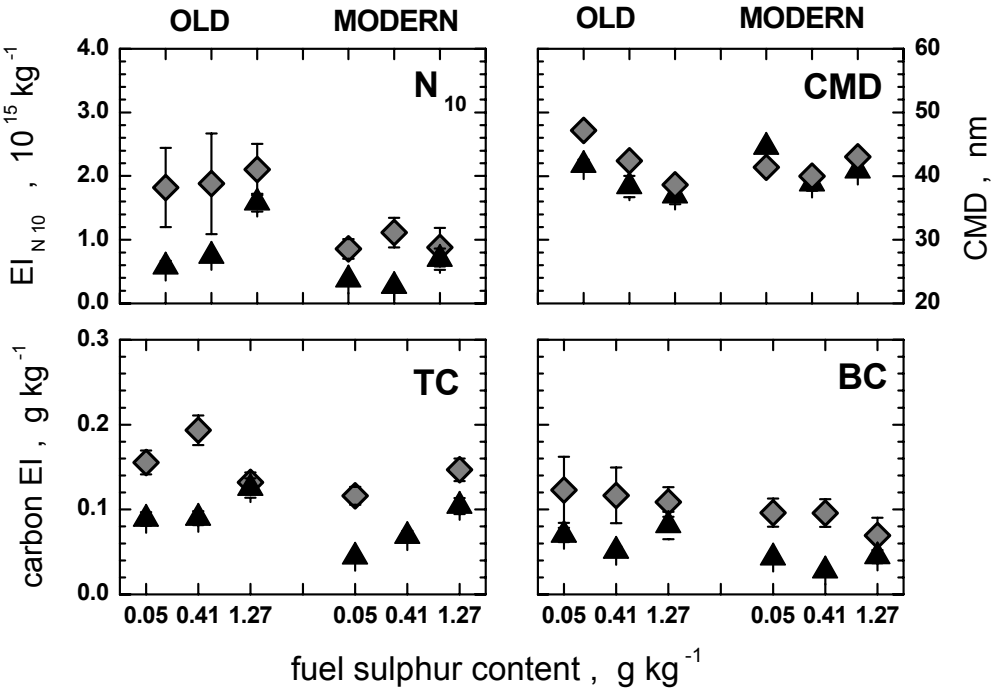

Figure 6.3. *Emission indices in terms of number (N_{10}), total carbon mass (TC), black carbon mass (BC) and CMD of the combustion aerosol for the Combustor exit (triangles) and the HES low pressure stage (diamonds); values are given for old and modern operation conditions as a function of the fuel sulphur content, error bars indicate signal variability in terms of ± 1 standard deviation; taken from [10].*

Figure 6.4 demonstrates the variation of black carbon mass emission and number emission indices from the combustor exit through the HES to the exit of the low pressure stage. The increase between the emission factors from the combustor to the combustor-HES combination is likely due to the fact that the operation conditions varied slightly between the two experiments.

As a first but very important conclusion, PartEmis demonstrated that the emission properties of an aircraft engine concerning carbonaceous combustion particles – which are considered the particle fraction in the exhaust of highest relevance - is almost completely determined by the combustor, while the remaining part of the engine has no significant influence. Any reduction of particle emissions from aircraft engines has thus to focus on the improvement of the combustion process.

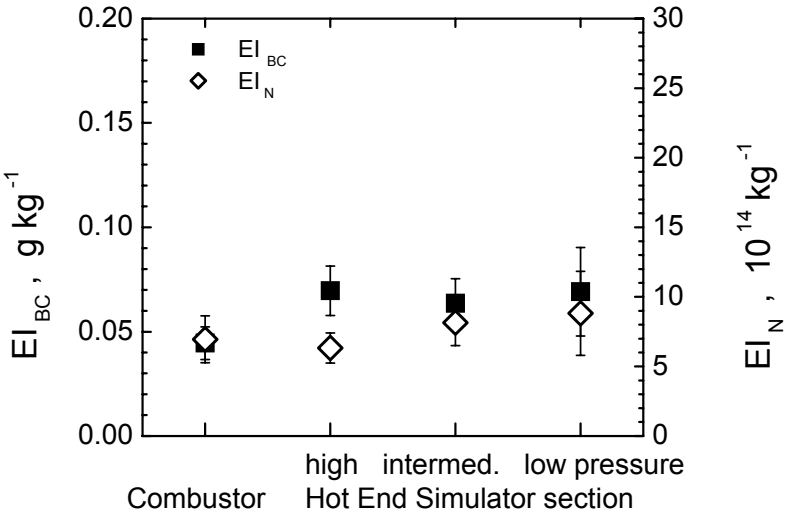

Figure 6.4. *Effect of the HES on the emission properties of the combustor-HES combi-nation operated at modern conditions, error bars indicate signal variability in terms of ± 1 standard deviation; taken from [10].*

Besides the carbonaceous combustion particles, also particles nucleated from gaseous precursors were detected. These particles occurred preferably in the size range D < 10 nm. The formation of volatile particles by nucleation was strongly depending on the fuel sulphur content. No particle nucleation was observed in the low and medium fuel sulphur experiments, while strong nucleation was measured during the high sulphur fuel experiments. Modelling studies using these experimental observations (Vancassel et al., 2003) supported the hypothesis, that the particle nucleation took place downstream the HES exit when the sample air was diluted. Nucleating particles are thus only indirect particulate exhaust products of an aircraft engine. Additional to the fuel sulphur content, another threshold condition for particle nucleation was the surface area of combustion particles being present in the exhaust gas. This aerosol surface may act as an additional sink for condensable gases and suppress thus particle nucleation. Indeed, particle nucleation was only observed when the surface are was below a threshold of 2300 $\mu m^2 cm^{-3}$.

The size of these nucleating particles was determined from an analysis of particle volatility. Nucleated particles are thermally not stable at T > 350°C, while combustion particle are thermally stable. Figure 6.5 shows the fraction of nonvolatile particles of the total aerosol for particles of size D = 15 nm as a function of the abundance of sub-10 nm particles in the total

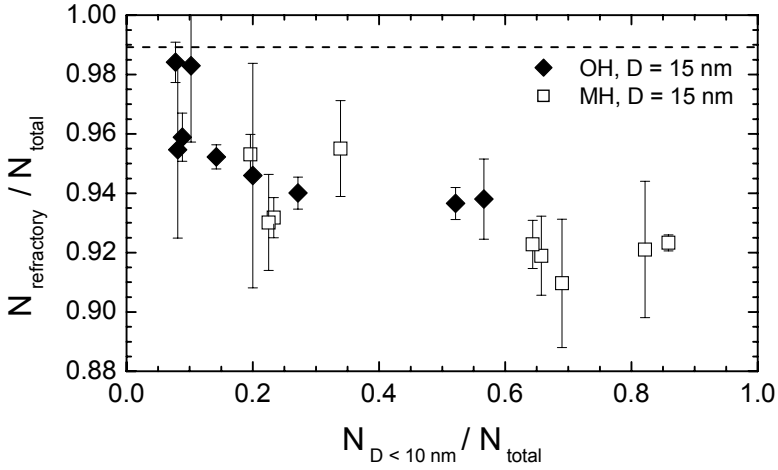

Figure 6.5. *Fraction of refractory particles (T = 625 K) of the total aerosol as a function of the fraction of ultrafine particles of size D < 10 nm of the total aerosol for sizes D = 15 nm (symbols) and D ≥ 30 nm (dashed line); taken from [9].*

aerosol. Even when sub-10 nm particles contributed 80% to the number concentration of the total aerosol, their contribution to particles of size D = 15 nm was < 10%, while their contribution to particles of size D = 30 nm was negligible. Hence, nucleating particles remained in the size range D > 10 nm, while combustion particles where to the largest extent > 10 nm.

The aerosol occurring in the exhaust of an aircraft engine is thus constituted by two different categories of particles:

(1) volatile H_2SO_4 - H_2O particles of size D ≤ 10 nm, which form downstream the engine in the plume or in the sampling line,

(2) nonvolatile carbonaceous combustion particles of size D > 10 nm which are covered by a thin H_2SO_4 - H_2O layer of less than 5% of the particle volume.

Modelling studies based on observations of particle and contrail properties at cruise altitude (e.g., Kärcher et al., 1998) predicted a contribution from liquid H_2SO_4 - H_2O particles to the formation of contrails. The role of these nucleated particles and the effect of the sulphuric

acid coating on the activation of combustion particles for the formation of cloud droplets are discussed in detail in the following Section 7.

Further to the detailed particle characterisation and the interaction of particle microphysics and particle chemistry in the process of cloud droplet formation, PartEmis provided numerous results of scientific importance which are summarised in [10]. The discussion of the PartEmis achievements in this section, however, was focused on the areas where the author made leading contributions to the experiment.

7 The Effects of Organic and Sulphur-containing Compounds on the CCN Activation of Combustion Particles

In PartEmis, data sets on aerosol microphysics, particle chemical composition, hygroscopic growth and cloud condensation nuclei activation were collected simultaneously from the exhaust gas of a real aircraft engine combustor. In this section, the effect of particle chemical composition and particle micro-physical properties on the potential cloud condensation nuclei activation of the combustion particles is discussed. The interaction of emitted combustion particles with the atmospheric water vapour in terms of cloud formation is one of the most important pathways of how exhaust particles may affect global climate. The material is published in *Atmospheric Chemistry and Physics* (Petzold et al., 2005).

7.1 Chemical Composition of Combustion Particles

During sampling the sampling probe was moved at fixed positions across the combustor exit plane in order to get a profile of the emissions, see Figure 7.1 and Wilson et al. (2004) for more details. The sampling probe was kept at each position for at least 20 min to allow for a sufficient sampling volume for each measurement method. In the case of filter samples, several probe positions were merged in order to meet the minimum required sample mass.

Due to the operation principle of an aircraft engine combustor, dilution air is fed into the combustion chamber downstream the combustion zone through holes in the wall of the chamber. As shown in Figure 7.1, the air to fuel ratio was distinctly higher at the outer

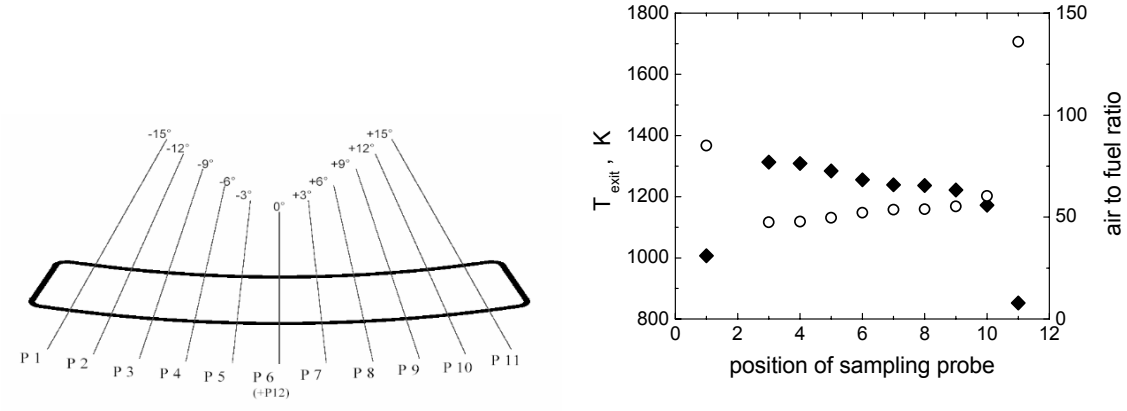

Figure 7.1. *Combustor exit temperature T_{ext} (filled symbols) and ratio of air to fuel (open symbols) for the sampling probe positions on the combustor exit nozzle plane (upper panel) during the operation at old cruise conditions.*

positions of the sampling probe close to the walls. The combustor exit temperature T_{exit} was lowest at the edge position and highest in the centre of the combustor exit plane. The emitted combustion aerosol was measured by in-situ methods for aerosol microphysical properties, hygroscopic growth factor and CCN activation, and collected on filter samples for chemical analysis [10]. Since the methods used for the characterisation of aerosol microphysical and hygroscopic properties worked in situ and were measuring simultaneously on the same aerosol sample, artefacts from wall effects or sample storage could be excluded.

The basic aerosol properties used for the presented study were the number density and particle size distribution of the combustion aerosol, the hygroscopic growth factors for defined particle sizes and relative humidity (Gysel et al., 2003), and the number of combustion particles activated as CCN at a supersaturation with respect to water of 0.6 - 0.7% (Hitzenberger et al., 2003). The fraction of CCN activated particles, or the activation ratio, respectively, was determined from the ratio of the number density of CCN and the number density N_{20} of combustion aerosol particles of size $D > 20$ nm in the sampled gas. The lower cut-off diameter of 20 nm was chosen in order to exclude possibly nucleated condensation particles from the analysis and to focus exclusively on the combustion aerosol particles.

The composition of the carbonaceous particle fraction was determined using multi-step combustion methods for the determination of TC and EC, and evolved gas analysis methods

EGA (Puxbaum, 1979) for measuring thermograms of the thermal stability of carbonaceous compounds. Figure 7.2 shows a set of thermograms. The CO_2 evolving at a given sample analysis temperature corresponds to the fraction of carbonaceous material which is oxidised at this temperature. Scanning the temperature up to approximately 850°C oxidises the complete carbonaceous material collected on the filter. A laser beam monitors the current transmittance of the filter sample. The definitions of carbonaceous material are: semivolatile organic carbon OC which evolves for T < 300°C, nonvolatile OC which evolves for T > 300°C but does not influence the filter transmittance, and EC which evolves at T > 600°C and increases filter transmittance. The total carbon is TC = semivol OV + nonvol OC + EC.

The TC and EC contents of the filter samples were determined simultaneously using multi-step combustion methods: TC was measured by burning the entire filter sample and measuring the evolving CO_2. EC was determined according to Cachier et al. (1989) by oxidising the OC during two hours of filter treatment at 340°C, the remaining carbonaceous material is then defined as EC. BC was determined using Multi-Angle Absorption Photometry [7].

The OC fraction of TC depends on the exhaust gas temperature and thus on the air to fuel ratio and on the combustion temperature, see Figure 7.3. Higher combustion temperature and thus a more complete combustion lead to a lower OC fraction of TC. Exemplary thermograms are compiled in Figure 7.2 for different sectors of the combustor exit plane. While the EC peak dominates the spectrum for all cases, the intensity of semi- and nonvolatile OC peaks vary distinctly with the sampling probe position. Since the combustor exit temperature varied with the position of the sampling probe, a similar effect is expected for the combustor exit plane profile of the CCN activation ratio, if the OC/EC partitioning has an effect on the CCN activation.

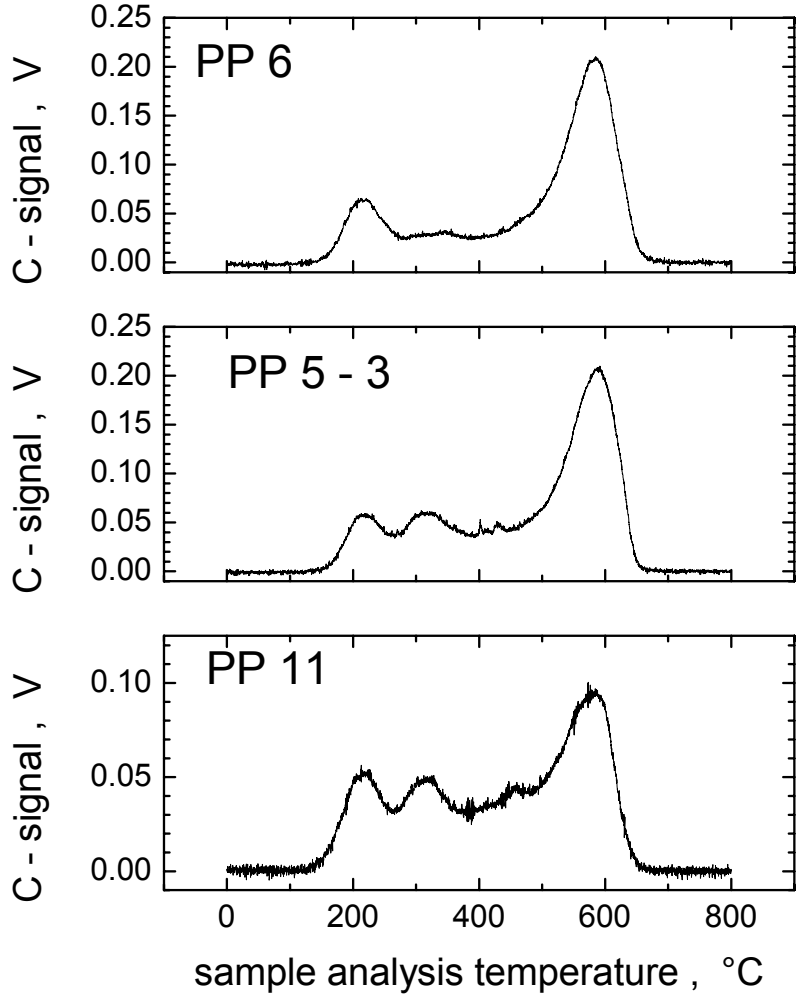

***Figure 7.2**. Thermograms of filter samples taken at central (top panel), intermediate (mid panel) and edge (bottom panel) positions of the combustor exit plane; the temperature ramp was 20 K min^{-1}.*

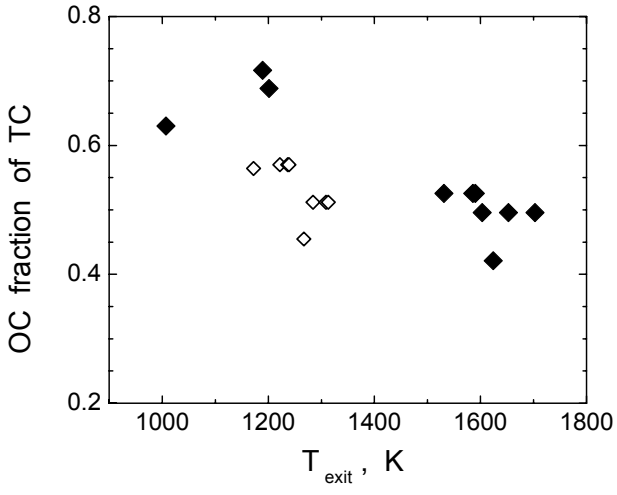

***Figure 7.3.** The organic fraction of total carbon as a function of the combustor exit temperature for the medium FSC case; open (full) symbols indicate data for old (modern) cruise conditions.*

7.2 CCN Activation of Sulphuric Acid-Coated Combustion Particles

The activation of combustion particles can be described in terms of Köhler theory (Pruppacher and Klett, 1997). The Köhler equation relates the equilibrium saturation ratio S_w with respect to water for a given solution droplet to its chemical composition or water activity, respectively, and to the droplet size

$$S_w = a_w \times \exp\left[\frac{4\, M_w\, \sigma_{sol}}{RT\, \rho_w\, D_{eq}}\right] \quad .$$

Water activity a_w and surface tension σ_{sol} of the solution are parameterised as a function of ist chemical composition. M_w and ρ_w are water molecular weight and water density. In the case of combustion aerosol covered by a sulphuric acid layer, the carbonaceous particle core is treated as an insoluble nucleus. The solution forming on the particle at a given saturation ratio S_w is composed of H_2SO_4 and H_2O. Depending on the water activity of the solution, the equilibrium water vapour pressure above the droplet may be below water saturation over a flat water surface ($S_w < 1$), or above ($S_w > 1$). The saturation ratio at subsaturated conditions is

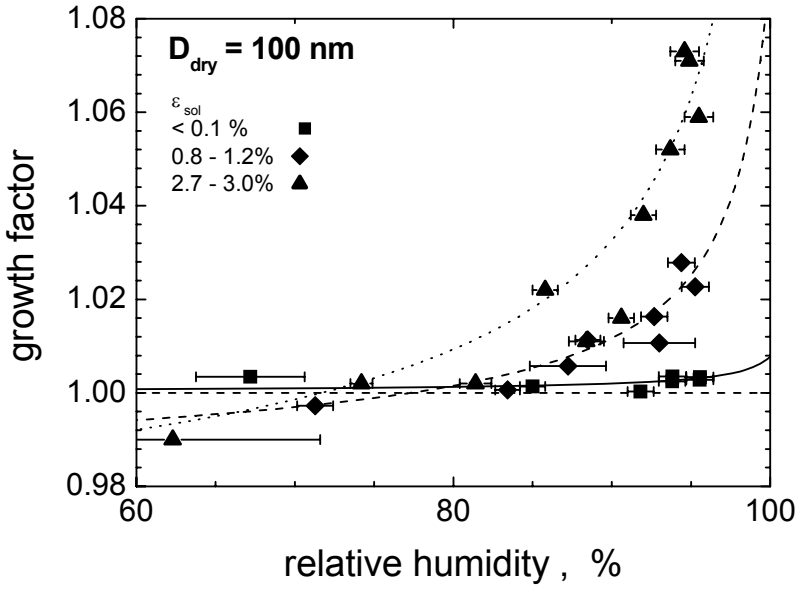

Figure 7.4. *Humidity growth of particles of initial size D_{dry} = 100 nm as a function of relative humidity for low, medium and high fuel sulphur cases; lines represent growth curves determined from Köhler theory for the indicated volume fractions of soluble matter* ε_{sol} .

also expressed as relative humidity with RH = 100 S_w . If the particle contains no water-soluble components, $a_w = 1$ and the Köhler equation reduces to the Kelvin equation.

Basically two models were deployed to calculate activation diameters for certain supersaturations and resulting activation ratios for the measured size distributions. The roughest approximation is the assumption of an insoluble graphite core which undergoes a Kelvin-type activation process. A more sophisticated approach is based on a coated-sphere model, where the activation diameter is estimated from measured particle humidity growth factors. This model uses experimental growth factor data and does not require any assumptions on particle composition and solubility.

The growth factor is defined as the ratio between the particle diameter at a certain saturation ratio and the particle diameter of the dry particle

$$g = \frac{D_{eq}(S_w)}{D_{dry}} = \frac{D_{eq}(RH)}{D_{dry}} \quad .$$

If the particle contains an insoluble core which is coated by a water-soluble layer of volume fraction ε_{sol}, only the water-soluble material can grow by water uptake (Gysel et al., 2003)

$$g(S_w) = \left[1 + \varepsilon_{sol}\left(g_{sol}^3(S_w) - 1\right)\right]^{1/3}$$

$g_{sol}(S_w)$ denotes the theoretical growth factor for a pure soluble particle of similar size and can be calculated by Köhler theory.

The experimental particle growth factors were determined using the Hygroscopicity Tandem Differential Mobility Analyser technique H-TDMA (Weingartner et al., 2002; Gysel et al., 2002). Figure 7.4 shows growth curves for particles of dry size 100 nm, measured with a H-TDMA and modelled with Köhler theory. The volume fraction of water-soluble matter ε_{sol} was used as a fitting parameter. The obtained volume fractions were $\varepsilon_{sol} < 0.1\%$ for low FSC, $\varepsilon_{sol} = 0.8 - 1.2\%$ for medium FSC and $\varepsilon_{sol} = 2.7 - 3.0\%$ for high FSC. Respective values for smaller particles are given by Gysel et al. (2003).

Table 7.1: Activation ratios N_{CCN} / N for liquid water clouds and Contrails for pure insoluble particles ($\varepsilon_{sol} = 0\%$) and coated combustion particles ($\varepsilon_{sol} = 3\%$).

	S_w	ε_{sol}	N_{CCN} / N
Water cloud	1.006	0%	10^{-4}
		3%	$\geq 10^{-2}$
Contrail	1.05	0%	0.25
		3%	0.53

Substituting D_{eq} by $g \times D_{dry}$ yields the modified Köhler equation

$$S_w = a_w \times \exp\left[\frac{4\, M_w\, \sigma_{sol}}{RT\, \rho_w\, g\,(S_w\,,\, \varepsilon_{sol})\, D_{dry}}\right] \quad .$$

From this equation, the equilibrium water vapour pressure can be calculated over particles, consisting of an insoluble core and a layer of water-soluble sulphuric acid of volume fraction of ε_{sol}.

Figure 7.5 shows these so-called Köhler curves for various values of ε_{sol}. The grey shaded area indicates the saturation ratio with respect to water at which the CCN counter used during PartEmis (Giebl et al., 2002) was operated. The drop diameter corresponding to the maximum S_w value, or critical saturation ratio respectively, is the critical diameter which is required for droplet activation at S_w. The mid panel of Figure 7.5 shows the corresponding critical saturation ratios required for the activation of a coated particle of size D_{dry} for droplet formation. The impact of the sulphuric acid coating of the combustion particles on their activation for cloud droplet formation becomes clearly visible.

For the experimental determination of the activation diameter, the number of droplets forming in the CCN counter was normalised to the number of combustion particles entering the counter. The corresponding number size distributions were integrated from the maximum diameter 0.5 µm to smaller sizes until the integrated fraction equalled the activation ratio. The threshold diameter was set as activation diameter D_{CCN}, i.e.,

$$\frac{N_{CCN}}{N_{20}} = \frac{\int_{D_{CCN}}^{0.5} n(D)\, d\log D}{\int_{0.02}^{0.5} n(D)\, d\log D} \quad .$$

As is demonstrated in the bottom panel of Figure 7.5, all average activation diameters determined for the different fuel sulphur runs of the combustor agree well with a saturation ratio of 1.006 inside the CCN counter. This saturation ratio is of similar magnitude as observed in natural liquid water clouds.

Table 7.1 summarises the activation ratios expected for a typical combustion aerosol size distribution as measured in the exhaust of the PartEmis combustor. Values are compiled for pure insoluble graphite particles without coating ($\varepsilon_{sol} = 0\%$) and for combustion particles coated with 3 vol.-% sulphuric acid. Considered cases are a liquid water cloud at $S_w = 1.006$ and a contrail in its early stage at $S_w = 1.05$. The coating of graphite particles with sulphuric acid increases the activation ratio for liquid water cloud conditions by two orders of magnitude from 10^{-4} to $> 10^{-2}$. However, even coated but young combustion particles are still poor CCN.

At high saturation ratios of 1.05 occurring in very young contrails, about one fourth of all particles become activated if they are not coated. In the case of coated particles, every second particle becomes activated. It is known from observations in contrails, that 1/3 of emitted combustion particles are incorporated into or attached to contrail ice particles ([2]; Schröder et al., 1998; Kuhn et al., 1998). This fraction of combustion particles associated with the contrail ice phase at cruise altitude is in remarkably close agreement with the conclusions drawn from PartEmis for the activation of combustion particles in contrails.

The position of the activation diameters with respect to the size distribution of the combustion aerosol measured during PartEmis is shown in Figure 7.6. The ratios of the marked areas to the total area under the size distribution illustrate the activation ratio for a certain condition. Since for $S_w = 1.006$ D_{CCN} is positioned at the large-size tail of the size distribution, a small decrease in D_{CCN} has a large effect on the activation ratio. In contrast, the activation diameter for contrail conditions of $S_w = 1.05$ lies close to the maximum of the size distribution. Thus, a decrease in D_{CCN} has only a weak effect on the activation ratio.

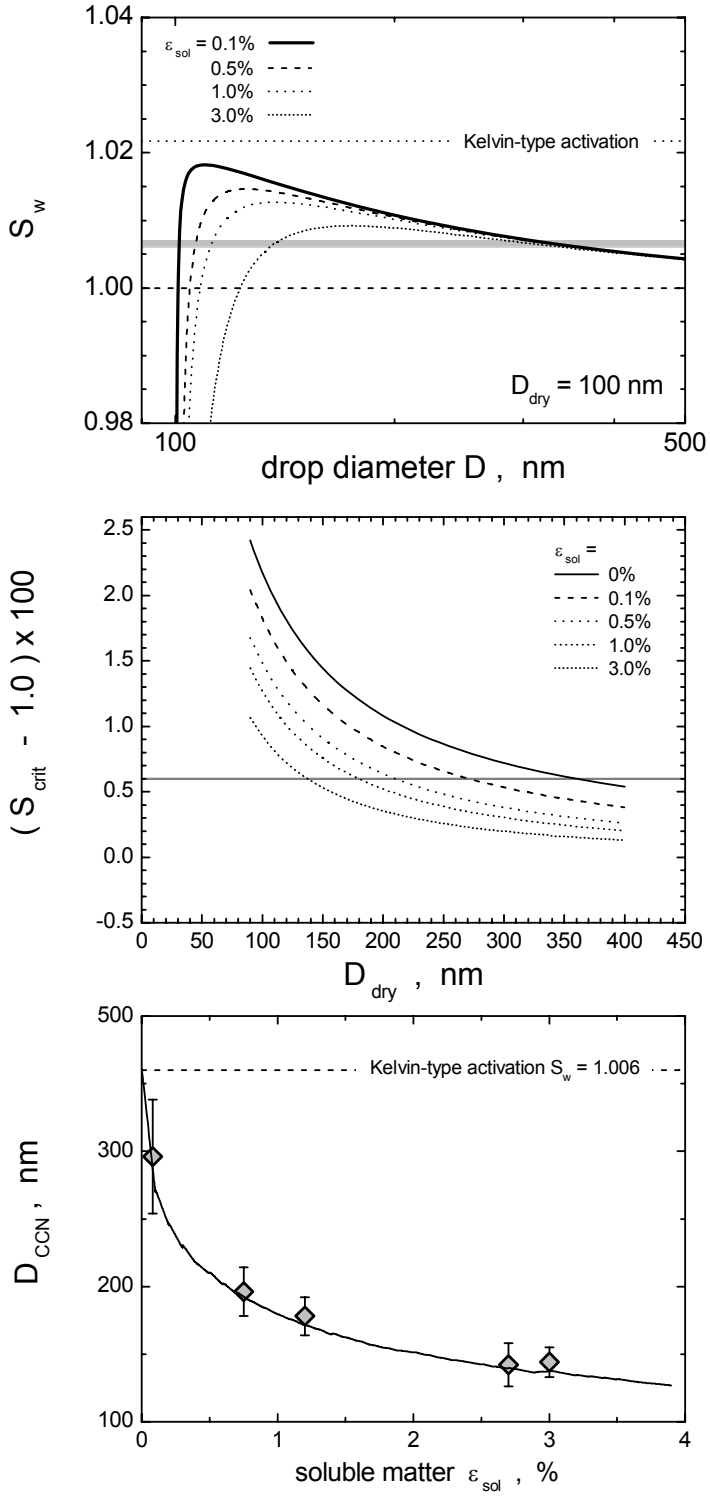

Figure 7.5. *Top panel: variation of the equilibrium vapour pressure over an aqueous solution drop formed from an insoluble carbonaceous nucleus covered with ε_{sol} volume-% of sulphuric acid in the dry particle state; mid panel: critical saturation ratio for coated particles of dry size D_{dry}; bottom panel: activation diameter D_{CCN} for insoluble particles coated with ε_{sol} volume-% of sulphuric acid, symbols represent the measured activation diameters, the lines show results from Köhler theory for the indicated saturation ratios.*

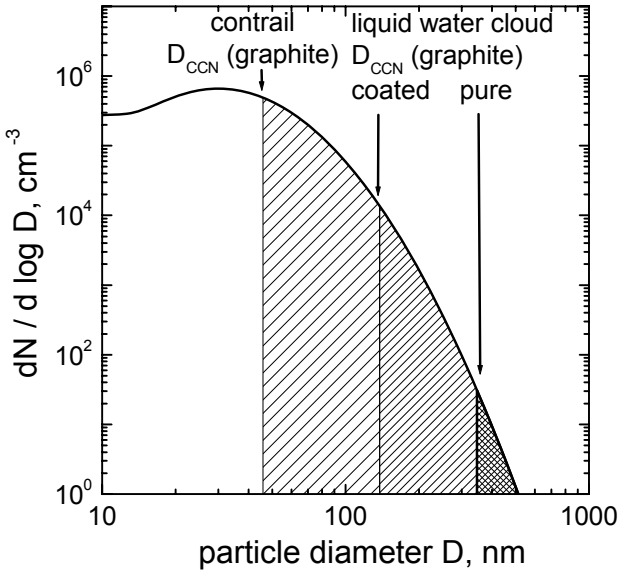

Figure 7.6. *CCN activation diameters for pure and coated particles at liquid water cloud conditions (S_w = 1.006) and contrail conditions (S_w = 1.05), marked areas under the combustion particle size distribution represent the number of activated particles.*

The values listed in Table 7.1 also indicate that a coating of combustion particles with sulphuric acid has only a weak effect on the activation of combustion particles for contrail formation at high saturation ratios. The activation ratio increases from 0.25 for pure insoluble particles to ≥ 0.5 for coated particles which is a factor of 2. Referring to the observations of the impact of the fuel sulphur content on the properties of contrails [1], only a weak effect of the FSC on the number of contrail particles was found.

As discussed in Section 2, the number of ice crystals in the contrail of the ATTAS aircraft increased from 1500 to 2000 particles per cm^3 when the fuel sulphur content was increased from 2 to 2700 mg kg^{-1}. A microphysical explanation for this observation is given in Figure 7.6.

7.3 CCN Activation of Combustion Particles with a High OC Fraction

The humidity growth factors and resulting CCN activation diameters for the different experimental parameters, i.e., old and modern conditions and fuel sulphur content levels, were determined from one set of data points at each experimental condition. Each data set consisted of humidity growth factors which were measured during the scan of the sampling probe

across the nozzle exit plane. The overall humidity growth behaviour of the combustion particles at the given experimental condition was determined from the entire data set, as can be seen in Figure 7.4.

The scans of the sampling probe included the edge positions, which showed a significant deviation in the OC-fraction of TC compared to the samples from the centre of the nozzle exit plane. Figure 7.7 demonstrates exemplary that not only the OC-TC fraction was different for particles sampled at the edge positions, but also the growth behaviour. This observation was a first indicator of a likely influence of the OC fraction of TC on the growth behaviour of combustion particles.

In order to investigate whether there is an impact of the OC fraction of TC on the CCN activation, the activation diameters measured at each sampling probe position were normalised to the ensemble value determined from the growth curves via Köhler theory. In Figure7.8, these ratios D_{CCN}(exp) / D_{CCN}(mod) are plotted as function of the semivolatile OC fraction of TC (left) and the nonvolatile OC fraction of TC (right). Increasing the fraction of nonvolatile OC increases the activation diameter. i.e., less particles are activated as is shown in the mid panel of Figure 7.6, and the activation ratio N_{CCN} / N decreases.

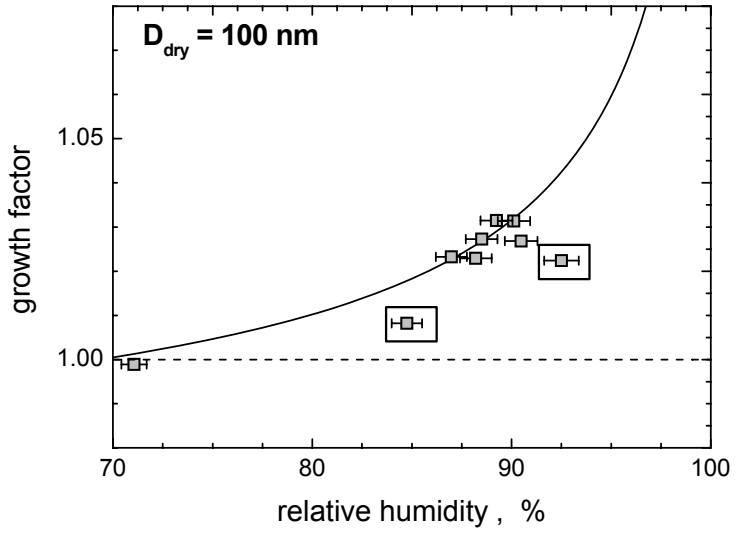

Figure 7.7. *Humidity growth of particles of initial size D_0 = 100 nm as a function of relative humidity for the high fuel sulphur case; the indicated data points correspond to sampling points at the edge positions of the combustor exit nozzle plane.*

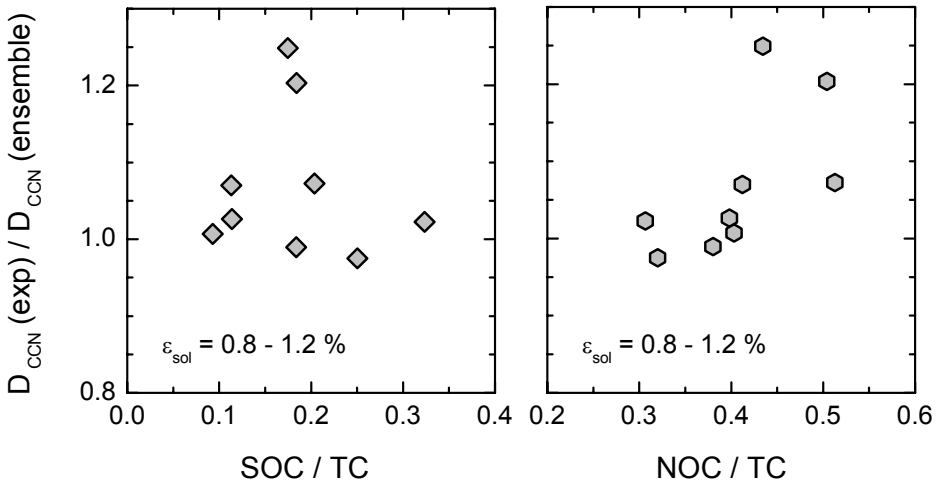

Figure 7.8. *Ratio of experimental CCN activation diameter to the ensemble CCN diameter determined from humidity growth factors, as a function of the semivolatile OC fraction of TC (left) and the nonvolatile OC fraction of TC (right).*

Table 7.2: Activation diameter D_{CCN} and activation ratio N_{CCN} / N for the investigated coated and non-coated combustion particles for a saturation ratio $S_w = 1.006$

	Coating	Activation diameter	Activation ratio
Particle type	ε_{sol} , %	D_{CCN} , nm	N_{CCN} / N
insoluble	0	360	10^{-4}
H_2SO_4 - coated	0.1	290 ± 43	$(8 \pm 2) \times 10^{-4}$
H_2SO_4 - coated	0.8	190 ± 12	$(2 \pm 0.6) \times 10^{-3}$
H_2SO_4 - coated	1.2	178 ± 14	$(4 \pm 1) \times 10^{-3}$
H_2SO_4 - coated,	0.8	237	9×10^{-4}
nonvol. OC fraction = 0.5	1.2	205	3×10^{-3}
H_2SO_4 - coated	2.7	144 ± 6	$(7 \pm 1) \times 10^{-3}$
H_2SO_4 - coated	3.0	142 ± 9	$(1 \pm 0.5) \times 10^{-2}$

Thus, an increasing fraction of nonvolatile OC compounds reduces the ability of combustion particles for CCN activation significantly. For the semivolatile OC no such trend is observable. The maximum increase in CCN activation diameter is ≅ 30% which translates into a reduction of the activation ratio from 2×10^{-3} to 9×10^{-4} for particles coated with 0.8% sulphuric acid. Table 7.2 summarises the effects of particle coating and organic content on the CCN activation of combustion particles, based on the observations during PartEmis. Already

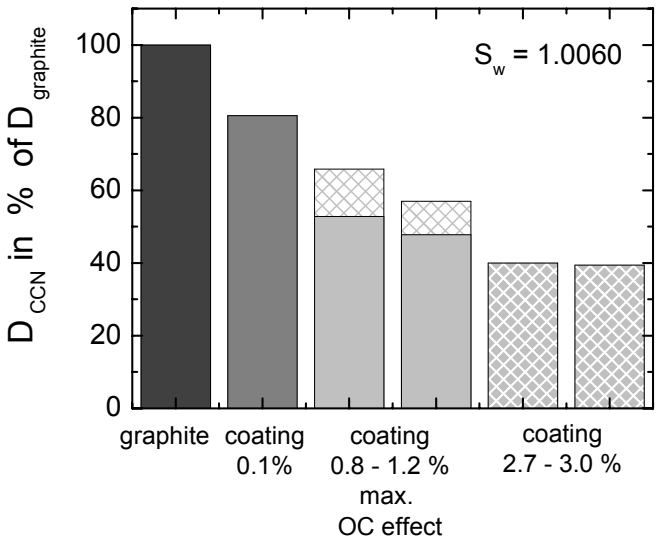

Figure 7.9. *Relative contribution of particle coating with sulphuric acid and large fraction of non-volatile OC to the change in the activation diameter of an initial graphite particle.*

a large effect occurs at the transition from the pure insoluble particle to the particle coated weakly with water-soluble substances.

The presented analysis is far from being quantitative, and the experimental data are limited. However, it presents important experimental material for the discussion on how organic components influence the CCN activity of internally mixed particles. Research on this subject focused so far on the role of organic acids and water soluble organic matter. The experiments showed that soluble organic compounds activate according to Köhler theory whereas highly insoluble species do not activate at atmospherically relevant super-saturations (e.g., Novakov and Corrigan, 1996; Giebl et al., 2002; Broekhuizen et al., 2004). For an urban aerosol which likely contains larger fractions of combustion particles, Saxena and co-workers (1995) reported that organic compounds diminish water adsorption of the inorganic fraction by about 30%, while for non-urban aerosol the organic fraction increases the water adsorption. The PartEmis results for combustion particles point in the same direction as the observations for urban aerosol particles.

As a final assessment of the competing effects of sulphur-containing and organic compounds on the CCN activation of combustion particles, the reduction of the activation diameter with

respect to a Kelvin-type activation of insoluble graphite particles is plotted in Figure 7.9. Coating the insoluble particle with 0.1 volume-% of sulphuric acid reduces the activation diameter by 15% with respect to Kelvin type activation. Coating the particle with approx. 1.0 and 3.0 volume-%, respectively, the reduction of the CCN activation diameter is ≅ 50% and 60%. In contrast, a high fraction of nonvolatile organic compounds increases the activation diameter by maximum 30%.

Summarising, a large fraction of nonvolatile organic compounds of combustion aerosol particles has a significant effect on the potential CCN activation. While a coating with water-soluble sulphuric acid increases the potential CCN activation, or reduces the activation diameter, respectively, the organic compounds compensate this sulphuric acid-related improvement in CCN activation by about one third of the effect.

8 Assessment of the Atmospheric Impact of Particle Emissions from Aviation and Outlook

The discussion of the aerosol-climate interaction in Section 1 and the scientific results presented in Sections 2 to 7 highlighted the importance of particulate black carbon for the impact of aviation on atmosphere and climate. The particulate emissions from aviation were characterised under real conditions at cruise altitude ([1] – [6]) and under simulated cruise conditions in test stand experiments at ground [9; 10]. A new method for the measurement of particulate black carbon was introduced [7; 8] and applied to the measurement in exhaust gas samples and in the clean polluted troposphere.

The final section combines the results presented in the preceding sections with yet unpublished observations of aerosol properties in the troposphere by the author in order to assess the impact of particulate emissions from aviation on the global climate on an observational basis. The results will be compared to the recent global assessment of aviation impact on the global climate from the European TRADEOFF project.

Applying the correlation method [6] to an inventory of globally operating aircraft and taking appropriate mission patterns into account, the altitude profiles of fuel consumption and BC emission as shown in Figure 8.1 were obtained. During ground operation and climb up to

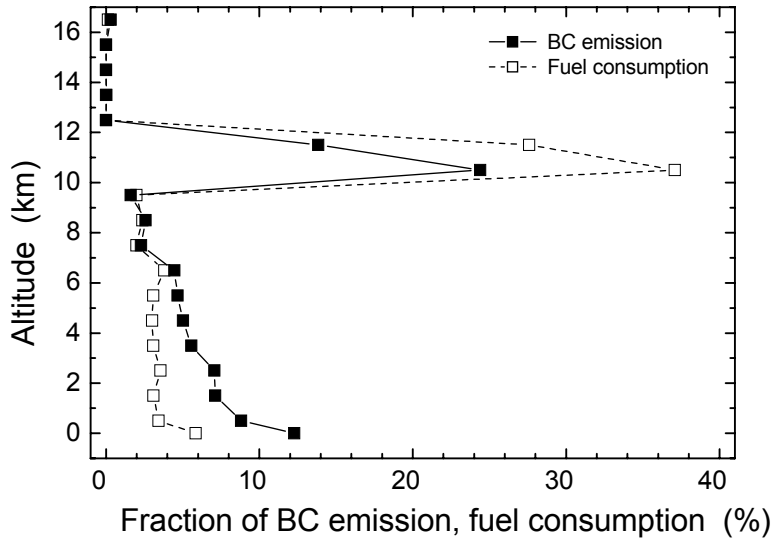

Figure 8.1. *Vertical distribution of aircraft-related BC emission and fuel consumption.*

3 km altitude, 16% of total fuel is consumed and 35% of aviation-related BC is emitted, while 67% of total fuel consumption and 40% of aviation BC emissions occur in the main air traffic altitude band at 9 – 13 km altitude in the upper troposphere-lowermost stratosphere, or UTLS region, respectively.

The mesoscale impact of aviation on the BC loading of the upper troposphere and lower stratosphere, e.g., in the North Atlantic flight corridor region, was estimated from an aircraft fleet-averaged ratio $EI(BC)/EI(NO_x) \cong 2.6\times10^{-3}$ g BC $(g\ NO_2)^{-1}$ at the engine nozzle exit plane (Döpelheuer, 1997, 2002) and an overall increase of the atmospheric NO_x level in the flight corridor by 100 pmol mol^{-1} due to aviation (Schlager et al., 1997). This estimate yields an aviation-related excess BC mass loading of 0.54 ng m^{-3} in the North Atlantic flight corridor [6]. Using average combustion particle size distributions in the exhaust plume, this value transfers into an excess number density of 17 cm^{-3}. This value is close to the observed number density enhancement of 30 cm^{-3} attributed to aircraft in the North Atlantic flight corridor (Schlager et al., 1997).

A rough estimate of BC deposited by aircraft in the tropopause region of the northern hemisphere yielded an excess BC mass concentration of ≤ 0.1 ng m^{-3} , when an annual fuel consumption of 1.36×10^{11} kg and an average tropopause residence time of 15 days were assumed. There are currently no accepted measurements of the tropospheric background black carbon mass concentration available. The average value of $\cong 1$ ng m^{-3} as reported by Blake and Kato (1995) is still under debate because wire impactors with unknown collection efficiency were used for sampling (Strawa et al., 1999). Nevertheless, the observations reported in [2] and by Kuhn et al. (1998) indicated a background value of a similar magnitude.

Another approach for estimating the tropospheric background level uses results from long-term measurements of the black carbon mass concentration with MAAP on the high-alpine research station Jungfraujoch at an elevation of 3450 m above sea level. The first annual cycle from MAAP data is shown in Figure 8.2. The minimum mass concentration in November 2003 was 3 ng m^{-3}. A statistical analysis of the entire data set yields a 5-percentile value of 8 ng m^{-3}. The measurement station is expected to be in late fall in the free background troposphere. An analysis of the vertical profiles of nonvolatile particles over Europe during

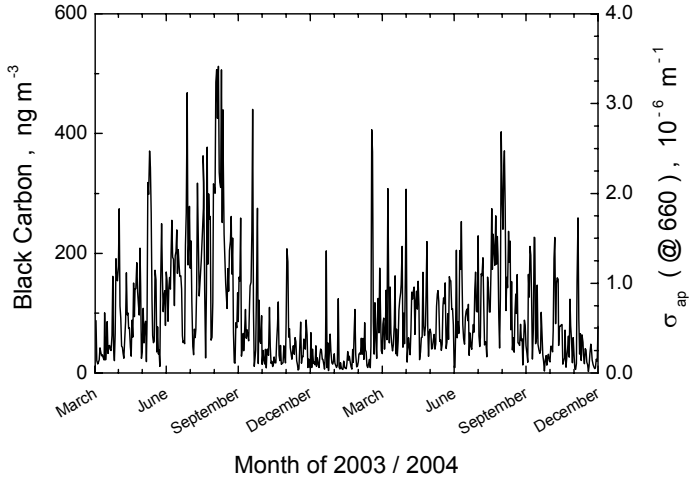

Figure 8.2. *Annual variation of the 24h average black carbon mass concentration on the high-alpine research station Jungfraujoch (CH) at an elevation of 3450 m above sea level; the BC mass concentration was calculated from the aerosol absorption coefficient.*

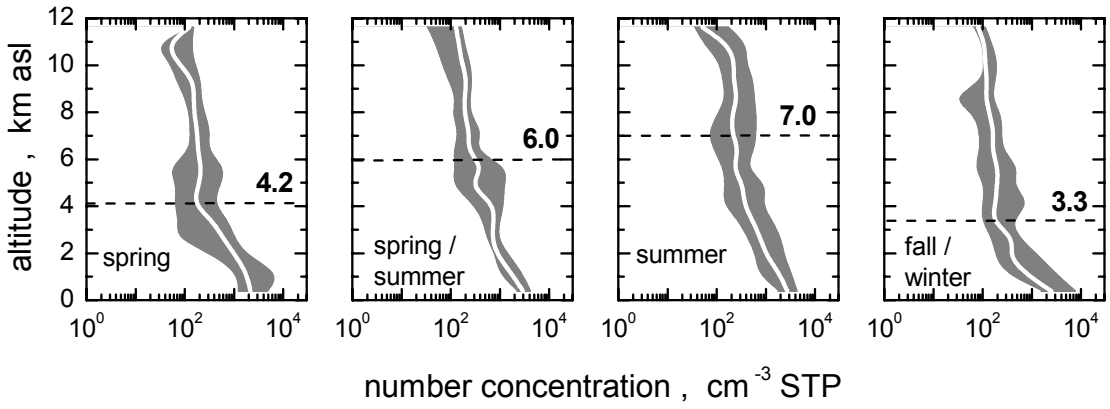

Figure 8.3. *Vertical profiles of the nonvolatile particles in the tropospheric aerosol; the data were collected over continental Europe during the indicated seasons in the years 2000 to 2002. Vertical profiles are given as median concentration values (white line) for standard conditions (273 K, 1013 hPa), the variability is indicated by the difference between 90-percentile and 10-percetile values (grey area). The inserted lines indicate the transition altitude between boundary-layer influenced lower troposphere and hemispheric background free troposphere.*

different seasons of the year supports this assumption. The vertical distributions used for this analysis originate from several aerosol-focused field experiments in continental Europe between 1998 and 2002 with the leading participation of the author. Some data are already

Table 8.1: Number concentration N of non-volatile particles in the upper free troposphere UT of the northern hemisphere NH and at the level of the Jungfraujoch JFJ research station, derived from the vertical aerosol profiles; black carbon mass concentration c_{BC} at JFJ and extrapolated UT concentration level

	Spring	Summer	Fall/ Winter
NH continental N, cm^{-3} AMB			
UT (9 - 11 km)	55	55	30
JFJ (3.5 km)	150	270	110
Jungfraujoch c_{BC}, $ng\ m^{-3}$			
5-percetile			8
Minimum			3
UT estimated			< 1 - 2.5

published, e.g., for the Lindenberg Aerosol Characterisation Experiment LACE 98 (Petzold et al., 2002b) and for the INCA experiment (Minikin et al., 2003). Figure 8.3 summarises the vertical distribution of nonvolatile particles as observed during these field experiments. All profiles exhibit similar features: (1) in the lower altitudes a clear influence of ground-based sources is identified and results in a vertical gradient of the number density; (2) at a certain altitude, the number density gradient almost vanishes and the free tropospheric background is entered; (3) close to the tropopause level, the influence of clean stratospheric air masses becomes visible.

Assuming that the vertical profile of black carbon mass concentration is proportional to the vertical profile of the nonvolatile particles, the free tropospheric background at 10 km altitude can be estimated. 5% of the measured BC mass concentration data at Jungfraujoch are below $8\ ng\ m^{-3}$. In late fall/winter, the number concentration of nonvolatile particles over continental Europe lowers from $110\ cm^{-3}$ at JFJ altitude to $30\ cm^{-3}$ at UT altitude. The corresponding BC mass concentration level at UT altitude is $2.5\ ng\ m^{-3}$ with respect to the 5-percentile value and $< 1\ ng\ m^{-3}$ with respect to the minimum value. The discussed values are compiled in Table 8.1. They are in close agreement with values estimated from observations (Baumgardner et al., 2004) and with results from recent model studies (Hendricks et al., 2004). Hendricks et al. (2004) report a range of $0.1 – 10\ ng\ m^{-3}$ for BC mass concentration in the global UTLS region and $> 1\ ng\ m^{-3}$ at northern midlatitudes. The radiative impact of aviation related particle emissions on the atmosphere is estimated from the excess BC mass.

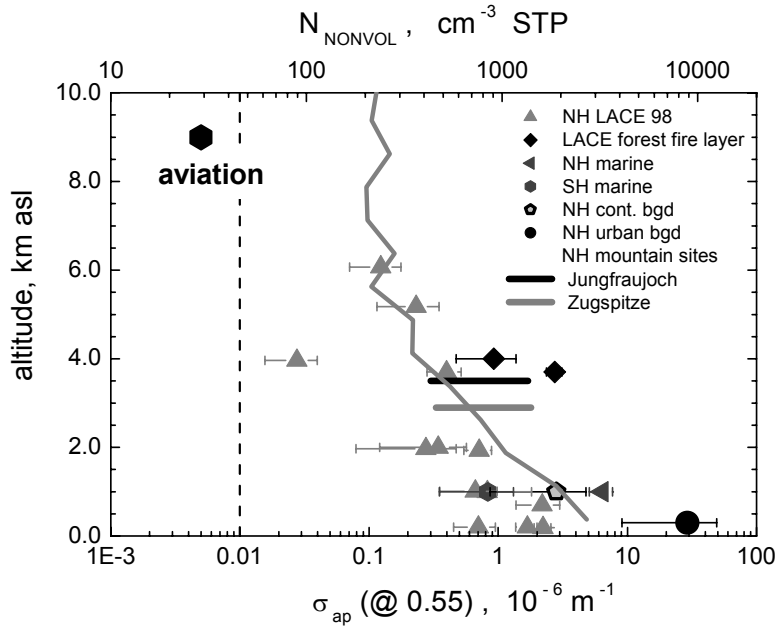

Figure 8.4. *Aerosol absorption coefficients measured at various sites in the northern hemisphere during the experiments LACE 98 (Petzold et al., 2002b) and INCA (Minikin et al., 2003) and during the testing of the MAAP on Zugspitze, Jungfraujoch (JFJ) and at urban sites [7], and in the southern hemisphere (INCA); the vertical profile of nonvolatile particles over continental Europe in summer was taken from Figure 8.3. The contribution of aviation is estimated from the excess black carbon released by aviation into the upper free troposphere.*

Aviation releases 0.5 ng m^{-3} into the atmosphere in air traffic polluted regions. Using a mass-specific absorption coefficient $b_{ap}^{(BC)} = 10\ m^2\ g^{-1}$ at $\lambda = 550$ nm, yields an absorption coefficient $\sigma_{ap} = 5 \times 10^{-9}\ m^{-1}$ via $\sigma_{ap} = c_{BC} \times b_{ap}^{(BC)}$. If the excess BC mass loading extends over the entire flight corridor altitude from 9 to 13 km, this loading causes an additional optical depth of 2×10^{-5}.

Applying the concept of radiative forcing potential by Haywood and Shine (1995), the aerosol forcing term $\Delta F\uparrow$ as a function of δ_λ can be calculated for a single aerosol layer in combination with the solar constant S_0, the atmospheric transmission T_{at}, the fractional cloud coverage A_c, and the surface albedo R_s

$$\Delta F\uparrow / \delta_\lambda \cong -\tfrac{1}{2} S_0\ T_{at}^2\ (1-A_c)\ \omega_0\ \overline{\beta}\ \left\{(1-R_s)^2 - (2R_s / \overline{\beta})\ (1/\omega_0 - 1)\right\}$$

The factor ½ accounts for the day length. To obtain results comparable to literature data,

S_0 = 1370 W m^{-2}, T_{at} = 0.76, A_c = 0.6 and R_s = 0.15 are to be used. Input data ω_0 and $\bar{\beta}$ were calculated for black carbon particles in aircraft engine exhaust.

Petzold et al. (2002b) determined forcing terms for continental aerosol of –20 to – 30 W m^{-2}, indicating a negative forcing or cooling effect. For a typical aircraft exhaust aerosol [5], a value of +35 W m^{-2} is found. Although this combustion aerosol would cause a highly net positive forcing, this translates into a direct aviation-related forcing in the flight corridor of only 0.7 mW m^{-2} due to the very low optical depth of 2×10^{-5}. The radiative effects of sulphate-water particles from aviation are highly speculative because the size of these particles depends strongly on atmospheric conditions like air temperature and relative humidity. An estimate for the radiative effects caused by volatile particles is thus not given here.

Table 8.2 compiles estimated radiative effects from the air traffic-impacted UTLS region in flight corridors and radiative forcing terms determined in the course of the European TRADEOFF project (Sausen et al., 2005) for the entire tropospheric column, including landing and take-off emissions. The estimated direct forcing in the flight corridor is of similar magnitude as the value calculated from emission inventories and global fuel consumption in TRADEOFF. Although flight corridor values and global-scale values are not comparable, the good agreement of at least the order of magnitude of the radiative effects supports the presented estimate based on observational data.

Table 8.2: Climate effects of aviation: values are estimated from observations and taken from the European TRADEOFF study (Sausen et al., 2005)

Observations		
Aerosol optical depth	NH midlatitudes	0.3
	Flight corridor	2×10^{-5}
direct BC forcing	Flight corridor	0.7 mW m^{-2}
TRADEOFF		
direct BC forcing	Troposphere	2.5 mW m^{-2}
Contrails		7 mW m^{-2}
Aviation	excluding cirrus	51 mW m^{-2}

Summarising the impact of particulate emissions from aviation on the light-absorbing and potential ice-nuclei forming carbonaceous particles in the upper free troposphere,

(1) the contribution of ≤ 0.1 ng m^{-3} to the background black carbon mass concentration of $\cong 1$ ng m^{-3} on a hemispheric scale is small;
(2) the contribution of $\cong 0.5$ ng m^{-3} to the background black carbon mass concentration in air traffic polluted air masses is significant;
(3) the direct fording of 0.7 mW m^{-2} in the flight corridor contributes $< 2\%$ to the total radiative forcing of aviation, when cirrus effects are excluded;
(4) the air traffic related excess number density of > 10 nonvolatile particles per cm^3 in flight corridors is a significant contribution to the number of potential ice nuclei and may influence cirrus formation in these air masses.

The still open key question is, whether there is an indirect effect of aviation on cirrus clouds. A full assessment of the environmental compatibility of aviation cannot be made without answering this question. As discussed in Section 7, combustion particles emitted from an aircraft engine are very inefficient cloud condensation nuclei under atmospheric conditions. However, similar knowledge on the ice nuclei potential is still missing, because there is a severe gap in instrumentation capabilities for the detection of ice nuclei under atmospheric conditions.

Research on the atmospheric impact of aviation – and beyond even on the atmospheric and climate impact of the global transportation system – has started with the INCA experiment to shift towards the investigation of aerosol-cirrus interactions. The methodology and instrumentation developed in the course of the presented work is expected to make significant contributions to this developing research area. As was already outlined in Section 1, this will particularly be the case within the projects IAGOS ("Integration of routine aircraft measurements into a global observing system"), focusing on the development of a global observing system on atmospheric constituents using scheduled aircraft, and QUANTIFY ("Quantifying the Climate Impact of Global and European Transport Systems"), focusing on the climate impact of the global transportation sector.

9 Acknowledgements

My sincere thanks go to Prof. Dr. Ulrich Schumann for his cordial support throughout my work. His reliance on me fostered all aspects of my research activities. Through numerous discussions he encouraged me to move to new scientific fields. The institute always offered a fruitful and creative atmosphere, which made my work possible. I am deeply grateful to Prof. Dr. Joseph Egger for his continuous interest in and support of my work. He invited me to contribute to the activities of the Meteorological Institute of the University of Munich. Dr. Hans Schlager supported my activities on the measurement of airborne particles and on the development of measurement techniques in every sense. I am grateful for the essential contributions of and close collaborations with numerous colleagues of DLR, only a few of whom can be named here. Franz Schröder, Markus Fiebig and Andreas Minikin shared through many years the huge efforts in establishing and successfully running our small but nice “Aerosol Group”. Gerhard Ehret and the entire Lidar group supported us whenever needed in discussions and during joint projects.

Many thanks are expressed to all the colleagues I had the pleasure to work with during various international projects. In particular I want to mention Regina Hitzenberger and Hans Puxbaum at the University and Technical University of Vienna, respectively, Urs Baltensperger and the entire Laboratory for Atmospheric Chemistry at the Paul Scherrer Institute in Switzerland and Chris W. Wilson and his former colleagues at Qinetiq in the United Kingdom who shared the challenging experience of PartEmis with me. I want to express my thanks also to Patrick J. Sheridan from NOAA and to W. Patrick Arnott from DRI who made my participation in the Reno Aerosol Optics Study possible, and to Darrel Baumgardner who introduced me to the secrets of optical particle spectrometers The financial support by the DLR for the project “Partikel und Zirren”, by the EU for the projects PartEmis and INCA, and the national funding from the BMBF for the Lindenberg Aerosol Characterisation Experiment LACE 98 as well as the funding from the Deutsche Bundesstiftung Umwelt for the development of the multi-angle absorption photometer are gratefully acknowledged.

10. References

Section 10.1 lists the publications which are explicitly discussed in the manuscript. Section 10.2 contains a selection of references with contributions by the author, which are cited in the manuscript. Further external references, cited in the manuscript, are listed in Section 10.3.

10.1 Integrated References

[1] Petzold, A., R. Busen, F.P. Schröder, R. Baumann, M. Kuhn, J. Ström, D.E. Hagen, P.D. Whitefield, D. Baumgardner, F. Arnold, S. Borrmann, and U. Schumann (1997) Near field measurements on contrail properties from fuels with different sulfur content, *J. Geophys. Res., 102*, 29,867-29,880.

[2] Petzold, A., J. Ström, S. Ohlsson and F.P. Schröder (1998) Elemental composition and morphology of ice crystal residual particles in cirrus clouds and contrails, *Atmos. Res., 49,* 21-34.

[3] Petzold, A. and F.P. Schröder (1998) Jet engine exhaust aerosol characterization, *Aerosol Sci. Technol., 28*, 62-76.

[4] Petzold, A. and A. Döpelheuer (1998) Reexamination of black carbon mass emission indices of a jet engine, *Aerosol Sci. Technol., 29,* 355-356.

[5] Petzold, A., J. Ström, F.P. Schröder, and B. Kärcher (1999) Carbonaceous aerosol in jet exhaust: emission characteristics and implications for heterogeneous reactions, *Atmos. Environ.*, 33*,* 2689-2698.

[6] Petzold, A., A. Döpelheuer, C.A. Brock, and F.P. Schröder (1999) In situ observations and model calculations of black carbon emission by aircraft at cruise altitude, *J. Geophys. Res.*, *104*, 22171-22181.

[7] Petzold, A., and Schönlinner, M. (2004) Multi-angle absorption photometry - a new method for the measurement of aerosol light absorption and atmospheric black carbon, *J. Aerosol Sci.*, *35,* 421-441.

[8] Petzold, A., H. Schloesser, P.J. Sheridan, W.P. Arnott, J.A. Ogren, and A. Virkkula (2005) Evaluation of multi-angle absorption photometry for measuring aerosol light absorption, *Aerosol Sci. Technol.*, 39, 40-51.

[9] Petzold , A., C. Stein, S. Nyeki, M. Gysel, E. Weingartner, U. Baltensperger, H. Giebl, R. Hitzenberger, A. Döpelheuer, S. Vrchoticky, H. Puxbaum, M. Johnson, C.D. Hurley, R. Marsh, and C.W. Wilson, (2003) Properties of jet engine combustor particles during the PartEmis experiment. Microphysical and chemical properties. *Geophys. Res. Lett.,* 30**,** 1719, doi:10.1029/2003GL017283.

[10] Petzold, A., M. Fiebig , L. Fritzsche, C. Stein , U. Schumann, C.W. Wilson , C.D. Hurley , F. Arnold , E. Katragkou, U. Baltensperger, M. Gysel , S. Nyeki , R. Hitzenberger, H. Giebl , K. J. Hughes, R. Kurtenbach, P. Wiesen, P. Madden, H. Puxbaum , S. Vrchoticky , C. Wahl, (2005) Particle emissions from aircraft engines – A survey of the European project PartEmis, *Meteorol, Z.* 14, 465-476.

10.2 Selected Author's Contributions

AIR 5892 (2004) *Nonvolatile Exhaust Particle Measurement Techniques*, Aerospace Information Report, SAE International, 2004.

Brock, C.A., et al. (2000) Ultrafine particle size distributions measured in aircraft exhaust plumes, *J. Geophys. Res.*, *105*, 26,555-26,567.

EC (2001a) *European research in the stratosphere 1996 – 2000*, European Commission, EUR 19867, Brussels.

EC (2001b) *Aviation, aerosols, contrails and cirrus clouds*, Proceedings of a European Workshop, Air pollution research report 74, European Commission, Brussels.

EC (2004) *Aviation, Atmosphere and Climate*, Proceedings of a European Conference, Air pollution research report 83, European Commission, Brussels.

Gayet, J.-F., F. Auriol, A. Minikin, J. Ström, A. Petzold, G. Febre, U. Schumann (2002) On the reliability of four different in situ probes for the quantitative measurement of the microphysical and optical properties of cirrus clouds during INCA experiment: Evidence of small ice crystals, *Geophys. Res. Lett.*, *29*, (10.1029/2001GL014342), 83-1-83-4.

Gayet, J.-F., J. Ovarlez, V. Shcherbakov, J. Stro¨m, U. Schumann, A. Minikin, F. Auriol, A. Petzold, and M. Monier (2004), Cirrus cloud microphysical and optical properties at southern and northern midlatitudes during the INCA experiment, *J. Geophys. Res.*, 39 109, doi:10.1029/2004JD004803.

Gysel, M., S.Nyeki, E. Weingartner, U. Baltensperger, H. Giebl, R. Hitzenberger, A. Petzold, and C.W. Wilson (2003) Properties of jet engine combustor particles during the PartEmis experiment. Hygroscopicity at subsaturated conditions, *Geophys. Res. Lett.*, *30*, 1566, doi:10.1029/2003GL016896.

Hitzenberger, R., H. Giebl, A. Petzold, M. Gysel, S. Nyeki, E. Weingartner, U. Baltensperger, C.W. Wilson (2003) Properties of jet engine combustor particles during the PartEmis experiment. Hygroscopic properties at supersaturated conditions, *Geophys. Res. Lett.*, *30***,** 1779, doi:10.1029/2003GL017294.

IPCC (1999) *Aviation and the Global Atmosphere*, Intergovernmental Panel on Climate Change, Cambridge University Press, Cambridge.

Kärcher, B., R. Busen, A. Petzold, F.P. Schröder, U. Schumann, and E. Jensen (1998) Physicochemistry of aircraft generated liquid aerosols, soot, and ice particles - II. Comparison with observations and sensitivity studies, *J. Geophys. Res.*, *103*, 17,129-17,147.

Kuhn, M. A. Petzold, D. Baumgardner, and F.P. Schröder (1998) Particle composition of a young condensation trail and of upper tropospheric background aerosol, *Geophys. Res. Lett.*, *25*, 2679-2682.

Minikin, A., Petzold, A., Ström, J., Krejci, R., Seifert, M., et al. (2003) Aircraft observations of the upper tropospheric fine particle aerosol in the northern and southern hemispheres at midlatitudes, *Geophys. Res. Lett., 30*, doi 10.1029/2002GL016458.

Nyeki, S., M. Gysel, E. Weingartner, U. Baltensperger, R. Hitzenberger, A. Petzold, C.W. Wilson (2004) Properties of jet engine combustion particles during the PartEmis experiment: Particle size spectra (d > 15 nm) and volatility, *Geophys. Res. Lett*., *31*, L18195, doi:10.1029/2004GL020569.

Petzold, A. and Niessner, R. (1995a) Method comparison study on soot-selective techniques., *Mikrochim. Acta*, *117*, 215-237.

Petzold, A. and R. Niessner (1995b) Novel design of a resonant photoacoustic spectrophone for elemental carbon mass monitoring, *Appl. Phys. Lett., 66*, 1285-1287.

Petzold, A. and Niessner, R. (1996) Photoacoustic soot sensor for in-situ black carbon monitoring. *Appl. Phys.*, *B63***,** 191-197.

Petzold, A., Kopp, C., and Niessner, R. (1997) The dependence of the specific attenuation cross-section on black carbon mass fraction and particle size. *Atmos. Environ.*, *31*, 661-672.

Petzold, A., Kramer, H., and Schönlinner, M. (2002a) Continuous measurement of atmospheric black carbon using a multi-angle absorption photometer. *Environ. Sci. Poll. Res.* Special issue, *4*, 78-82.

Petzold, A., M. Fiebig, H Flentje, A. Keil, U. Leiterer, F. Schröder, A. Stifter, M. Wendisch, P. Wendling (2002b) Vertical variability of aerosol properties observed at a continental site during LACE 98, *J. Geophys. Res.*, *107* (10.1029/2001JD001043), LAC 10-1 – LAC 10-18.

Petzold, A., M. Gysel, X. Vancassel, R. Hitzenberger, H. Puxbaum, S. Vrochticky, E. Weingartner, U. Baltensperger , and P. Mirabel (2005) On the effects of organic matter and sulphur-containing compounds on the CCN activation of combustion particles, *Atmos. Chem. Phys., 5*, 3187–3203.

Schröder, F.P., B. Kärcher, A. Petzold, R. Baumann, R. Busen, C. Hoell, and U. Schumann (1998) Ultrafine aerosol particles in aircraft plumes: In situ observations, *Geophys. Res. Lett.*, *25*, 2789-2793.

Schröder, F., C. Brock, R. Baumann, A. Petzold, R. Busen, P. Schulte, and M. Fiebig (2000) In-situ studies on volatile jet exhaust particle emissions: Impact of fuel sulfur content and thermodynamic conditions on nuclei-mode aerosols, *J-. Geophys. Res.*, 105, 19,941-19,954.

Schröder, F. B. Kärcher, C. Duroure, J. Ström, A. Petzold, J.F. Gayet, B. Strauss, P.Wendling, S. Borrmann (2000) The Transition of Contrails into Cirrus Clouds, *J. Atmos. Sci.*, 57, 464-480.

Schumann, U. , F. Arnold, R. Busen, J. Curtius, B. Kärcher, A. Kiendler, A. Petzold, H. Schlager, F. Schröder, and K.-H. Wohlfrom (2002) Influence of fuels sulfur on the composition of aircraft exhaust plumes: The experiments SULFUR 1-7, *J. Geophys. Res.*, *107* (10.1029/2001JD000813), AAC 2-1 – AAC 2-27.

Sheridan, P.J., Arnott, W.P., Ogren, J.A., Andrews, E., Atkinson, D.B., Covert, D.S., Moosmüller, H., Petzold, A., Schmidt, B., Strawa, A.W., Varma, R., and Virkkula, A. (2004) The Reno Aerosol Optics Study: Overview and Summary of Results, *Aerosol Sci. Technol.*, in press.

Vancassel, X., A. Sorokin , P. Mirabel , A. Petzold , and C.W. Wilson (2004) Volatile particles formation during PartEmis: a modelling study, *Atmos. Chem. Phys.*, *4*, 439-447.

Wilson, C.W., A. Petzold, S. Nyeki, U. Schumann, and R. Zellner (2004) Measurement and Prediction of Emissions of Aerosols and Gaseous Precursors from Gas Turbine Engines (PartEmis): An Overview, *Aerosp. Sci. Technol*., *8*, 131 – 143.

10.3 External References

Adams, K. M. (1988), Real-time in situ measurements of atmospheric optical absorption in the visible via photoacoustic spectroscopy. 1: Evaluation of photoacoustic cells, *Appl. Opt.*, *27*, 4052-4056

Anderson, B.E., W.R. Cofer, D.R. Bagwell, J.W. Barrick, C.H. Hudgins, and K.E. Brunke (1998a) Airborne observations of aircraft aerosol emissions I: Total nonvolatile particle emission indices, *Geophys. Res. Lett., 25*, 1689-1692.

Anderson, B.E., W.R. Cofer, D.R. Bagwell, J.W. Barrick, and C.H. Hudgins (1998b) Airborne observations of aircraft aerosol emissions II: Factors controlling volatile particle production, *Geophys. Res. Lett., 25*, 1693-1696.

Andreae, M.O. (2001) The dark side of aerosols. *Nature*, *409*, 671-672.

Arnott, W.P., H. Mosmüller, C.F. Rogers, T. Jin, and R. Bruch (1999) Photoacoustic spectrometer for measuring light absorption by aerosol: Instrument description. *Atmos. Environ.*, *33*, 2845-2852.

Baumgardner, D., G. Kok, and G. Raga (2004) Warming of the arctic lower stratosphere by light absorbing particles, *Geophys. Res. Lett.*, *31,* L06117, doi: 10.1029/2003GL018883.

Blake, D.F. and K. Kato (1995) Latitudinal distribution of black carbon soot in the upper troposphere and lower stratosphere, *J. Geophys. Res., 100*, 7195-7202.

Bohren, C.F and Huffman, D.R. (1983) *Absorption and Scattering of Light by Small Particles*. John Wiley, New York.

Bond, T.C., Anderson, T.L., and Campbell, D. (1999) Calibration and intercomparison of filter-based measurements of visible light absorption by aerosols. *Aerosol Sci. Technol.*, *30*, 582-600.

Boucher O. (1999) Influence of air traffic on cirrus occurrence, *Nature*, *397*, 30-31.

Broekhuizen, K., P.Pradeep Kumar, and J.P.D. Abbatt (2004) Partially soluble organics as cloud condensation nuclei: Role of trace soluble and surface active species, *Geophys. Res. Lett.*, *31*,

L01107, doi: 10.1029/2003GL018203.

Brühl, C. and P.J. Crutzen (1988) Scenarios of possible changes in the atmospheric temperatures and ozone concentrations due to man's activities, estimated with a one-dimensional coupled photochemical climate model, *Chemical Dynamics*, *2*, 173 – 203.

Busen, R. and U. Schumann (1995) Visible contrail formation from fuels with different sulfur contents, *Geophys. Res. Lett.*, *22*, 1357-1360.

Cachier, H., M.P. Bremond, P. Biat-Ménard (1989) Determination of atmospheric soot carbon with a simple thermal method, *Tellus*, *41B*, 379-390.

Charlson, R.J., J.E. Lovelock, M.O. Andreae, and S.G. Warren (1989) Sulphate aerosols and climate, *Nature*, *340*, 437-438.

Charlson, R.J., J. Langner, and H. Rohde, Sulphate aerosol and climate (1990) *Nature*, *348*, 22.

Charlosn, R.J., J. Langner, H. Rohde, C.B. Leovy, and S.G. Warren (1991) Perturbation of the northern hemisphere radiative balance by backscattering from anthropogenic sulphate aerosols, *Tellus*, *43AB*, 152-163.

Charlson, R.J. and J. Heintzenberg (Eds.) (1995) *Aerosol Forcing of Climate*, John Wiley, New York.

Clarke, A.D., Noone, K.J., Heintzenberg, J., Warren, S.G., and Covert, D.S. (1987) Aerosol light absorption measurement techniques: Analysis and Intercomparisons. *Atmos. Environ.*, *21*, 1455-1465.

Coakley, J.A. and Chylek, P. (1975) The two-stream approximation in radiative transfer: Including the angle of incident radiation. *J. Atmos. Sci., 32*, 409-418.

Crutzen, P.J. (1971) Ozone production rate in an oxygen-hydrogen-nitrogen oxide atmosphere, *J. Geophys. Res.*, *76*, 7311 - 7327.

Delumyea, R.G., Chu, L.-C., and Macias, E.D. (1980) Determination of elemental carbon component of soot in ambient aerosol samples. *Atmos. Environ.*, *14*, 647-652.

Döpelheuer, A. (1997) *Berechnung der Produkte unvollständiger Verbrennung aus Luftfahrttrieb-werken*, IB-325-09-97, DLR, Institut für Antriebstechnik, Köln.

Döpelheuer, A. (2002) Anwendungsorientierte Verfahren zur Bestimmung von CO, HC und Ruß aus Luftfahrttriebwerken, FB 2002-10, DLR Köln.

DLR (1994) *Impact of Emissions from Aircraft and Spacecraft Upon the Atmosphere,* Proceedings of an International Scientific Colloquium, *DLR-Mitteilung 94-06.*

Fahey, D.W., Keim, E.R., Woodbridge E.L., Gao, R.S., Boering, K.A., Daube, B.C., Wofsy, S.C., Lohmann, R.P., Hintsa E.J., Dessler, A.E., Webster C.R., May, R.D., Brock, C.A., Wilson, J.C., Miake-Lye, R.C., Brown, R.C., Rodriguez, J.M., Loewenstein, M., Proffitt, M.H., Stimpfle, R.M., Bowen, S.W. and Chan, K.R. (1995a) In-situ Observations in Aircraft Plumes in the Lower Stratosphere at Midlatitudes, *J. Geophys. Res., 100*, 3065-3074.

Fahey, D.W., Keim, E.R., Boering, K.A., Brock, C.A., Wilson, J.C., Jonsson, H.H., Anthony, S., Hanisco,

T.F., Wennberg, P.O., Miake-Lye, R.C., Salawitch, R.J., Louisnard, N., Woodbridge, E.L., Gao, R.S., Donnelly, S.G., Wamsley, R.C., Del Negro, L.A., Solomon, S., Daube, B.C., Wofsy, S.C., Webster, C.R., May, R.D., Kelly, K.K., Loewenstein, M., Podolsk, J.R. and Chan, K.R. (1995b) Emission Measurements of the Concorde Supersonic Aircraft in the Lower Stratosphere, *Science, 270*, 70-73.

Gerber, H.E. and E.E. Hindman (1982) *Light Absoretion b yAerosol Particles*, Spectrum Press, Hampton.

Giebl, H., A. Berner, G. Reischl, H. Puxbaum, and R. Hitzenberger (2002) CCN activation of oxalic acid and malonic acid test aerosols with the Univ. of Vienna cloud condensation nuclei counter, *J. Aerosol Sci.*, *33*, 1623-1634.

Glassman, I. (1996) *Combustion* 3rd Edition, Academic Press, San Diego.

Goldberg, E.D. (1985) *Black Carbon in the Environment*, John Wiley, New York.

Gysel., M., E. Weingartner, and U. Baltenspergr (2002) Hygroscopicity of Aerosol particles at low temperatures: 2. Theoretical and experimental hygroscopic properties of laboratory generated aerosols, *Environ. Sci. Technol.*, *36*, 63-68.

Hänel, G. (1987) Radiation budget of the boundary layer: Part II, Simultaneous measurement of mean solar volume absorption and extinction coefficients of particles, *Beitr. Phys. Atmosph.*, *60,* 241-247.

Hagen, D.E., P.D. Whitefield and H. Schlager (1996) Particle emissions in the exhaust plume from commercial jet aircraft under cruise conditions, *J. Geophys. Res.*, *101*, 19,551-19,557.

Hansen, A.D.A., Rosen, H., and Novakov, T. (1984) The aethalometer - an instrument for the real-time measurement of optical absorption by aerosol particles. *Sci. Total Envir.*, *36*, 191-196.

Hartmann, D.L. (1994) *Global Physical Climatology*, Academic Press, San Diego.

Heintzenberg, J. (1982) Workshop measurements of the aerosol absorption coefficient with an Integrating Plate method and an Integrating Sphere Photometer, in *Light Absorption by Aerosol Particles*, edited by H.E. Gerber and E.E. Hindman, Spectrum Press, Hampton, 267-274.

Heintzenberg, J., R.J. Charlson, A.D. Clarke, C. Liousse, V. Ramaswamy, K.P. Shine, M. Wendisch, and G. Helas (1997) Measure-ments and modelling of aerosol single-scattering albedo: Progress, problems, and prospects. *Beitr. Phys. Atmosph.*, *70*, 249-263.

Hitzenberger, R. (1993) Absorption measurements with an integrating plate photometer, calibration and error analysis. *Aerosol Sci. Technol.*, *18*, 70-84.

Hofmann, D.J. and J.M. Rosen, Balloon observations of a particle layer injected by stratospheric aircraft at 23 km, *Geophys. Res. Lett.*, *5*, 511-514, 1978.

IPCC (2001) *Climate Change 2001: The Scientific Basis*, Intergovernmental Panel on Climate Change, Cambridge University Press, Cambridge.

Johnston, H.S. (1971) Reduction of stratospheric ozone by nitrogen oxide catalysts from supersonic transport exhaust, *Science*, *173*, 517 - 522.

Kärcher, B. (1996), Aircraft-generated aerosols and visible contrails, *Geophys. Res. Lett.*, *23*, 1933-1936.

Kärcher , B., Th. Peter and R. Ottmann (1995) Contrail formation: Homogeneous nucleation of H_2SO_4-H_2O droplets, *Geophys. Res. Lett.*, *22*, 1501-1504.

Kärcher, B., Th. Peter, U.M. Biermann and U. Schumann (1996) The initial composition of jet condensation trails, *J. Atmos. Sci.*, *53*, 3066-3083.

Lin, C.L., M.B. Baker, and R.J. Charlson (1973) Absorption coefficient for atmospheric aerosols: a method for measurement, *Appl. Opt*., *12*,1356-1363.

Melton, L.A. (1984) Soot diagnostics based on laser heating, *Appl. Opt.*, *23*, 2201-2208.

Miake-Lye, R.C., R.C. Brown, M.R. Anderson and C.E. Kolb (1994) Calculations of condensation and chemistry in an aircraft contrail, *DLR-Mitteilung 94-06*, 274-279.

Novakov, T. and C.E. Corrigan (1996) Cloud condensation nucleus activity of the organic component of biomass smoke particles, *Geophys. Res. Lett.*, *23*, 2141-2144.

Penner, J.E., R.E. Dickinson, and C.A. O'Neill (1992) Effects of aerosol from biomass burning on the global radiation budget, *Science*, *256*, 1432-1433.

Pitchford, M., J.G. Hudson, and J. Hallet (1991) Size and critical supersaturation for condensation of jet engine exhaust particles, *J. Geophys. Res.*, *96*, 20787 – 20793.

Pruppacher, H. R., and J.D. Klett (1997) *Microphysics of Clouds and Precipitation*, Kluwer 2nd edition, Academic Publishers, Dordrecht.

Puxbaum, H. (1979) Thermo-Gasanalysator zur Charakterisierung von Kohlenstoff und Schwefelverbindungen in luftgetragenen Stäuben, *Fresenius Z. Anal. Chem.*, *298*, 250-259.

Rosen, H., A.D.A. Hansen, L. Gundel, and T. Novakov (1978) Identification of the optically absorbing component in urban aerosols, *Appl. Opt.*, *17*, 3859-3861.

Rosen, H. and T. Novakov. (1983) Optical transmission through aerosol deposits on diffusely reflecting filters: a method for measuring the absorbing component of aerosol particles. *Appl. Opt.* , *22*, 1265-1267.

Sausen, R., I. Isaksen,V. Grewe, D.S. Lee, G. Myhre, U. Schumann, F. Stordal, and C. Zerefos (2005) Aviation radiative forcing in 2000: An update on IPCC (1999), *Meteorol. Z.*, *14*, 555-561.

Saxena, P., L.M. Hildemann, P.H. McMurry, and J.H. Seinfeld (1995) Organics alter hygroscopic behaviour of atmospheric particles, *J. Geophys. Res.*, *100*, 18755-18770.

Schlager, H., P. Konopka, P. Schulte, U. Schumann, H. Ziereis, F. Arnold, M. Klemm, D.E. Hagen, P.D. Whitefield, and J. Ovarlez (1997) In situ observations of air traffic emission signatures in the North Atlantic flight corridor, *J. Geophys. Res.*, *102*, 10,739-10,750.

Schmid, H., *et al.* (2001), Results of the "carbon conference" international aerosol carbon round robin test stage I. *Atmos. Environ.*, *35*, 2111-2121.

Schumann, U. (Ed.) (1990) Air Traffic and the Environment – Background, Tendencies and Potential Global Atmospheric Effects. *Proceedings of a DLR International Colloquium*. Bonn, November 15 – 16 1990, Lecture notes in Engineering, Vol. 60, Springer, Berlin.

Schumann, U. (1996) On conditions for contrail formation from aircraft exhausts, *Meteorol. Z., NF 5*, 4-23.

Schumann U., J. Ström, R. Busen, R. Baumann, K. Gierens, M. Krautstrunk, F.P. Schröder and J. Stingl (1996) In situ observations of particles in jet aircraft exhausts and contrails for different sulfur-containing fuels, *J. Geophys. Res.*, *101*, 6853-6869.

Twohy, C.H. and B.W. Gandrud (1998) Electron microscope analysis of residual particles from aircraft contrails, *Geophys. Res. Lett.*, *25*, 1359-1362.

Twomey, S. (1977) The influence of pollution on the shortwave albedo of clouds, *J. Atmos. Sci.*, *34*, 1149-1152.

Weingartner, E., M. Gysel, and U. Baltenspergr (2002) Hygroscopicity of aerosol particles at low temperatures: 1. New low-temperature H-TDMA instrument: Setup and first applications, *Environ. Sci. Technol.*, *36*, 55-62.

Weingartner, E., H. Saathoff, M. Schnaiter, N. Streit, B. Bitnar, and U. Baltensperger (2003), Absorption of light by soot particles: Determination of the absorption coefficient by means of aethalometers, *J. Aerosol Sci., 34*, 1445-1463.